UC Davis
UC Davis Electronic Theses and Dissertations

Title

The Qualitative Identification of Cardenolide-Containing Plants Using Ultra High Performance Liquid Chromatography — High Resolution Mass Spectrometry Chromatograms at Select Ions

Permalink

https://escholarship.org/uc/item/2j52r2q0

Author

Ng, Megan

Publication Date

2023

Peer reviewed|Thesis/dissertation

eScholarship.org Powered by the California Digital Library
University of California

The Qualitative Identification of Cardenolide-Containing Plants Using Ultra High Performance Liquid Chromatography – High Resolution Mass Spectrometry Chromatograms at Select Ions

By

MEGAN NG
THESIS

Submitted in partial satisfaction of the requirements for the degree of

MASTER OF SCIENCE

in

Forensic Science

in the

OFFICE OF GRADUATE STUDIES

of the

UNIVERSITY OF CALIFORNIA

DAVIS

Approved:

Robeert Poppenga, Chair

Wilson Rumbeiha

Benjamin Moeller

Committee in Charge

2023

Abstract

Cardiac glycosides (CGs), classified as cardenolides or bufadienolides, are toxins found in a variety of flora and fauna. CGs have historically been used to treat heart failure, but despite their place in medicine, they are still toxic to humans and animals. Currently, liquid chromatography paired with mass spectrometry (LC-MS) is used to screen for CGs. However, this requires using specific, costly, and often unavailable CG standards for reference. This study investigated the potential of identifying a cardenolide-containing (CC) plant using a plant's overall cardenolide composition, represented by unique ions in the 300 to 400 *m/z* region in their mass spectra, rather than individual toxins. The chromatographic patterns of different plants at these select ions may provide unique "fingerprints" to serve as a means of identification. Not only would this provide an alternative to the standards, but it could also aid the diagnosis of cardenolide toxicosis in humans and animals, especially in cases where exposure history is unknown. To accomplish this, cardenolide standards in methanol were analyzed using LC-MS and ions in the 300 to 400 *m/z* region exhibiting the "loss of 18 *m/z*" pattern were noted. These ions were grouped into "high", "medium", "low", based on their masses, and "genin". Next, 14 CC plants were individually homogenized in methanol and analyzed in replicate. The extracted ion chromatograms (EICs) at each ion of interest were observed for all plants. Blind tests were conducted to assess the ability to, using the EICs at the select ions, distinguish between CC and non-CC plants (Blind Test 1) and identify a CC plant (Blind Test 2). Blind Test 1 had a success probability of 1.0 across all ion groups, while Blind Test 2 had a success probability of 1.0 for the "high" and "medium" groups, and a success probability of 0.990 for the "low" and "genin" groups. Overall, this present study shows a promising start in using select ion chromatographic finger prints as a means of qualitatively identifying CC plants.

Acknowledgements

First, I would like to thank the UC Davis Arboretum, UC Davis Botanical Conservatory, and UC Davis Herbarium, for helping me identify suitable plants to include in my research and most of all, for allowing me to use plants from their collection.

I am grateful to the California Animal Health and Food Safety Laboratory in Davis for allowing me to complete my thesis project using their facilities. I cannot thank the entire toxicology department enough, who welcomed me with open arms and were eager to show me around. Most notably, I would like to thank Dr. Robert Poppenga, for being my Principle Investigator and providing insightful suggestions, Mike Filigenzi, for mentoring me throughout this project and thoroughly explaining topics so that I understand them, and Jim Langston who was always open to my questions. I would also like to thank my thesis committee members Dr. Wilson Rumbeiha and Dr. Ben Moeller, for investing time and care in my thesis. Thank you everyone for your involvement with my thesis.

Finally, I'd like to thank my friends and family who have shown their support throughout my journey to reach this milestone, through both the highs and the lows. I am very grateful for everyone's support.

Table of Contents

Abstract ii

Acknowledgements iii

1. Introduction 1

1.1 Cardiac Glycosides 1

1.2 Bufadienolides 3

1.3 Cardenolides 5

1.3.1 Sources 5

1.3.2. Toxin Distribution Within a Plant 6

1.3.3 Toxicity 6

1.3.4 Ingestion in Humans, Animals 7

1.4 Current Research 8

1.4.1 In Medicine 8

1.4.2 Sequestration and Resistance 9

1.5 Cardenolide Mass Spectrometry Fragmentation 10

1.6 Research Objective 11

2. Materials and Methods 14

2.1 Location 14

2.2 Reagents 14

2.3 Plants Collected 14

2.4 Preparation of Standards 16

2.5 Plant Selection 17

2.5.1 *Adenium* spp. 17

2.5.2 *Carissa macrocarpa* 17

2.6.3 *Ornithogalum fimbrimarginatum* 18

2.6.4 *Taxus baccata, Heteromeles arbitufolia, Prunus laurocerasus* 18

2.6.5. Attempted Plants 18

2.6 Preparation of Plant Samples 20

2.6.1 Attempted dSPE Cleanup 20

2.7 Instrumentation 22

2.7.1 Liquid Chromatography 22

2.7.2 Mass Spectrometry 22
2.8 Data Analysis 23
2.9 Validation 23
2.10 Blind Tests 26
2.10.1 Blind Test 1 – Identification of Cardenolide-containing Plants 26
2.10.2 Blind Test 2 – Individual Plant Classifications 26
2.10.3 Blind Test Statistics 27
2.10.4 Blind Test Sample Size Calculation 31
3. Results 36
3.1 Standards 36
3.2 Exemplary Extracted Ion Chromatograms of Each Plant 40
3.2.1 *Adenium boehmianum* 41
3.2.2 *Adenium obesum* 43
3.2.3 *Adenium oleifolium* 45
3.2.4 *Adenium socotranum* 47
3.2.5 *Asclepias curassavica* 49
3.2.6 *Asclepias fascicularis* 51
3.2.7 *Asclepias speciosa* 53
3.2.8 *Carissa macrocarpa* 55
3.2.9 *Cerbera odollam* 57
3.2.10 *Convallaria majalis* 59
3.2.11 *Digitalis purpurea* 61
3.2.12 *Nerium oleander* 63
3.2.13 *Ornithogalum fimbrimarginatum* 65
3.2.14 *Thevetia peruviana* 67
3.2.15 *Heteromeles arbitufolia* 69
3.2.16 *Taxus baccata* 71
3.2.17 *Prunus laurocerasus* 73
3.3 Blind Test 1: Identification of Cardenolide-containing Plants 75
3.3.1 Using "High" Ion Grouping 75
3.3.2 Using "Medium" Ion Grouping 75

3.3.3 Using "Low" Ion Grouping 75
3.3.4 Using "Genin" Ion Grouping 75
3.4 Blind Test 2: Individual Plant Classifications 76
3.4.1 Using "High" Ion Grouping 76
3.4.2 Using "Medium" Ion Grouping 77
3.4.3 Using "Low" Ion Grouping 78
3.4.4 Using "Genins" Ion Grouping 79
4. Discussion 79
4.1 Extracted Ion Chromatograms of Standards 80
4.2 Extracted Ion Chromatograms of Plants and Blind Test Identification 80
4.3 Blind Test Ion Performance 82
4.3.1 Blind Test 1 82
4.3.2 Blind Test 2 83
4.4 Blind Test Issues 87
4.5 Future Endeavors 88
4.5.1 Additional Plants and Ions 88
4.5.2 Blind Test Changes 89
4.5.3 Other Matrices 89
5. Conclusion 90
References 91
Appendix 105

1. Introduction

1.1 Cardiac Glycosides

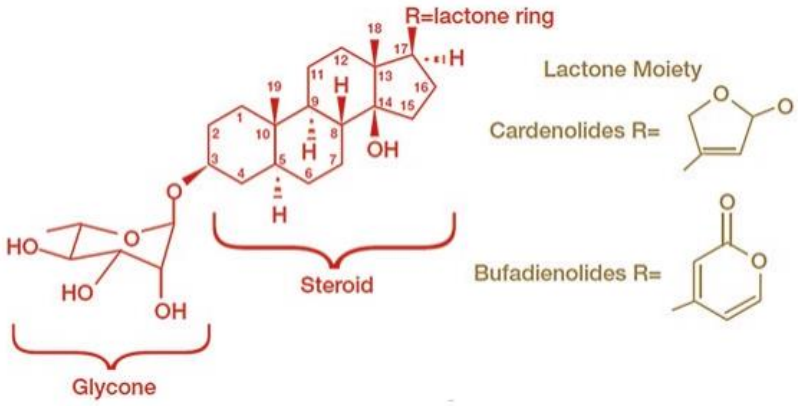

Figure 1. *The general structure of cardiac glycoside.*

From "Therapeutic Potential of Cardiac Glycosides Against Cancer" by Siti-Syarifah, M., & Yunos, N. 2018. In Anticancer Plants: Natural Products and Biotechnological Implements *(pp. 67–81).*

Plants are not simply passive organisms as they are equipped with defense mechanisms against predators. These defenses can be physical, such as thorns, spikes, or barbs, or chemicals, like the secretion of toxins. One such group of toxins found in plants are cardiac glycosides.

Cardiac glycosides (CGs) are naturally occurring toxic compounds found in a variety of flora and fauna. Their general structure consists of a lactone ring and steroid nucleus, forming the aglycone, with a sugar side chain (Figure 1). Their name is attributed to their ability to inhibit sodium potassium pump (Na^+/K^+-ATPase) functionality in cardiac tissues and the glycosidic linkage between the sugar component and the steroid nucleus. There are over 500 known CGs, with even more likely to be discovered (Singh and Rastogi, 1970; Kreis and Müller-Uri, 2010: Agrawal et al., 2012). "Cardiac glycosides" is a broad term that encompasses all toxins sharing the same general structure of a steroid nucleus, sugar, and lactone ring. However, they can be further categorized as bufadienolides or cardenolides.

The unique toxic properties of CGs offer a broad range of applications. Unsurprisingly, their toxicity has made them popular homicide and suicide agents. *Thevetia peruviana* is a major culprit of the thousands of self-harm poisoning cases occurring annually in parts of India and Sri Lanka (Gaillard et al., 2004; Eddleston et al., 1999). CGs also serve as hunting aids, as in the case of the San people in southern Africa who coat their hunting arrows with the sap of the CG-containing *Acokanthera oppositifolia* (Akinmoladun et al., 2014). CGs can also be employed as natural pesticides and even serve as a better alternative to synthetic pesticides. The CGs neriifolin and cerberin in *Adenium obesum* have higher molluscicidal activity than conventional molluscicides such as the carbamates methomyl and methiocarb (Alzabib et al., 2019).

On the opposite end of the spectrum, CGs also have a long-intertwined history with medicine as treatment for an array of ailments. *Chan Su*, a traditional Chinese medicine made from CG-containing toad venom, has been used to treat sore throat, tonsillitis, and palpitations for over 1,000 years (Chen, 1967). Digoxin was first recorded in 1785 as treatment for edema, a symptom of congestive heart failure (Wilkins, 1985). This foxglove toxin has since become an approved therapy for various heart conditions such as atrial fibrillation and heart failure (Bavendiek et al., 2017).

1.2 Bufadienolides

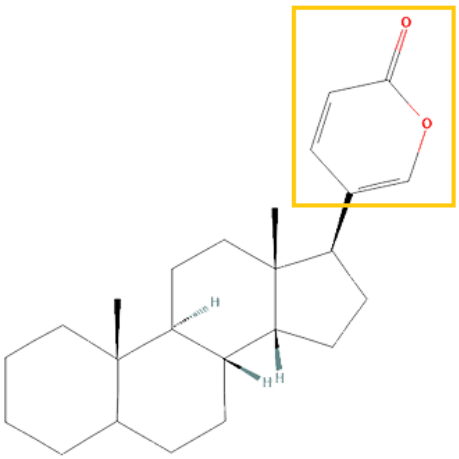

Figure 2. *The general structure of a bufadienolide aglycone.*
From PubChem. PubChem Identifier: CID 46173848 URL: https://pubchem.ncbi.nlm.nih.gov/compound/46173848#section=2D-Structure

Bufadienolides are C24 steroids containing a six membered lactone ring at the C17 position (Figure 2). Also known as "toad venom," bufadienolides derive their name from the members of the true toad family *Bufonidae* such as *Bufo gargarizans* (Asiatic Toad) that secretes the CGs bufalin, cinobufagin, and bufotalin among other bufotoxins from its skin glands (Jin et al., 2021). Bufadienolides are also observed in invertebrates such as *Photinus* fireflies of the *Lampyridae* family that produce lucibufagin, a defensive bufotoxin that makes them unpalatable to predators (Eisner et al., 1978). More recently, there is increasing evidence of endogenous bufadienolides in humans which are produced in the placenta and adrenal cortex, but their exact biosynthetic pathways and function remain unknown (Hilton et al., 1996; Dmitrieva et al., 2000; Carullo et al., 2023)

Bufadienolides are also produced in at least five different plant families such as *Crassulaceae, Ranunculaceae, Hyacynthinacae, Leguminosae,* and *Sterculiaceae*, with some notable plants being *Helleborus (Ranunculaecae), Kalanchoe (Crassulaceae*), and *Drimia maritima (Asparagaceae*) (Gao et al., 2011).

Bufadienolides can also be found in animals that do not produce the toxins themselves but acquire it from prey that produce them. For example, *Rhabdophis tigrinus* (Tiger Keelback Snake) sequesters bufotoxins from *Bufo* toads they eat; the toxins are then stored in their nuchal glands and incorporated into their own defense systems (Hutchinson et al., 2007). Likewise, *Spilostethus pandurus* (Milkweed Bug) sequesters bufadienolides from the *Drimia maritma* (Sea Squill) they consume (Pokharel et al., 2020).

1.3 Cardenolides

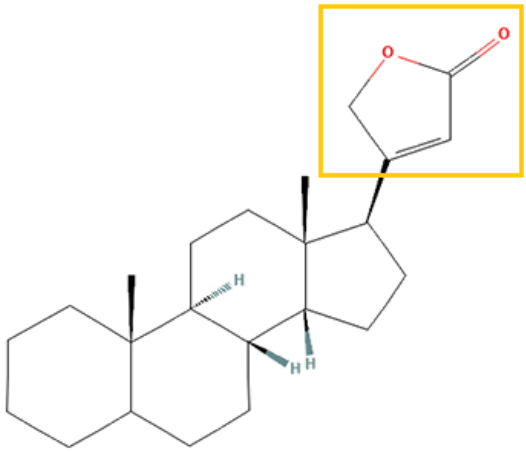

Figure 3. *The general structure of a cardenolide aglycone.*
From PubChem. PubChem Identifier: CID 53957771 URL: https://pubchem.ncbi.nlm.nih.gov/compound/53957771#section=2D-Structure

1.3.1 Sources

Cardenolides are C23 steroids containing a five-member lactone ring, or butenolide, at the C17 position (Figure 3). They are a class of structurally diverse toxins predominantly found and produced in plants, existing in at least 13 families of flora, such as *Apocynaceae*, *Asparagaceae*, *Brassicaceae*, *Celastraceae*, *Combretaceae*, *Euphorbiaceae*, *Fabaceae*, *Liliaceae*, *Moraceae*, *Plantaginaceae*, *Ranunculaceae*, *Scrophulariaceae, and Solanaceae* (Kreis and Müller-Uri, 2010). Among these plant families, cardenolides are most dominant in *Apocynaceae*, where over 30 genera have been reported to produce them (Agrawal et al., 2012). Well-known examples of cardenolide-containing plants include *Nerium oleander* (Oleander), *Digitalis purpurea* (Purple Foxglove), and *Adonis aestivalis* (Summer Pheasant's Eye).

Like bufadienolides, cardenolides can also be found in a handful of invertebrates that are not primary producers of the toxins but eat plants that produce them. *Danaus plexippus* (Monarch Butterfly) is famously known to feed on *Asclepias* plants from which they sequester cardenolides like calactin and calotropin (Cheung et al., 1988). In fact, these sequestered toxins

make them unpalatable to predators, thereby serving as a defense mechanism (Brower et al. 1967).

1.3.2. Toxin Distribution Within a Plant

In most cases, cardenolides are present in all parts of plants, making the entire plant toxic, such as is the case with *N. oleander* (Langford 1996). However, the distribution of toxins within a plant can vary across different plant species. In *Asclepias humistrata,* for example, the cardenolide concentration in the latex is greater than that in the leaves by 90-fold (Zalucki et al 2001). In *D. purpurea*, the upper leaves had the highest concentration of cardenolides while its roots possess the least (Evans and Cowley 1972). Moreover, the distribution of individual cardenolides among plant parts can vary depending on a toxin's polarity. In *Asclepias eriocarpa*, polar cardenolides are concentrated in the roots, while less polar cardenolides like labriformin are found in the latex (Nelson et al. 1981).

1.3.3 Toxicity

Many cardenolide-containing (CC) plants are extremely potent. A single *Nerium oleander* leaf can be fatal to children, while the lethal dose of *N. oleander* for a human adult has been observed to vary from about 5 to 15 leaves (Shaw 1979; Osterloh 1982). As low as 0.005% of body weight in dried *N. oleander* leaves can be lethal for an animal, which is equivalent to as little as 10 to 20 leaves for an adult horse (Galey 1996). Ingesting only half of a *Cerbera odollam* seed is enough to cause death (Saxena 2023). Furthermore, cardenolides are structurally stable; plant leaves remain toxic whether they have been desiccated or boiled (Rahnama-Moghadam et al. 2015).

1.3.4 Ingestion in Humans, Animals

Cardenolide-containing plants are often ornamental plants used for public landscaping, making them ubiquitous despite their toxicity. Although generally uncommon, there were over 2,000 human cases of CG plant related poisonings in the United States in 2021, of which over 20% were attributed to *N. oleander* alone (Gummin et al., 2021). Accidental ingestion of CC plants by companion animals also occurs. In France, *Convallaria majalis* and *N. oleander* are a common cause of plant-related poisonings in cats and dogs, often resulting in severe and potentially lethal cardiac disorders (Gault et al., 1995: Berney et al., 2010).

Cardenolide poisoning is a more pressing concern in livestock, as fodder may become inadvertently contaminated with CC plants and given to animals for consumption. For example, from 1992 to 2005, seven outbreaks of acute *N. oleander* poisoning in cattle occurred in Northeastern Brazil. Residual pruning waste of *N. oleander* had been left on the grazing land, ground up, and incorporated into feed; as a result, 67% of the affected cattle died (Soto-Blanco et al. 2006). Similarly, in all 12 cases of oleander toxicosis in camelids from 1995 to 2006, oleander was either present in the hay feed or areas where the llamas and alpacas resided (Kozikowski et al. 2009). Horses that consumed hay contaminated with *Adonis aestavalis* suffered from gastrointestinal gaseous distension (Woods et al. 2004). While plants containing cardenolides are unpalatable to animals, this appears only relevant for fresh leaves, as cattle are not deterred from eating dried oleander clippings (Galey, 1996).

1.4 Current Research

1.4.1 In Medicine

Cardiac glycoside (CG) inhibition of Na^+/K^+-ATPase increases intracellular sodium ion concentrations, resulting in a build-up in calcium ions in cardiac tissue which ultimately increases the contractility of the cardiac muscles (Ren et al 2020). While this effect could be fatal, it has also given CGs a place in medicine, primarily as treatment for atrial fibrillation and heart failure with reduced ejection fraction (Bavendiek et al. 2017). However, the narrow therapeutic window of CGs and the emergence of safer and more effective alternatives, such as beta-blockers and calcium channel antagonists, have discouraged the prescription of CGs as first-choice medications; it is recommended that CGs are used in conjunction with other therapies rather than as the sole form of medication (Fauchier et al. 2016; Rosca et al. 2021). There has been investigations into their potential as cancer and antiviral therapies, as well as other medical applications.

1.4.1.1 Anticancer Potential

Cardenolide cytotoxicity on cancer cell lines is likely attributed to their Na^+/K^+-ATPase inhibition properties. Pan et al. (2017) confirmed that oleandrin suppresses colon cancer cell growth without significantly hindering the viability of normal colon cells. Tian et al. (2018) established that calotropin promoted apoptosis while downregulating the expression of anti-apoptosis proteins, therefore inhibiting tumor growth. Guerrero et al. (2019) found that ouabain is a senolytic agent that may work synergistically with existing anti-cancer medications to eliminate tumor and even senescent cells. The variation of cytotoxicity among different CGs may be due to the expression of different isoforms of Na+/K+-ATPase and Na+-Ca2+ exchangers in cancer cells (Rajkovic 2023).

1.4.1.2 Antiviral Potential

The exploration of CG's potential as antiviral agents, especially with the recent COVID-19 pandemic, has been an ongoing effort. Cheung et al. (2014) observed a dose-dependent relationship between the reduction of dengue viral RNA and increasing lanatoside C concentrations. Laird et al. (2014) demonstrated that cardenolides such as convallotoxin, cymarin, and digitoxin, can inhibit HIV-1 gene expression and structural protein synthesis by altering RNA processing. Jin et al. (2021) found that digitoxin and bufadienolides like bufalin, telocinobufagin, and bufotalin, among others, all exhibited anti-coronaviral activity towards MERS-CoV, SARS-CoV, and SARS-CoV-2.

1.4.2 Sequestration and Resistance

Despite the potency of CG toxins, there are numerous examples of invertebrates whose diet consists of CG-containing plants or animals. These animals have developed biological adaptations that result in either the sequestration of or resistance to CGs. Agrawal et al. (2021) determined that *D. plexippus* have Na^+/K^+-ATPase 50 to 100 times more resistant towards cardenolides than porcine Na^+/K^+-ATPase, providing insight into their tolerance to milkweed toxins. Mohammadi et al. (2017) revealed that *Thamnophis elegans* (Western Terrestrial Garter Snake) expresses high levels of mutant cardiac Na^+/K^+-ATPase mRNA, which might explain their resistance to bufadienolides in frogs. Ujvari et al. (2013) concluded that resistant Na^+/K^+-ATPase exhibited in *Bufo* frog-eating Asian and African varanids could be attributed to two amino acid replacements in their Na^+/K^+-ATPase α3 subunit, as they have a 3000-fold increased resistance to bufalin compared to their Australian counterparts lacking this mutation. Similarly, Groen et al. (2021) found that *Pheucticus melanocephalus* (Black-Headed Grosbeak) also have Na^+/K^+-ATPase amino acid substitutions that allow them to prey on monarch butterflies.

1.5 Cardenolide Mass Spectrometry Fragmentation

Liquid Chromatography – Mass Spectrometry (LC-MS) is at the forefront of quantitative and qualitative analysis, not only for its sensitivity, specificity, and resolution, but also its broad application in the analysis of a variety of different compounds. Analytes are first separated based on their relative affinities for the mobile phase and column. They are then ionized, sometimes fragmented, and sorted by their mass to charge ratios, eventually reaching the detector. Naturally, LC-MS is also the method of choice for the analysis of cardenolides. Cardenolides share a distinct fragmentation pattern. During fragmentation, a cardenolide's sugar moiety leaves first. The remaining aglycone consisting of the steroid nucleus and lactone ring is also known as the genin. Consider the CG oleandrin, which becomes oleandrigenin once it has lost its sugar moiety (Figure 4). A successive loss of small molecules, namely H_2O, from the genin then ensues, indicated by a successive loss of 18 *m/z* in the 300 to 400 *m/z* region of a cardenolide's mass spectra (Higashi et al., 1999). In oleandrin, this pattern is observed at ions 373, 355, and 337 (Figure 5). The mass range of this "trio of ions" can vary slightly due to the inherently different molecular weights of each toxin. For example, digitoxin also exhibits this mass spectra pattern, which is observed at ions 375, 357, and 339 (Figure 6).

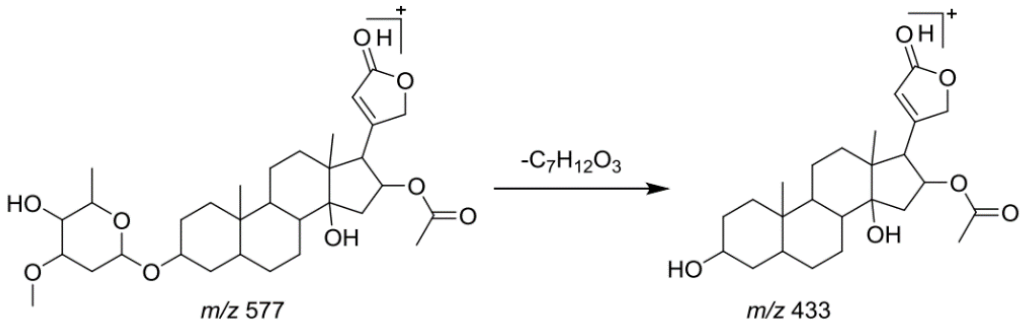

Figure 4. *The fragmentation of Oleandrin (left) into Oleandrigenin (right).*

From "Structural Analysis of Diastereomeric Cardiac Glycosides and Their Genins Using Ultraperformance Liquid Chromatography-Tandem Mass Spectrometry" by Singh et al. 2021. Journal of the American Society for Mass Spectrometry, *32(5), 1205–1214. Supporting Information list.*

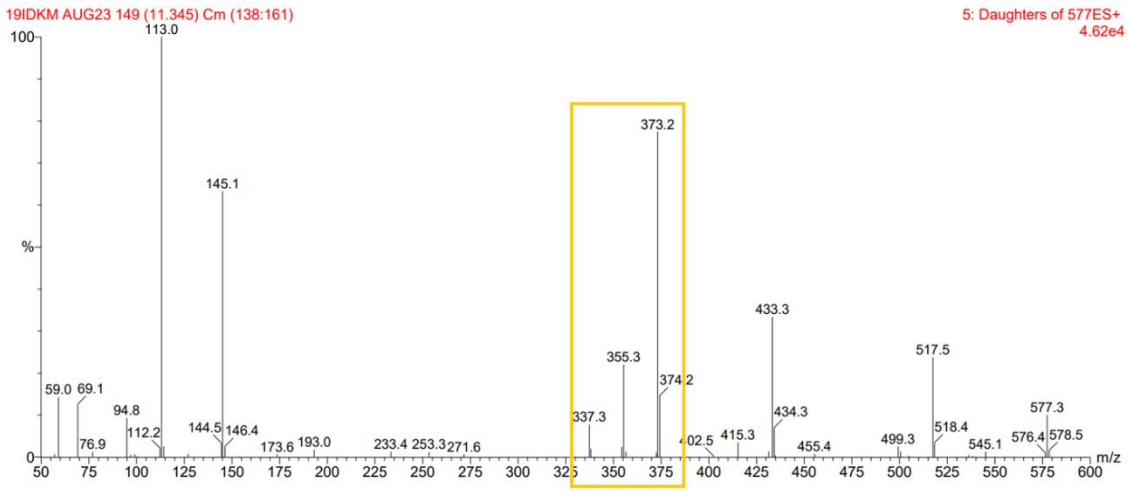

Figure 5. *The LC-MS/MS spectra of Oleandrin.*

From "Structural Analysis of Diastereomeric Cardiac Glycosides and Their Genins Using Ultraperformance Liquid Chromatography-Tandem Mass Spectrometry" by Singh et al. 2021. Journal of the American Society for Mass Spectrometry, *32(5), 1205–1214. Supporting Information list.*

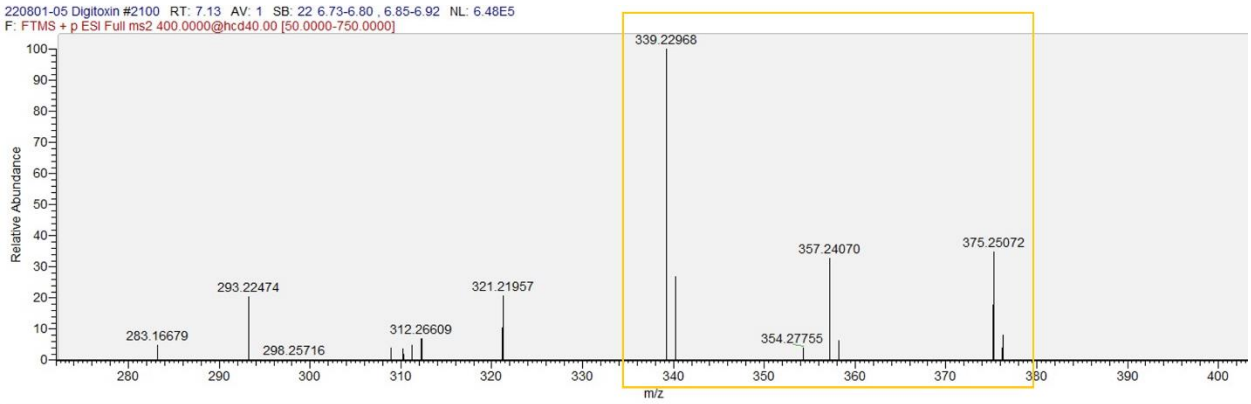

Figure 6. *The LC-MS/MS spectra of Digitoxin.*

Digitoxin standard prepared at 10ug/mL in MeOH and injected at 500ng/mL.

1.6 Research Objective

Currently, liquid chromatography – mass spectrometry is used to screen for CGs. However, this requires the use of standards of specific toxins expected to be encountered for reference, which are often expensive or not readily available. Furthermore, a single plant can contain up to 30 different cardenolides, from milkweeds that can produce more than 20 different cardenolides within a single species to *Digitalis* sp. which are known to produce over 100

different cardenolide forms (Agrawal et al. 2012; Luckner and Witchl 2000: Petschenka et al., 2018). The number of cardenolides in a single plant can make it difficult to know what to specifically target for analysis.. Any slight variation in a compound, be it in functional groups of the sugar or steroid nucleus itself, results in a different cardenolide. For example, the change in stereochemistry of a single hydrogen from a *cis* to *trans* configuration turns digitoxigenin into uzarigenin (Figure 7). With a seemingly infinite number of potential cardenolides, it would not be cost-effective nor practical to employ standards for individual cardenolides, nor to attempt to look for all of them.

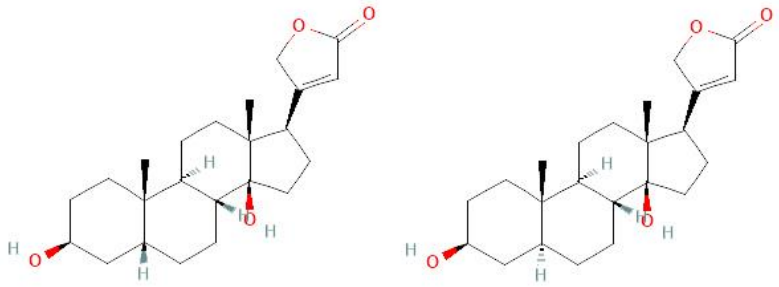

Figure 7. *Digitoxigenin (left) and Uzarigenin (right).*
From PubChem. PubChem Identifier: CID 4369270 URL: https://pubchem.ncbi.nlm.nih.gov/compound/4369270#section=2D-Structure, PubChem Identifier: CID 92760 URL: https://pubchem.ncbi.nlm.nih.gov/compound/92760#section=2D-Structure

The 300 to 400 *m/z* mass spectral region is especially helpful not only due to its striking uniqueness, but because it is the region for identification of genins rather than individual cardenolides. There are fewer genins than cardenolides since a single genin can serve as the foundation for the natural synthesis of many different cardenolides. For example, digitoxin, neriifolin, and cerberin are all derivatives of digitoxigenin and consequently exhibit an ion pattern of 375, 357, 339 (Ravi et al., 2020a). On the other hand, calotropin, calotoxin, and calactin are all derivatives of calotropagenin so they exhibit product ion spectra at ions 387, 369, and 351 (Kanojiya et al., 2012). Consequently, different cardenolides can share the same “trio of

ions" in the 300 to 400 *m/z* region. Therefore, by focusing on select ions in this specific region, many CGs can be accounted for instead of laboring to identify specific CGs.

The purpose of this research was to investigate the potential of identifying a cardenolide-containing plant using the overall cardenolide composition of a plant, represented by the "trio of ions" in the 300 to 400 *m/z* region discussed earlier, rather than individual toxins themselves. This is a possible alternative to relying on costly or unavailable reference standards. In addition, the chromatographic patterns of different plants at these select ions might provide unique "finger prints" to serve as a means of identifying a CC plant.

Moreover, this method could have applications in the diagnosis of cardenolide intoxications in humans and animals. Cardenolide intoxications are often diagnosed based on a corroboration of history of exposure to a CC plant, such as consumption, and consistent clinical signs observed. It could be difficult to make diagnoses and attribute intoxication to a particular plant when exposure to a CC plant is unknown. In these cases, the detection of cardenolides can confirm exposure to a plant. For example, Papi et al. (2012) investigated the death of two individuals found in a pine forest whose stomach contents contained unrecognizable vegetable matter. With no exposure history nor distinct leaves in the stomach for identification, they suspected oleander poisoning due to the plant growing in the surrounding area. The radioimmunoassay they conducted, designed to detect digoxin but cross reacts with oleandrin, resulted positive; this indicated the presence of a CC plant, which was likely oleander. Therefore, a general method for the qualitative identification of a CC plant using cardenolide compositions would be useful, especially in cases where exposure history is not known and vegetable matter in stomach contents cannot be identified visually.

2. Materials and Methods

2.1 Location

Research was conducted at the California Animal Health and Food Safety Laboratory in Davis, California (CAHFS-Davis).

2.2 Reagents

HPLC-grade acetonitrile (ACN), submicron filtered water, methanol (MeOH), and formic acid were purchased from Thermo Fisher Scientific (Fair Lawn, NJ, USA).

2.3 Plants Collected

Fourteen cardenolide-containing plants were sampled in this study (Table 1). Eleven plants were available and collected from the University of California, Davis (UC Davis) main campus, UC Davis Arboretum, UC Davis Botanical Conservatory, UC Davis School of Veterinary Medicine, and the California Animal Health and Food Safety Laboratory, Davis (CAHFS-Davis). The remaining three plants were purchased from online vendors on an e-commerce website. Three non-cardenolide-containing (NCC) plants were also collected (Table 2). Plants were located and identified by the UC Davis Arboretum, UC Davis Botanical Conservatory, and the UC Davis Herbarium , who identified the three purchased plants and NCC plants. Leaves were collected from the plants and air-dried for a minimum of three days, with the exception of *Cerbera odollam,* which were available at CAHFS-Davis as seeds. A minimum of 1 gram of plant material (desiccated) was collected for each plant.

Table 1. *Cardenolide-containing plants collected.*

Family	Subfamily	Species	Common Name(s)	Location collected
Apocynaceae	*Apocynoideae*	*Nerium oleander*	Common Oleander	UC Davis Arboretum
		Adenium boehmianum *Adenium obesum* *Adenium oleifolium* *Adenium socotranum*	Desert Rose	UCD Botanical Conservatory
	-	*Carissa macrocarpa*	-	
	-	*Cerbera odollam*	Pong Pong Nut	CAHFS-Davis
	-	*Thevetia peruviana*	Yellow oleander	Purchased online
	Asclepiadoideae	*Asclepias curassavica* *Asclepias fascicularis* *Asclepias speciosa*	Tropical Milkweed Narrow-leaf Milkweed Showy Milkweed	UC Davis Arboretum
Asparagaceae	*Nolinoideae*	*Convallaria majalis*	Lily of the Valley	Purchased online
	Scilloideae	*Ornithogalum fimbrimarginatum*	Fringe-leafed Star of Bethlehem	UCD Botanical Conservatory
Plantaginaceae	-	*Digitalis purpurea*	Purple Foxglove	Purchased online

Table 2. *Non-Cardenolide-containing plants collected.*

Family	Species	Common Name(s)	Location collected
Taxaceae	*Taxus baccata*	English Yew	UC Davis Main Campus
Rosaceae	*Heteromeles arbitufolia*	Toyon, California Holly	UC Davis Arboretum
	Prunus laurocerasus	Common laurel, cherry laurel	UC Davis School of Veterinary Medicine

2.4 Preparation of Standards

Table 3*. Cardenolide standards used.*

Chemical	Supplier	Details
Cerberin	Toronto Research Chemicals	98% purity
Convallotoxin	Phytolab/The Nature Network	81% purity
Cymarin	-	Existing working stock solution at CAHFS-Davis
Digitoxin	Sigma Aldrich	≥ 92% purity
Digitoxigenin	Sigma Aldrich	97%
Digoxigenin	Fluka	99.7% purity
Digoxin	Fluka	97.7% purity
Gitoxin	-	Existing working stock solution at CAHFS-Davis
17-beta-Nerifolin	Toronto Research Chemicals	96% purity

Cardenolide standards were prepared at a concentration of 1mg/mL in MeOH, with the exception of gitoxin and cymarin, which were already prepared at 1mg/mL in MeOH (Table 3). In a 5mL volumetric flask, 5 mg of each standard was weighed out, filled to volume with MeOH, and vortexed. Each 1 mg/mL standard was diluted to 10 μg/mL in a 10 mL volumetric flask, in which 100 μL of the prepared 1 mg/mL standard solution was dispensed and filled to volume with MeOH. The 10 μg/mL working solutions were transferred to a 12 mL amber vial and refrigerated.

The working solutions were diluted to 500 ng/mL in autosampler vials and injected onto the UHPLC-HRMS. The “trio of ions” observed in the mass spectra, their chromatographic peaks, and retention times were recorded. This phase was to determine the ions specific to cardenolides, such as the “trio of ions” and genins, and their exact masses (*m/z*). EIC templates were made for each “trio of ions” pattern observed. These ions were also grouped by mass and EIC templates were made for the groupings. These templates were later used to aid the identification of unknown samples during the subsequent blind tests.

2.5 Plant Selection

Plants were selected on the basis of whether or not they contained cardenolides according to literature and their availability at the UC Davis main campus. Plants selected were confirmed to contain cardenolides by consulting literature (Table 4). As leaves were sampled for 13 out of the 14 plants collected, studies discussing the cardenolide content in the leaves of plants were prioritized. For *C. odollam,* studies discussing the cardenolide content of the seeds were prioritized instead. The sources included experiment-oriented research, such as direct qualitative and quantitative analysis of cardenolides in plants or the extraction of cardenolides from plants for a broader research purpose.

2.5.1 *Adenium* spp.

There is much confusion of the plants in the *Adenium* genus with regard to species. *A. boehmianum, A. oleifolium,* and *A. socotranum* are often conflated as simply *A. obesum* or considered subspecies of *A. obesum* by some botanists (respectively, GD Rowley 1983; GD Rowley 1980; Lavranos 1996). Thus, literature discussing CGs found in the *Adenium* genus appears to primarily focus on *A. obesum.* However, given their botanical proximity to *A. obesum,* it is hypothesized that *A. boehmianum, A. oleifolium,* and *A. socotranum* likely contain cardenolides as well.

2.5.2 *Carissa macrocarpa*

Literature discussing CGs in the *Carissa* genus focuses on those found in *C. spinarum* rather than *C. macrocarpa* while literature on *C. macrocarpa* appears to focus on the bioactive properties of its phenolic compounds instead. However, given that they are in the same genus, it

is hypothesized that *C. macrocarpa* contains cardenolides as well, although their identification and concentrations are not clear.

2.6.3 *Ornithogalum fimbrimarginatum*

Literature discussing CGs in the *Ornithogalum* genus tends to focus on species like *O. nutans*, *O. umbellatum*, and *O. boucheanum*. Similar to *C. macrocarpa*, given that it is also in the *Ornithogalum* genus, it is hypothesized that *O. fimbrimarginatum* contains cardenolides as well.

2.6.4 *Taxus baccata, Heteromeles arbitufolia, Prunus laurocerasus*

Literature discussing *T. baccata*, *H. arbitufola*, and *P. laurocerasus* was consulted to confirm that they do not contain cardiac glycosides (Table 5).

2.6.5. Attempted Plants

Adonis aestivalis (Summer's Pheasants-Eye) and *Digitalis lanata* (Wooly Foxglove) were originally in the lineup of plants to sample as both are well-known CC plants. *A. aestivalis* contains strophanthidin, helveticoside, and cymarin (Kopp et al. 1992). *D. lanata* contains digoxin, digitoxin, verodoxin, and lanatoside C among at least 13 other cardenolides (Ravi et al. 2020b). At the time of this study, both plants were only available for purchase as seeds online. The seeds proved to be difficult to grow. Due to this and time constraints, both plants were omitted.

Table 4. *Literature on cardenolides in the selected plants.*

Plant	Author(s)	Part of plant	Cardenolides reported
A. boehmianum	Schmelzer et al. 2008	Roots, Stem Latex	Echujin, Digitalinum verum, Somalin, Abobioside
A. obesum	Hoffman et al. 1977	Leaves	Somalin/Honghelоside G, Hongelin, Honghelоside A, 16-acetylstrospeside/Neritaloside
	Arai et al. 2011		Digitoxigenin, Odoroside H, various derivatives of Gitoxigenin, Digitoxigenin, Oleandrigenin
	Azabib et al. 2019		Neriifolin, Cerberin
A. oleifolium	Schmelzer et al. 2008	Leaves	Honghelоside A, Echujin, Somalin, Odorotrioside G
A. curassavica	Warashina et al. 2008	Aerial parts	Uzarigenin, Xysmalogenin, Coroglaucigenin, Calactin, Asclepin, Uscharin, Uscharidin, Calotropin; various derivatives of Asclepin, Calactin, Uscharin, Uzarigenin, and others
	Zhang et al. 2014	Leaves	Calotropagenin, Calotropin, Calactin, Asclepin, Frugoside, Ascleposide, Digitoxigenin, Calactinic acid, and others
A. fascicularis	Duffey and Scudder 1971	Leaves	Three cardenolides detected and measured, but not identified
	Seiber et al. 1982		Cardenolides detected (low amount), but not identified
	Rasmann et al. 2009		Cardenolides detected and measured, but not identified
A. speciosa	Brower et al. 1984	Leaves	Uzarigenin, Syriogenin, other polar cardenolides
	Seiber et al. 1986	Aerial parts	Aspecioside, Syriobioside, Desglucosyrioside, Uzarigenin
*Carissa**	Wangteeraprasert et al. 2012 (*C. spinarum)*	Stems	Evomonoside, Odoroside H
	Kaunda et al. 2020 *(C. edulis/C. spinarum)*	Root/Bark	Carissaedulosides A, B, C, D, E, F
C. odollam	De Vry 1864	Seed	Cerberin
	Laphookhieo et al. 2004	Seed	Cerleaside A, 17α-neriifolin, 17α- neriifolin, Cerberin
	Cheenpracha et al. 2004	Seed	17β-neriifolin, Cerberin, Tanghinin, Deacetyltanghinin, Cerleaside A, 2'-O-acetyl-cerleaside A
C. majalis	Schrutka-Rechtenstamm et al. 1985	Leaves	Convallotoxin, Convalloside, Convallatoxol, various derivatives of Strophanthidin and others
	Kopp and Kubelka 1982		Strophanthidin, Cannogenol, Sarmentogenin; various derivatives of Strophanthidin, Cannogenol, Sarmentogenin
	Higano et al. 2007	Rhizomes	Convallotoxin, Convallatoxol
D. purpurea	Fujii et al. 1989	Leaves	Digitoxin, Gitoxin, Gitaloxin, Strospeside
	Ravi et al. 2020b		Digitoxin, Gitaloxin, Glucogitaloxin, Verodoxin, Purpurea glycoside A, Purpurea glycoside B, Digitoxigenin fucoside
	Kwon et al. 2011		Digitoxin, Gitoxin, Digitonin
*Ornithogalum**	Ghannamy et al. 1987 *(O. boucheanum)*	Leaves, bulbs	Various derivatives of Sarmentogenin, Syriogenin, Uzarigenin, and Digitoxigenin
	Ferth and Kopp 1992 (*O. umbellatum)*	Leaves, bulbs	Convallotoxin, Convalloside, Strophanthidin, Sarmentogenin; various derivatives of Strophanthidin and Sarmentogenin
	Ferth et al. 1992 (*O. nutans*)	Bulbs	Various derivatives of Bipindogenin, Sarmentogenin, Strophanthidin and others
N. oleander	Begum et al. 1999	Leaves	Odoroside H, Neritaloside, Neridiginoside
	Singh et al. 2021		Oleandrin, Digitalin, Oleandrigenin, Odorosides, Neritaloside; various derivatives of Oleandrigenin, Digitoxigenin, Gitoxigenin, Adynerigenin, Δ^{16}adynerigenin, and Δ^{16}anhydrogitoxigenin
T. peruviana	Abe et al. 1994	Leaves	Peruvoside, Thevetin A, Thevetin B, Cannogenin, Uzarigenin, Digitoxigenin; various derivatives of Digitoxigenin, Uzarigenin, Cannogenin
	Miyagawa et al. 2009	Bark	Peruvoside, Neriifolin, Thevefolin
	Tian et al. 2016	Seeds	Thevefolin, Peruvoside monoacetate, Perutosin; various derivatives of Digitoxigenin, Uzarigenin, Cannogenin

Table 5. *Literature on the toxic compounds in* T. baccata, H. arbitufola, and P. laurocerasus.

Plant	Author(s)	Compounds reported
T. baccata	Jacobs et al. 2023	Taxine alkaloids – Taxine A, Taxine B, Taxine I, Taxol A, Taxol B
H. arbitufola	Dement and Mooney 1974	Cyanogenic glycosides, tannins
	Wang et al. 2016	Butalin, Maslinic acid, Betulin, Catechin, etc.
P. laurocerasus	Sendker and Nahrstedt 2009	Cyanogenic glyco/glucosides - Prunasinamide, (2R)-b-D-glucopyranosyloxyacetamide
	Malaspina et al. 2022	Cyaanogenic glycosides - Prunasin, Amygdalin, Sambunigrin

2.6 Preparation of Plant Samples

Dried plant material was extracted in methanol (MeOH). Plant leaves were weighed in a 12 mL polystyrene falcon tube on a xs204 Mettler Toledo balance and the appropriate amount of MeOH was added to reach a concentration of 10 mg/mL. For *C. odollam*, a metal spatula was used to scrape off material from the soft seeds. Two steel ball bearings were added to each tube before they were put into a SPEX Sample Prep Genogrinder 2010 at 750 RPM for 5 minutes for homogenization. Ball bearings were removed using a magnet and the sample was allowed to settle for at least 15 minutes. One milliliter of the liquid extract, void of any sediment, was transferred to an autosampler vial. When necessary, the sample was diluted with MeOH in the autosampler vial. Autosampler vials containing the samples were vortexed before being loaded onto the instrument. Plant extracts were stored in a refrigerator.

2.6.1 Attempted dSPE Cleanup

Dispersive Solid Phase Extraction (dSPE) was considered as a cleanup step for the plant samples. Different dSPE sorbents, such as C18, Primary Secondary Amine (PSA), and Graphitized Carbon Black (GCB) in ACN were first evaluated on *N. oleander*. As the solvent of choice for dSPE is acetonitrile, the effects of extracting plant material in ACN were compared to extracting in MeOH. A 4mg/mL *N. oleander* extract in ACN (N. OL-ACN) and a 4mg/mL *N. oleander* extract in MeOH (N.OL-MEOH) were both prepared in duplicate as described earlier and analyzed on the instrument. The N.OL-ACN ions showed a decreased response compared to the N.OL-MEOH. As *N. oleander* is a plant with high cardenolide content, this dampening effect on abundances was expected to be more dramatic in the responses of plants with a lower cardenolide content than *N. oleander*.

Still, *N. oleander* extraction with various mixes of C18 and PSA in ACN, as well as in MeOH, were attempted (Table 6). In all cases, there were no significant improvements observed in abundances, signal-to-noise ratio, or overall peak shape compared to their N.OL-MeOH counterparts. C18 and PSA were not expected to be the most appropriate sorbents for dSPE, as they are usually used to remove lipids, fatty acids, sugars, and organic acids, which are typically absent in CC plants. GCB, typically used to remove pigments, is more relevant for the CC plant samples. Two-mL centrifuge tubes containing 150mg MgSO4 and 7.5mg GCB were purchased from United Chemical Technologies. Two individual 1.5 mL aliquots of *N. oleander* extracted in ACN and MeOH were transferred to their respective GCB tubes, vortexed, allowed to settle, and run on the instrument. Both versions of the GCB extracts were prepared in duplicate. Again, there were no significant improvements in abundances, signal-to-noise ratio, or overall peak shape observed for both versions of GCB extracts compared to the MeOH only extracts. Thus, MeOH extraction was considered to be as effective as other approaches.

Table 6. *Mixes of C18 and PSA with ACN or MeOH attempted for N.* oleander *extraction.*

C18 (mg)	PSA (mg)	Solvent	Solvent Volume
0	150	ACN	5 mL
150	0		
100	50		
75	75		
50	100		
0	150	MeOH	
150	0		
100	50		
75	75		
50	100		

2.7 Instrumentation

An existing HPLC-HRMS method at CAHFS-Davis for general compound screening was used for this experiment.

2.7.1 Liquid Chromatography

The HPLC system was a Thermo Scientific Dionex UltiMate 3000 with chromatographic separation accomplished in an Agilent EclipsePlus C18 RRHD 1.8um 2.1x100mm column. The flow rate was set at 0.350 mL/minute and an injection volume of 2 µL was used. The mobile phases used were 0.1% formic acid in water (A) and 0.1% formic acid in acetonitrile (B). Below is the gradient chart for the two mobile phases (Table7). The analytical method had a run time of 17 minutes, with divert valve parameters of 0 to 1 minute to waste, 1 to 16 minutes to the instrument, and 16 to 17 minutes to waste.

Table 7. *Solvent ratio for chromatographic separation at given times during the analytical run. Solvent A is 0.1% formic acid in water and Solvent B is 0.1% formic acid in acetonitrile.*

Time (minutes)	A%	B%
0	99	1
1.50	99	1
9.50	2	98
13.5	2	98
13.6	99	1
17.4	99	1
17.5	99	1
18.0	99	1

2.7.2 Mass Spectrometry

A Thermo Scientific Q-Exactive Orbitrap Mass Spectrometer was used for mass spectrometry analysis. Two non-targeted experiments were implemented, a Full MS scan and All Ion Fragmentation (AIF), a pseudo-MS/MS analysis, which occurred simultaneously with a runtime of 0 to 14 minutes. The scan range for Full MS was from 75 *m/z* to 1125 *m/z*. The scan

range of AIF was from 50 *m/z* to 750 *m/z* and involved stepped normalized collision (higher-energy collision dissociation, i.e. HCD) energy (NCE) at 35% and 45%. Heated electron spray ionization (HESI) was set to positive mode ($[M+H]^+$). HESI sheath gas was set at 45 arb. units, auxiliary gas at 15 arb. units heated at 280 C, sweep gas flow rate at 1 arb. units, spray voltage at 3.50 kV, capillary temperature at 320 C, and S-lens RF level at 100 arb. units.

2.8 Data Analysis

Positive ion chromatograms and mass spectral data were evaluated qualitatively on Thermo Xcalibur Qual Browser Software Version 3.1. From the standards, ions found in Full MS^2 were observed with a mass tolerance of 10 ppm while ions found in Full MS were observed with a mass tolerance of 5ppm. Templates showing the Extracted Ion Chromatograms (EIC) at the ions that appear in the "trio of ions" patterns in Full MS were created and applied to each plant sample analyzed during validation. The cardenolide fragmentation patterns were confirmed and the retention times (RTs) and presence of the chromatographic peaks characteristic to those ions were recorded. These ions were later grouped into "high," "medium," "low," and "genin" and EIC templates were made for these groupings. These particular EICs were used in the subsequent Blind Tests to identify unknown samples to compare the performance of ions (high, medium, low, or genins) in discerning between CC and NCC plants and the identification of specific CC plants.

2.9 Validation

Optimal concentrations, defined as the milligrams of plant material in milliliters of MeOH, were determined for each plant (Table 8). This refers to the weight of plant material in a volume of MeOH (mg/mL), not to the concentration of any particular cardenolide. However, it

does represent the amount of cardenolides present in a sample, as they are positively correlated. The goal was to obtain chromatographic peaks, using HPLC-HRMS, with abundances greater than or equal to E5 and signal-to-noise ratios of at least 3 for the ions of interest. This required preparing plant homogenates at varying concentrations and analyzing them across multiple runs. Plants were prepared in duplicate per run. Once an optimal concentration was found for each plant, a minimum of six replicates of each plant at that amount were analyzed to confirm the consistency of retention times and chromatographic peak shapes. Optimal concentrations, characteristic peaks, and their retention times found at this stage were used for the preparation and analysis of the unknown samples for the subsequent blind tests.

Table 8. *Validation of Plant Samples Runs and Optimal Concentrations Found.*

Plant	Concentrations attempted (mg/mL)	# replicates per concentration	# of runs/analyses per concentration	Acceptable Concentrations (mg/mL)	Optimal Concentration (mg/mL)
A. boehmianum	4	2	2	6-7	7
	6	2	2		
	7	4	10		
A. obesum	4	2	4	6-7	7
	6	2	2		
	7	4	6		
A. oleifolium	4	2	2	6 - 7	7
	6	2	2		
	7	2	4		
A. socotranum	4	6	6	4	4
A. curassavica	6	2	2	8	8
	8	6	6		
A. fascicularis	6	2	2	10	10
	8	4	4		
	10	6	6		
	12	2	2		
A. speciosa	6	2	2	10	10
	8	4	4		
	10	6	6		
	12	2	2		
C. macrocarpa	4	2	2	9	9
	5	2	2		
	6	2	2		
	7	2	2		
	8	2	2		
	9	8	14		
	10	2	2		
C. odollam	4	6	6	4	4
C. majalis	4	2	2	8-9	9
	5	2	2		
	6	2	2		
	9	8	12		
	10	2	2		
D. purpurea	2	2	2	8-9	9
	4	2	2		
	6	2	2		
	7	2	2		
	8	3	3		
	9	7	7		
N. oleander	1	2	2	4 - 6	6
	2	2	2		
	4	4	4		
	5	2	2		
	6	2	2		
O. fimbrimarginatum	4	2	2	9	9
	5	2	2		
	6	2	2		
	7	2	2		
	8	2	2		
	9	6	6		
	10	2	2		
T. peruviana	2	2	2	8-9	9
	4	4	4		
	5	2	2		
	6	2	2		
	7	2	2		
	8	2	2		
	9	6	6		

2.10 Blind Tests

Blind tests were performed to assess the ability of the method to 1) correctly determine whether or not a plant contained cardenolides and 2) to correctly identify the genus and species of a cardenolide-containing plant.

2.10.1 Blind Test 1 – Identification of Cardenolide-containing Plants

The first blind test assessed the ability of the method to discern between cardenolide-containing (CC) plants and non-cardenolide-containing (NCC) plants. The CC plants used in this were *N. oleander* and *T. peruviana*, while the NCC plants used were *H. arbitufola* and *P. laurocerasus*. Samples in this blind test were split evenly between CC and NCC plants. CC plants were distributed equally between *N. oleander* and *T. peruviana* while the non-CC plants were distributed evenly between *H. arbitufola* and *P. laurocerasus*. The unknown samples for this blind test were prepared the same way as samples were for validation, at their respective optimal concentrations. The subsequent vials were randomly shuffled before being put onto the instrument for analysis.

Templates showing the EICs at each ion grouping were applied to the unknown sample data. The presence of at least three defined peaks would be considered as a CC plant and the absence of any defined peaks was considered a non-CC plant.

2.10.2 Blind Test 2 – Individual Plant Classifications

The second blind test assessed the ability of the method to correctly identify the genus and species of a CC plant, and thus only included the plants containing cardenolides: *A. boehmianum, A. obesum, A. oleifolium, A. socotranum, A. curassavica, A. fascicularis, A. speciosa, C. macrocarpa, C. odollam, C. majalis, D. purpurea, N. oleander, O.*

fimbrimarginatum, and *T. peruviana*. The unknown samples were prepared the same way as samples were prepared during validation, at their respective optimal concentrations. Eight replicates were made of each plant, resulting in a total of 112 samples. However, only 105 of the samples were randomly chosen for analysis so that the individual performing the identifications did not have prior knowledge about the distribution of species in the unknown samples. This ensured that the identification of the unknown sample was based solely on the EICs, rather than experiment logistics. The analyst performed the identification using the next group of ions three days apart and by randomizing the order of the unknowns so they are identified in a different order. Moreover, characteristic peaks were noted for each unknown which is required to be considered sufficient for identification

As in Blind Test 1, templates showing the EICs at each ion grouping were applied to the unknown sample data. Identifications were performed by comparing the unknown sample chromatograms with the exemplary validation chromatograms at the ions of interest. A minimum of five observable peaks must be present for identification.

2.10.3 Blind Test Statistics

The variables measured in the blind test were categorical, where the assigned labels were compared to the "true" label of a sample. In Blind Test 1, the unknown samples were assigned as positive for "cardenolide-containing" or negative for "non-cardenolide-containing", and this was compared to the "true" label of whether or not the unknown sample was in fact a CC plant. In Blind Test 2, the proposed identity of an unknown sample, based on the chromatographic patterns observed in the EICs of selected ions, was compared to the true identity of that plant sample. Thus, categorical data analysis was conducted. Due to the qualitative nature of the

experiment, the measure of agreement was assessed, where a binomial test of the proportion of success was found for each blind test.

2.10.3.1 Overall Test

An Overall Test was conducted to determine if all classifications have the same "random guessing" proportion. This determined if the proposed identification was successful due to the information from the chromatographic patterns at the select ions, rather than mere guessing. The null hypothesis would be that the classifications are no better than what is expected due to chance, where:

$$H_0: The\ probability\ of\ correct\ classifications\ is\ no\ better\ than\ p = \frac{1}{\#\ of\ categories}$$

The alternative hypothesis would be that the classifications are better than what is expected due to chance, where:

$$H_a > \frac{1}{\#\ of\ categories}$$

For Blind Test 1, there are only two categories; the unknown sample *is* a CC plant, or it *is not* a CC plant. Therefore, the null and alternative hypotheses are:

$$H_0:\ p = \frac{1}{2}\ \ vs\ \ H_a:\ p > \frac{1}{2}$$

For Blind Test 2, the categories are the possible identifications of an unknown sample. The identity of an unknown sample may be any one of the fourteen plants sampled, resulting in fourteen categories. Therefore, the null and alternative hypotheses are:

$$H_0:\ p = \frac{1}{14}\ \ vs\ \ H_a:\ p > \frac{1}{14}$$

2.10.3.2 Individual Test

An individual test was conducted on each category, CC or NCC for Blind Test 1 and the individual species for Blind Test 2, to determine which was performing well. This shares the same null and alternative hypotheses as in the Overall Test. However, the probability compared to the null hypothesis would be the probability of a correctly identified sample per each individual category.

For Blind Test 1, this compared the probability of correctly determining a CC plant sample to the null hypothesis, and the probability of correctly determining a non-CC plant sample to the null hypothesis.

$$H_0: p = \frac{1}{2} \; vs \; H_a: \; p > \frac{1}{2}, where \; p = \frac{\#\; samples \; correctly \; determined \; as \; CC \; plant \; samples}{\#\; of \text{ "true" CC plant samples}}$$

$$H_0: p = \frac{1}{2} \; vs \; H_a: \; p > \frac{1}{2}, where \; p = \frac{\#\; samples \; correctly \; determined \; as \; non \; CC \; plant \; samples}{\#\; of \text{ "true" } non \; CC \; plant \; samples}$$

For Blind Test 2, this assessed how many proposed identifications matched the true identification for each unknown sample. In other words, the probability of correctly identifying a plant for each unknown sample will be compared to the null hypothesis of $H_0 = \frac{1}{14}$. For example, suppose there were 24 unknown samples whose true identification is *A. boehmianum*, and the proposed identification for 20 of these samples was *A. boehmianum* while the remaining 4 were identified incorrectly. The 20/24 are compared to the null hypothesis of 1/14, and the null hypothesis can be rejected ($\frac{20}{24} > \frac{1}{14}; H_a > \frac{1}{14}$). This was repeated for the other 13 plants.

2.10.3.3 Data Presentation

The results of the blind tests are presented in a contingency table that compares the proposed identifications of the unknown samples to their actual identifications.

Figure 8*. Example Contingency Table #1.*

	Plant 1	Plant 2	Plant 3	Plant 4	Total
Plant 1	4	0	0	0	4
Plant 2	0	6	0	0	6
Plant 3	0	0	5	0	5
Plant 4	0	0	0	5	5
Total	4	6	5	5	20

Overall Test	
$p = \frac{20}{20} = 1.0,\ H_a > \frac{1}{4}$	
Individual Test	
Plant 1	$p = \frac{4}{4} = 1.0,\ H_a > \frac{1}{4}$
Plant 2	$p = \frac{6}{6} = 1.0,\ H_a > \frac{1}{4}$
Plant 3	$p = \frac{5}{5} = 1.0,\ H_a > \frac{1}{4}$
Plant 4	$p = \frac{5}{5} = 1.0,\ H_a > \frac{1}{4}$

In this scenario, all of the unknown samples were correctly identified; all proposed identifications matched the true identifications of the samples.

Figure 9. *Example Contingency Table #2.*

	Plant 1	Plant 2	Plant 3	Plant 4	Total
Plant 1	4	2	0	0	6
Plant 2	0	4	0	0	4
Plant 3	0	0	4	0	4
Plant 4	0	0	1	5	6
Total	4	6	5	5	20

Overall Test	
$p = \frac{17}{20} = 1.0,\ H_a > \frac{1}{4}$	
Individual Test	
Plant 1	$p = \frac{4}{4} = 1.0,\ H_a > \frac{1}{4}$
Plant 2	$p = \frac{4}{6} = 0.67,\ H_a > \frac{1}{4}$
Plant 3	$p = \frac{4}{5} = 0.80,\ H_a > \frac{1}{4}$
Plant 4	$p = \frac{5}{5} = 1.0,\ H_a > \frac{1}{4}$

In this scenario, all of the Plant 1 and Plant 4 unknown samples were correctly identified as Plant 1 and 4. In other words, all proposed identifications of the Plant 1 and Plant 4 unknown samples matched their true identifications. Two of the Plant 2 samples were incorrectly identified as Plant 1 and one of the Plant 3 samples was incorrectly identified as Plant 4.

2.10.4 Blind Test Sample Size Calculation

A minimum sample size for both blind tests was determined using the following code inputted into SAS (Statistical Analysis System):

```
proc power;
onesamplefreq
power=0.95
ntotal=.
nullp=0.0625
proportion=.25
test=adjz
method=normal; * uses a normal approximation;
run;
```

A null hypothesis value of 1/14 was used for "nullp" and a power of "0.95" was used. The value for "proportion" refers to the "true value" of the alternative hypothesis (H_a). To find a suitable value for H_a, smaller scale versions of Blind Tests 1 and 2 were conducted, named "Pre-Blind Test 1" and "Pre-Blind Test 2", respectively. The probability found from the Overall Test in these smaller scale blind tests were averaged and used as the "proportion" value to determine a suitable sample size for the larger-scale blind tests.

2.10.4.1 Pre- Blind Test 1

The two cardenolide-containing plants used were *N. oleander* and *T. peruviana* while the two non-cardenolide-containing plants used were *H. arbitufola* and *T. baccata. C. odollam* and *P. laurocerasus* served as positive and negative controls, respectively and were prepared at 10 mg/mL. *N. oleander* and *T. peruviana* were prepared at their optimal concentrations found during validation. The resulting probabilities from the "Overall Test" were averaged and used as the "proportion" value (H_a) in the SAS formula discussed above to solve for sample size.

2.10.4.1.1 Using “High” Ion Grouping

	Cardenolide-containing (True)	Non-cardenolide-containing (True)
Cardenolide-containing (Proposed)	16	0
Non-cardenolide-containing (Proposed)	0	16

Overall Test: $\frac{32}{32} = 1.00$

2.10.4.1.2 Using “Medium” Ion Grouping

	Cardenolide-containing (True)	Non-cardenolide-containing (True)
Cardenolide-containing (Proposed)	16	0
Non-cardenolide-containing (Proposed)	0	16

Overall Test: $\frac{32}{32} = 1.00$

2.10.4.1.3 Using “Low” Ion Grouping

	Cardenolide-containing (True)	Non-cardenolide-containing (True)
Cardenolide-containing (Proposed)	16	0
Non-cardenolide-containing (Proposed)	0	16

Overall Test: $\frac{32}{32} = 1.00$

2.10.4.1.4 Using “Genin” Ion Grouping

	Cardenolide-containing (True)	Non-cardenolide-containing (True)
Cardenolide-containing (Proposed)	16	0
Non-cardenolide-containing (Proposed)	0	16

Overall Test: $\frac{32}{32} = 1.00$

2.10.4.2 Sample Size for Blind Test 1

H_a probability determined from Pre-Blind Test 1:

$$\frac{Overall_{High\ Ions} + Overall_{Medium\ Ions} + Overall_{Low\ Ions} + Overall_{Genin\ Ions}}{4} = 1.00$$

Sample Size Calculation:

```
proc power;
onesamplefreq
power=0.95
ntotal=.
nullp=0.50
proportion=0.99
test=adjz
method=normal
run;
```

The POWER Procedure
Z Test for Binomial Proportion with Continuity Adjustment

Fixed Scenario Elements	
Method	Normal approximation
Null Proportion	0.5
Binomial Proportion	0.99
Nominal Power	0.95
Variance Estimate	Null Variance
Number of Sides	2
Alpha	0.05
Computed N Total	
Actual Power	N Total
0.989	8

2.10.4.3 Pre-Blind Test 2

A total of 18 unknown samples were prepared, where each plant was represented at least once and *N. oleander*, *A. boehmianum*, *O. fimbrimarginatum*, and *A. fascicularis* were represented twice. One sample of *N. oleander* and *H. arbitufola* each served as positive and negative controls, respectively. All samples were prepared as they were during validation at their optimal concentrations. The resulting probabilities from the Overall Test were averaged and input as the "proportion" value in the SAS formula discussed above to solve for sample size.

2.10.4.3.1 Using “High” Ion Grouping

		True ID														
		A. boe	A. obe	A. ole	A. soc	A. cur	A. fas	A. spe	C. mac	C. odo	C. maj	D. pur	N. ole	O. fim	T. per	Proposed Total
Proposed ID	A. boe	2														
	A. obe		2													
	A. ole			1												
	A. soc				1											
	A. cur					1										
	A. fas						2									
	A. spe							2								
	C. mac								1					1		
	C. odo									0						
	C. maj										1					
	D. pur											1				
	N. ole												1			
	O. fim													1		
	T. per														1	
	True Total															18

$$Overall\text{: } \frac{17}{18} = 0.944$$

2.10.4.3.2 Using “Medium” Ion Grouping

		True ID														
		A. boe	A. obe	A. ole	A. soc	A. cur	A. fas	A. spe	C. mac	C. odo	C. maj	D. pur	N. ole	O. fim	T. per	Proposed Total
Proposed ID	A. boe	2														
	A. obe		2													
	A. ole			1												
	A. soc				1											
	A. cur					1										
	A. fas						2									
	A. spe							2								
	C. mac								1							
	C. odo									0						
	C. maj										1					
	D. pur											1				
	N. ole												1			
	O. fim													2		
	T. per														1	
	True Total															18

$$Overall\text{: } \frac{18}{18} = 1.00$$

2.10.4.3.3 Using “Low” Ion Grouping

		True ID														
		A. boe	A. obe	A. ole	A. soc	A. cur	A. fas	A. spe	C. mac	C. odo	C. maj	D. pur	N. ole	O. fim	T. per	Proposed Total
Proposed ID	A. boe	2														
	A. obe		2													
	A. ole			1												
	A. soc				1											
	A. cur					1										
	A. fas						1									
	A. spe							2								
	C. mac						1		1							
	C. odo									0						
	C. maj										1					
	D. pur											1				
	N. ole												1			
	O. fim													2		
	T. per														1	
	True Total															18

$$Overall\text{: } \frac{17}{18} = 0.944$$

2.10.4.3.4 Using “Genin” Ion Grouping

		True ID														
		A. boe	A. obe	A. ole	A. soc	A. cur	A. fas	A. spe	C. mac	C. odo	C. maj	D. pur	N. ole	O. fim	T. per	Proposed Total
Proposed ID	A. boe	2														
	A. obe		2													
	A. ole			1												
	A. soc				1											
	A. cur					1										
	A. fas						2									
	A. spe							2								
	C. mac								1							
	C. odo									0						
	C. maj										1					
	D. pur											1				
	N. ole												1			
	O. fim													2		
	T. per														1	
	True Total															18

$$Overall\text{: } \frac{18}{18} = 1.00$$

2.10.4.4 Sample Size for Blind Test 2

H_a probability determined from Pre-Blind Test 2:

$$\frac{Overall_{High\ Ions} + Overall_{Medium\ Ions} + Overall_{Low\ Ions} + Overall_{Genin\ Ions}}{4} = 0.972$$

Sample Size Calculations:

```
proc power;
onesamplefreq
power=0.95
ntotal=.
nullp=0.07143
proportion=0.972
test=adjz
method=normal
run;
```

The POWER Procedure
Z Test for Binomial Proportion with Continuity Adjustment

Fixed Scenario Elements	
Method	Normal approximation
Null Proportion	0.07143
Binomial Proportion	0.972
Nominal Power	0.95
Variance Estimate	Null Variance
Number of Sides	2
Alpha	0.05
Computed N Total	
Actual Power	N Total
0.994	2

2.10.4.5 Sample Sizes Used

In each smaller-scale blind test, the success probability was extremely high. Thus, the sample sizes determined on SAS were incredibly low. However, to be conservative and for redundancy, the actual sample sizes used for each blind test were much larger than needed according to the calculations. Blind Test 1 had a total sample size of 32 samples, which is the same number of samples as used in the Pre-Blind Test 1, whereas Blind Test 2 had a total sample size of 105 samples.

3. Results

3.1 Standards

Ions of interest and their exact masses (*m/z*) were determined from HPLC-HRMS analysis of the standards. The characteristic product ions discussed earlier, which exhibit a successive loss of 18 *m/z*, were observed in the standards. The exact masses of these ions were then recorded (Table 9). Ions corresponding to cardenolide genins were also observed and recorded from the analyzed standards and from the literature. The ions were then grouped by mass into "high," "medium", "low", and "genin" (Table 10). These groupings were then used to identify the unknown samples in the blind tests.

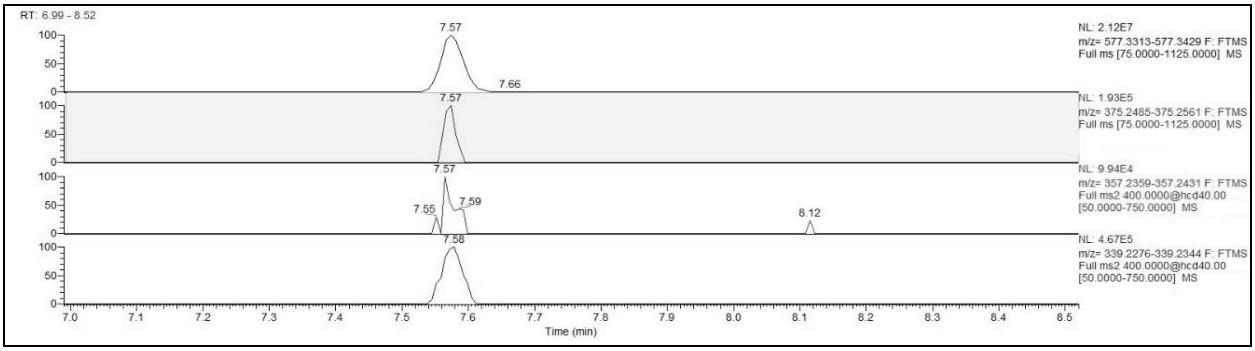

Figure 10. *Ions observed in Cerberin Standard.*

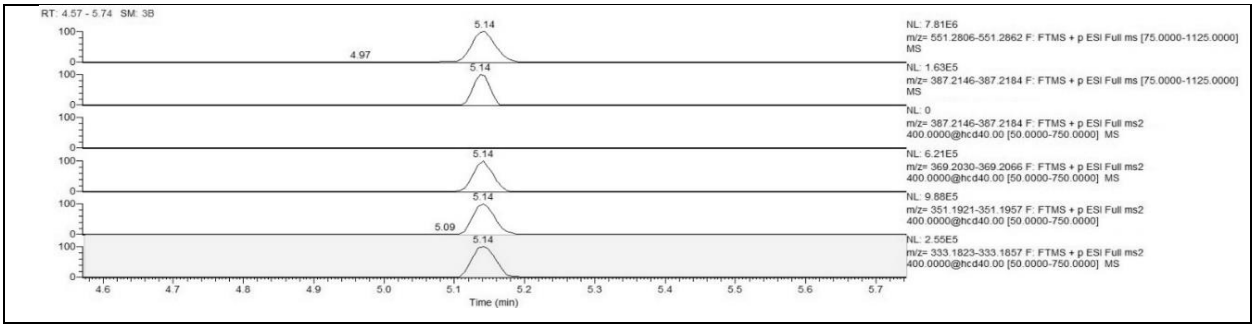

Figure 11. *Ions observed in Convallotoxin Standard.*

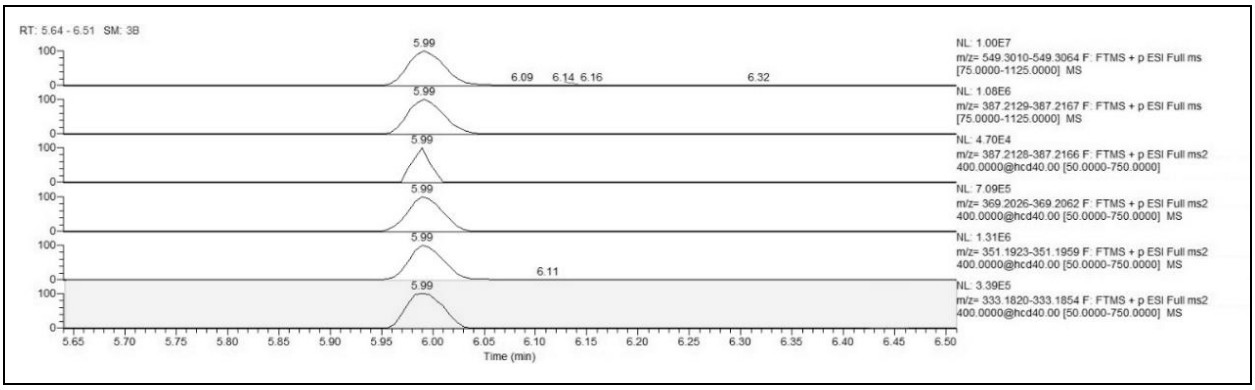

Figure 12. *Ions observed in Cymarin Standard.*

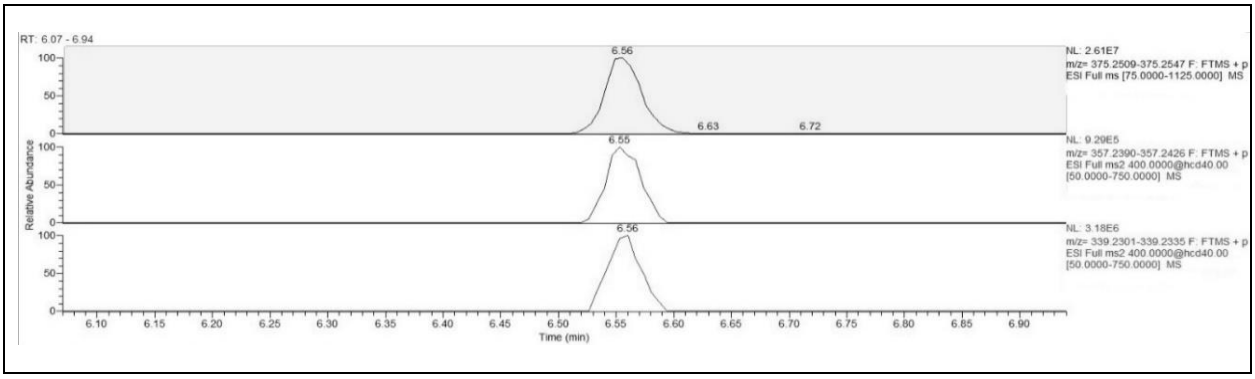

Figure 13. *Ions observed in Digitoxigenin Standard.*

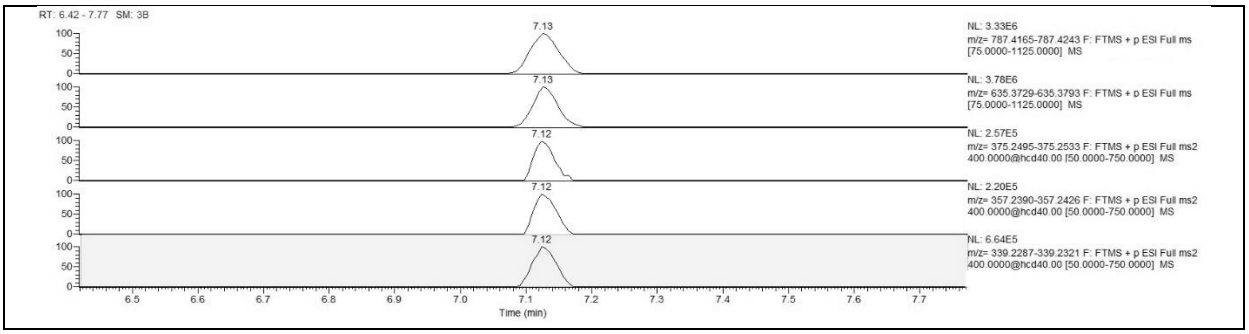

Figure 14. *Ions observed in Digitoxin Standard.*

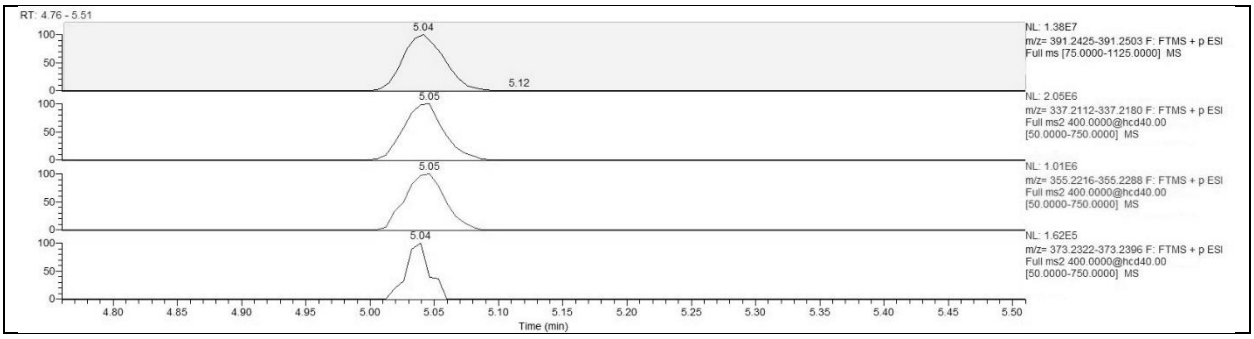

Figure 15. *Ions observed in Digoxigenin Standard.*

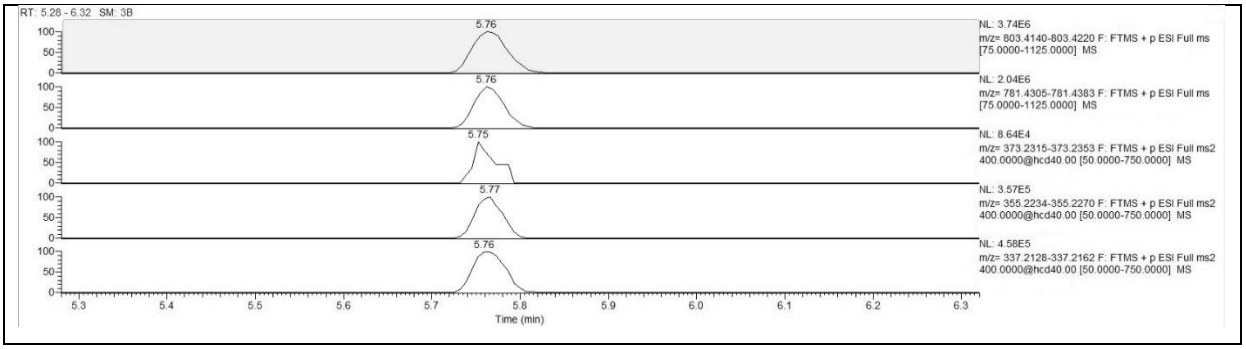

Figure 16. *Ions observed in Digoxin Standard.*

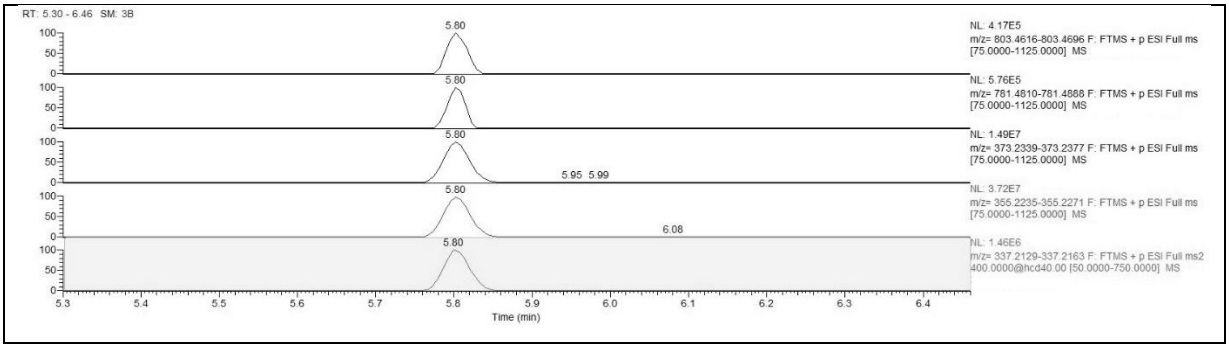

Figure 17. *Ions observed in Gitoxin Standard.*

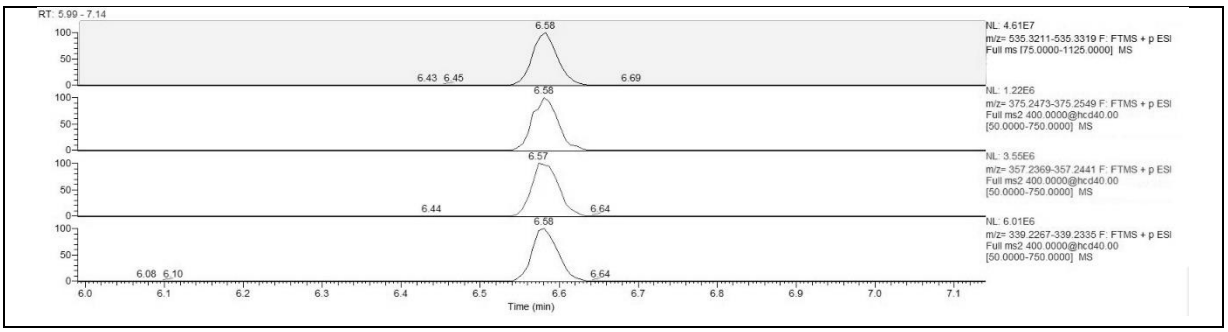

Figure 18. *Ions observed in Neriifolin Standard.*

***Table 9**. Summary of Ions of Interest found from standards and literature.*

Nominal *m/z*	**Observed (measured) *m/z***	**Delta ppm***	**Calculated *m/z***	**Elem. Comp. $[M+H]^+$**	**Mass Range for EICs in the present study**	**Examples of cardenolides that exhibit designated ions**
433	433.2577	-1.846	433.2585	$C_{25}H_{36}O_6$	433.2553 – 433.2597	Oleandrigenin (Singh et al. 2021)
405	405.2302	2.52 (mmu)	405.2272	$C_{23}H_{33}O_6$	405.2244 – 405.2284	Strophanthidin, Calotropagenin (Kanojiya et al. 2012)
405	405.2250	-4.109				Convallotoxin, Cymarin
391	391.2464	-3.912	391.2479	$C_{23}H_{35}O_5$	391.2441 – 391.2481	Digoxigenin/Digoxin
375	375.2512	-3.720	375.2530	$C_{23}H_{35}O_4$	375.2503 – 375.2541	Digitoxigenin/Digitoxin, Cerberin, Neriifolin
375	375.2507	-6.039		$C_{23}H_{35}O_4$	375.2508 – 375.2546	
357	357.2407	-4.819	357.2424	$C_{23}H_{33}O_3$	357.2407 – 357.2443	
339	339.2304	4.353	339.2319	$C_{23}H_{31}O_2$	339.2301 – 339.2335	
373	373.2359	-3.928	373.2373	$C_{23}H_{33}O_4$	373.2351 – 373.2389	Digoxigenin/Digoxin, Gitoxin, Oleandrin/Oleandrigenin, (Singh et al. 2021)
355	355.2252	-4.367	355.2268	$C_{23}H_{31}O_3$	355.2250 – 335.2286	
337	337.2146	-4.676	337.2162	$C_{23}H_{29}O_2$	337.2144 – 337.2178	
369	369.2052	-2.508	369.2060	$C_{23}H_{29}O_4$	369.2042 – 369.2078	Convallotoxin, Cymarin
351	351.1941	-3.933	351.1955	$C_{23}H_{27}O_3$	351.1936 – 351.1972	
333	333.1837	-3.711	333.1849	$C_{23}H_{25}O_2$	333.1826 – 333.1860	
371	371.2207	-2.693	371.2217	$C_{23}H_{31}O_4$	371.2198 – 371.2236	Δ^{16}Adynerigenin (Singh et al. 2021)
353	353.4	-	353.2111	$C_{23}H_{29}O_3$	353.2093 – 353.2129	
335	335.2	-	335.2006	$C_{23}H_{27}O_2$	335.1983 – 335.2017	

*Difference between observed mass and the calculated mass in ppm units for the elemental composition formula.

***Table 10.** Ion Groupings used for Blind Tests. Grouped by mass.*

Grouping	***m/z* range**	***m/z* (nominal)**
"High"	369 – 375	375 373 371 369
"Medium"	351 – 357	357 355 353 351
"Low"	333 – 339	339 337 335 333
"Genins"	375 – 433	433 405 391 375

3.2 Exemplary Extracted Ion Chromatograms of Each Plant

Below are exemplary Extracted Ion Chromatograms (EICs) at the select ions for each plant sampled. Included are notable peaks characteristic to a particular plant and the retention times at which they occur. This was determined from observations made at the select ions from the six replicates analyzed for each plant. While the retention times of the peaks remained consistent, the peak intensities varied among different samples of the same plant. Still, there were peaks whose intensities maintained a constant ratio over other peaks in the same chromatogram. Exceptional peaks like these are indicated in bold font.

3.2.1 *Adenium boehmianum*

Ions 369, 351, 333 *m/z*

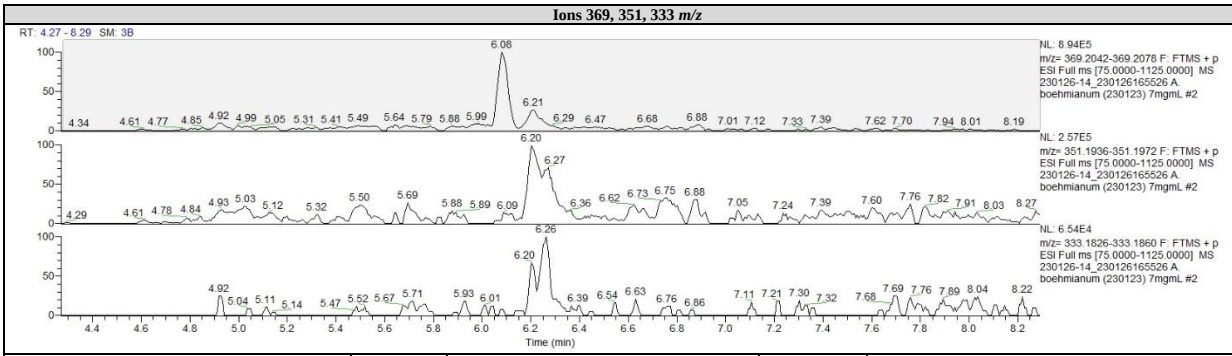

General Observations	RT	Observed Peaks	RT	Observed Peaks
Adequate abundances (> E5) for ions 369 and 351, where the abundance for ion 333 is typically the lowest. Chromatographic peak shapes may appear jagged.	4.91 – 4.93	Peak present for all ions.	**6.19 – 6.21**	**Major peak for all ions.**
	5.48 – 5.50, 5.68 – 5.70	Minor peaks present in ion 351.	**6.25 – 6.27**	**Major peak in ion 333. May appear as major peak in ion 351.**
	6.08 – 6.10	**Major peak in ion 369.**	6.60 – 6.62, 6.73 – 6.75	Peaks most prominent in ion 351, 333.

Ions 371, 353, 335 *m/z*

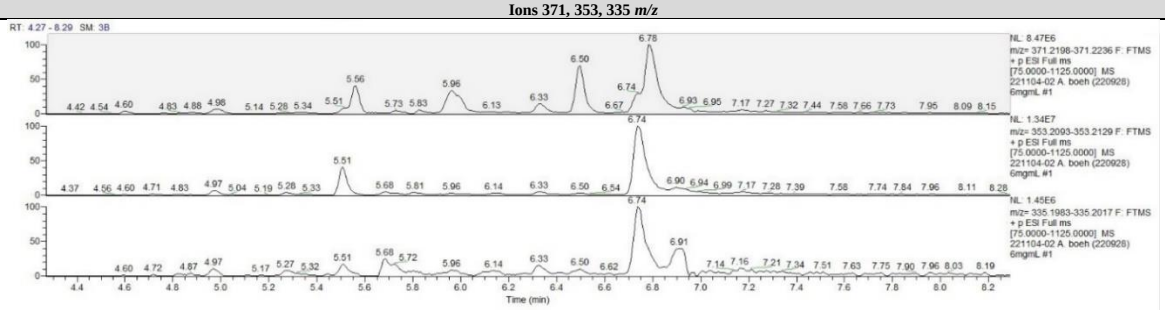

General Observations	RT	Observed Peaks	RT	Observed Peaks
Clean EICs, with very low baseline and little to no noise for ions 371, 353. Noisier spectrum for ion 335. Strong abundances (≥E6) for all ions. Good peak shape.	5.50 – 5.52	Present in all ions. Most prominent in ions 353, 335.	6.49 – 6.51	Present in all ions. Most prominent in ion 371.
	5.55 – 5.57	Present in all ions. Most prominent in ion 371.	**6.73 – 6.75**	**Major peak in all ions. May appear unresolved from 6.78 – 6.80 peak in ion 371.**
	5.95 – 5.97, 6.32 – 6.34	Present in all ions. Most prominent in ion 371.	6.90 – 6.92	Present in all ions. Most prominent in ion 335. May appear unresolved from 6.73 3- 6.75 peak in ion 335.

Ions 373, 355, 337 *m/z*

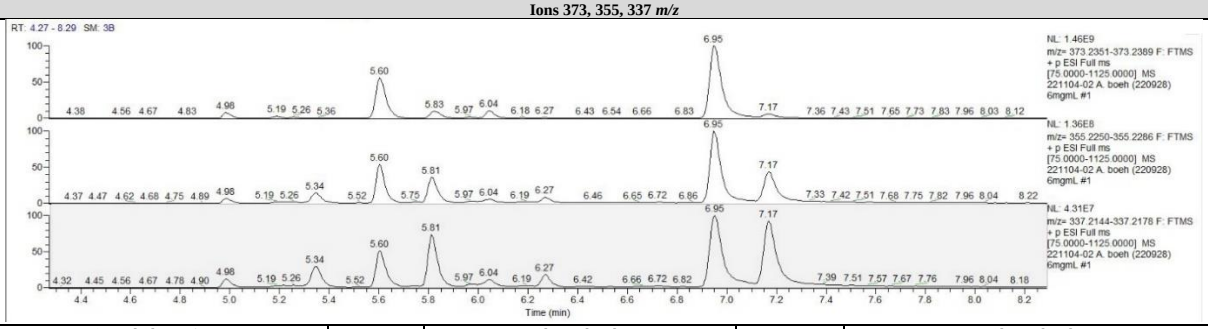

General Observations	RT	Observed Peaks	RT	Observed Peaks
Clean EICs with very low baseline and little to no noise across all ions. Strong abundances (≥E6) for all ions. Smooth peak shapes.	5.33 – 5.35	Small peak most prominent in ions 355, 337	6.26 – 6.28	Small peak most prominent in ions 355, 337
	5.59 – 5.61	Medium peak in all ions	**6.94 – 6.96**	**Major peak in all ions**
	5.80 – 5.82	**Major peak in ions 355, 337**	**7.16 – 7.18**	**Major peak in all ions. Most prominent in ions 355, 337.**

Ions 375, 357, 339 *m/z*

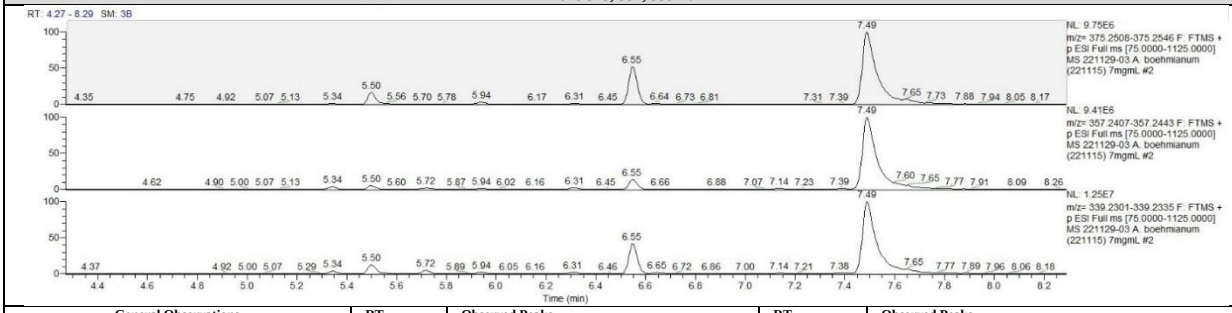

General Observations	RT	Observed Peaks	RT	Observed Peaks
Very clean EICs with very low baseline and little to no noise across all ions. Strong abundances (≥E6) for all ions. Smooth peak shapes for all ions. Very consistent chromatograms across replicates.	5.31 – 5.33	Small peak most prominent in ions 357, 339.	**6.54 – 6.55**	**Major peak in all ions.**
	5.49 – 5.50	Peak present in all ions.	**7.48 – 7.50**	**Major peak in all ions.**

Ions 433, 405, 391, 389, 375 *m/z* (genins)

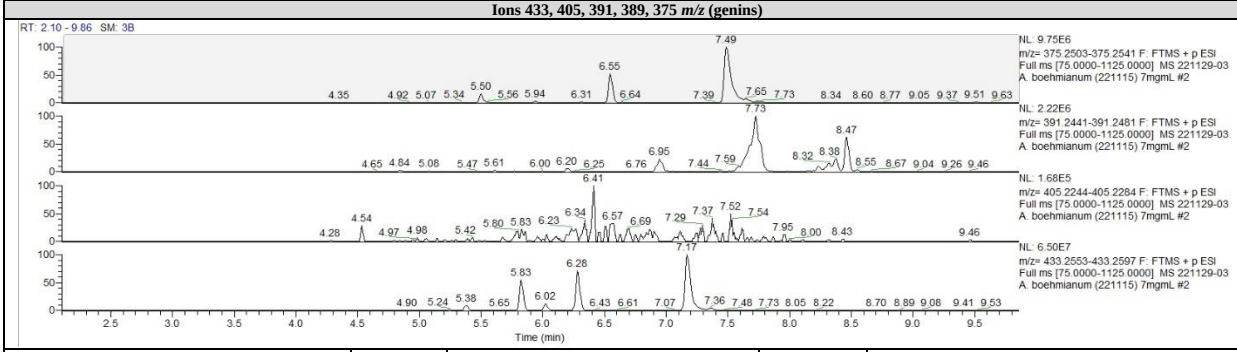

General Observations	RT	Observed Peaks	RT	Observed Peaks
Strong abundances (≥E6) for all ions. Most distinct peaks appear at ions 375 and 433. Noisy EIC for ion 405, without distinct peaks, concentrated around 5.80 to 7.50.	5.82 – 5.84	Present in ion 433	**7.16 – 7.18**	**Major peak in ion 433**
	6.27 – 6.29	Present in ion 433	**7.48 – 7.50**	**Major peak in ion 375**
	6.54 – 6.56	Present in ion 375	**7.72 – 7.74**	**Major peak in ion 391**
	6.94 – 6.96	Present in ion 391	8.46 – 8.48	Present in ion 391

3.2.2 *Adenium obesum*

Ions 369, 351, 333 *m/z*

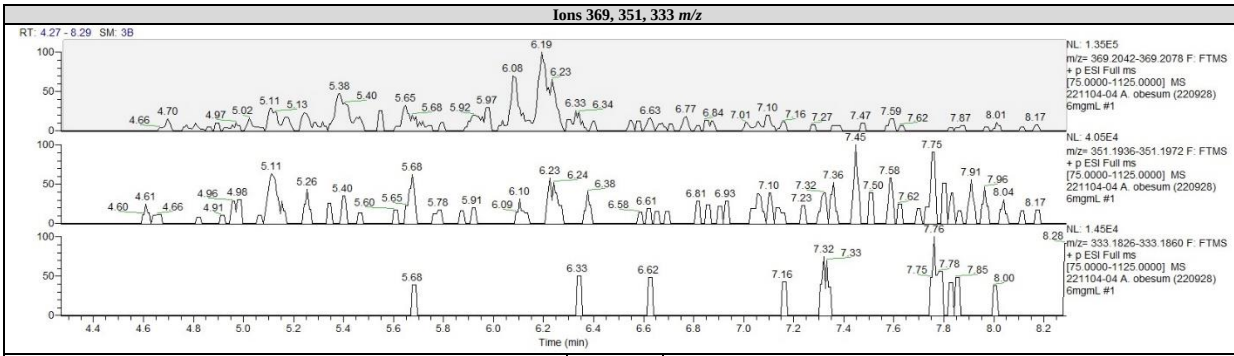

General Observations	RT	Observed Peaks
Poor EICs; poorly shaped peaks for ions 369, 351. Ion 333 does not appear to provide any peaks. B Inconsistent, inadequate abundances (≤E5) for ions 369, 351, 333. Ions 369 and 351 do not appear to be present in *A. obesum* in large amounts. Ion 333 does not appear to be present in *A. obesum*.	6.09 – 6.11	Most prominent in ion 369.
	6.18 – 6.20	Most prominent in ion 369.

Ions 371, 353, 335 *m/z*

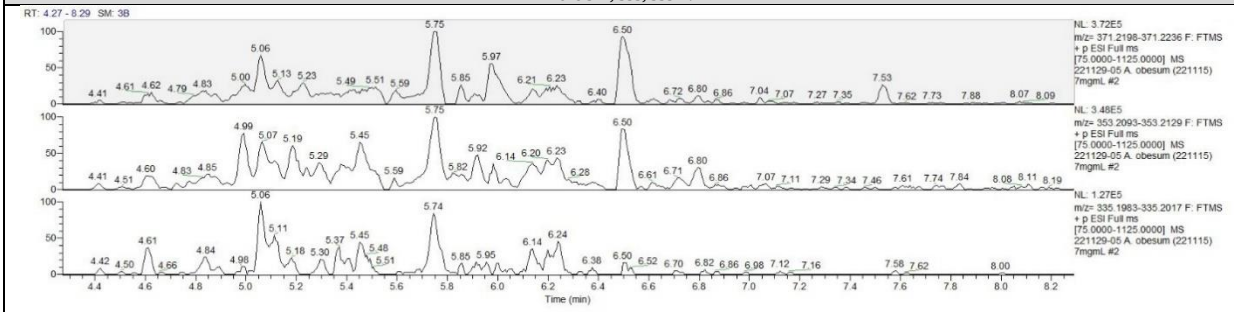

General Observations	RT	Observed Peaks	RT	Observed Peaks
Poor chromatogram; poorly shaped peaks for ions 371, 353, 335. Adequate abundances (≥E5) for all ions. Baseline very noisy.	5.05 – 5.08	Present in all ions.	**6.49 – 6.51**	**Major peak for ions 371, 353**
	5.74 – 5.76	**Major peak for all ions.**	7.52 – 7.54	Most prominent in ion 371.
	5.96 – 5.98	Most prominent in ion 371		

Ions 373, 355, 337 *m/z*

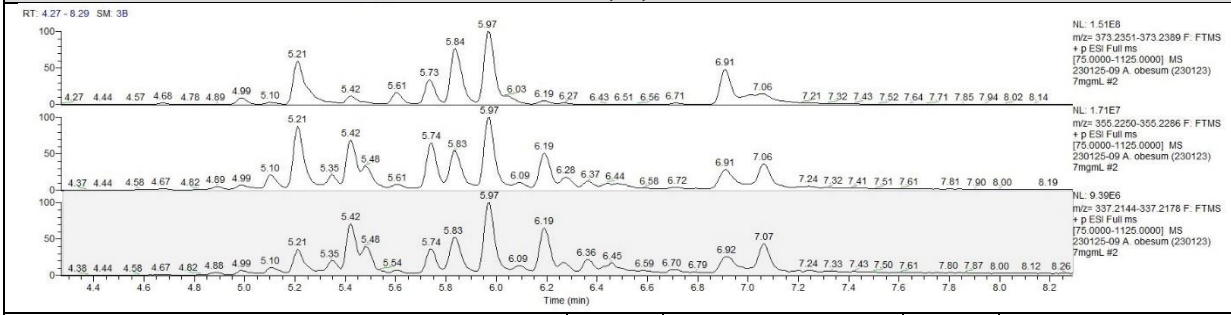

General Observations	RT	Observed Peaks	RT	Observed Peaks
Clean EICs with low baseline. Strong abundances (≥E6) and smooth peak shapes for all ions. Very consistent chromatograms across replicates.	**5.20 -5.22**	**Major peak in all ions.**	**5.96 – 5.98**	**Major peak in all ions.**
	5.41 – 5.43	Most prominent in ions 355, 337	6.18 – 6.20	Most prominent in ions 355, 337.
	5.73 – 5.75	**Major peak in all ions.**	6.90 – 6.92	Most prominent in ion 373.
	5.83 – 5.85	**Major peak in all ions.**	7.05 – 7.07	Most prominent in ions 355, 337.

Ions 375, 357, 339 *m/z*

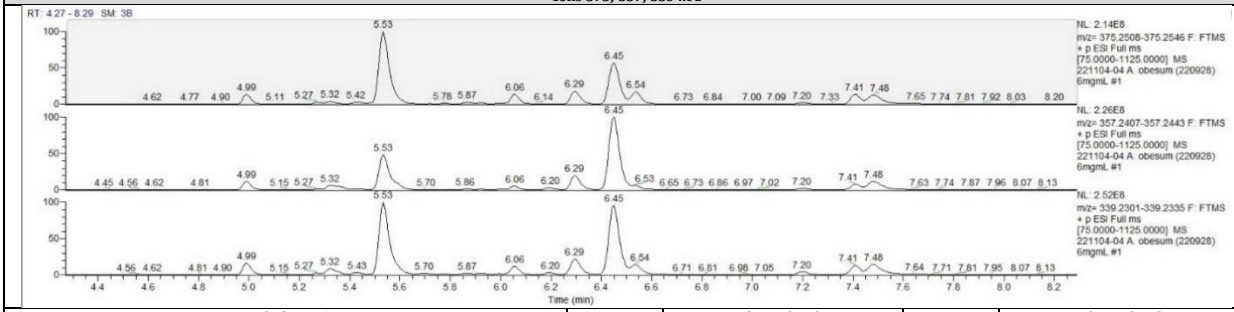

General Observations	RT	Observed Peaks	RT	Observed Peaks
Very clean EICs with very low baseline. Strong abundances (≥E6) and smooth peak shapes for all ions. Very consistent chromatograms across replicates.	4.98 – 5.00	May appear as major peak in all ions.	**6.44 – 6.46**	**Major peak in all ions.**
	5.52 – 5.54	**Major peak in all ions.**	7.40 -7.42	Present in all ions.
	6.28 – 6.30	Small peak present in all ions.	7.47 – 7.49	May appear as major peak in all ions.

Ions 433, 405, 391, 389, 375 *m/z* (genins)

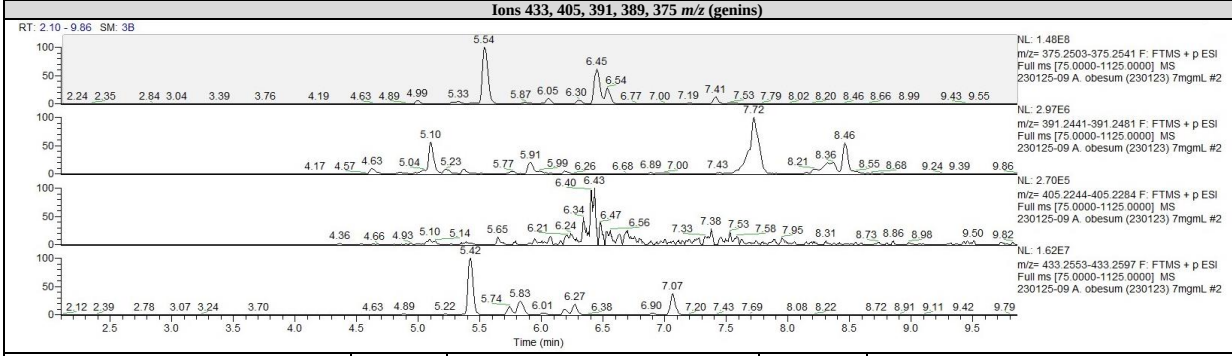

General Observations	RT	Observed Peaks	RT	Observed Peaks
Strong (≥E6) to adequate (≥E5) abundances for all ions. Most distinct peaks appear at ions 375 and 433. Noisy EIC for ion 405, without distinct peaks, concentrated around 6.20 to 8.00.	5.09 – 5.11	Present in ion 391.	6.53 – 6.55	Present in ion 375. May appear unresolved from 6.44 – 6.46 peak.
	5.41 – 5.43	**Major peak in ion 433.**	7.06 -7.08	Present in ion 433.
	5.53 – 5.55	**Major peak in ion 375.**	7.71 – 7.73	Major peak in ion 391.
	6.44 – 6.46	**Major peak in ion 375**	8.45 – 8.47	Present in ion 391.

3.2.3 *Adenium oleifolium*

Ions 369, 351, 333 *m/z*

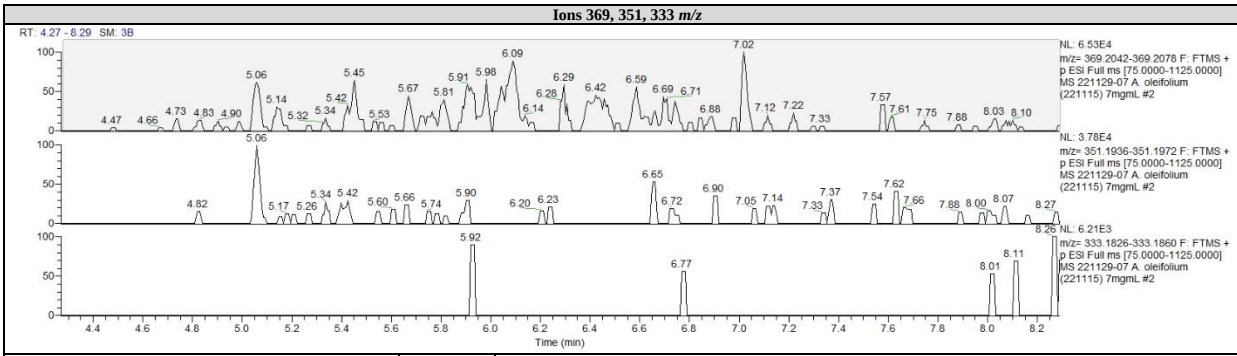

General Observations	RT	Observed Peaks
Poorly shaped peaks and noisy baseline. Inconsistent peaks across replicates. Poor abundances (E3 – E4) for all ions. Ions 369 and 351 do not appear to be present in *A. oleifolium* in large amounts. Ion 333 does not appear to be present in *A. oleifolium.*	5.05 – 5.07	Present in 369, 353.

Ions 371, 353, 335 *m/z*

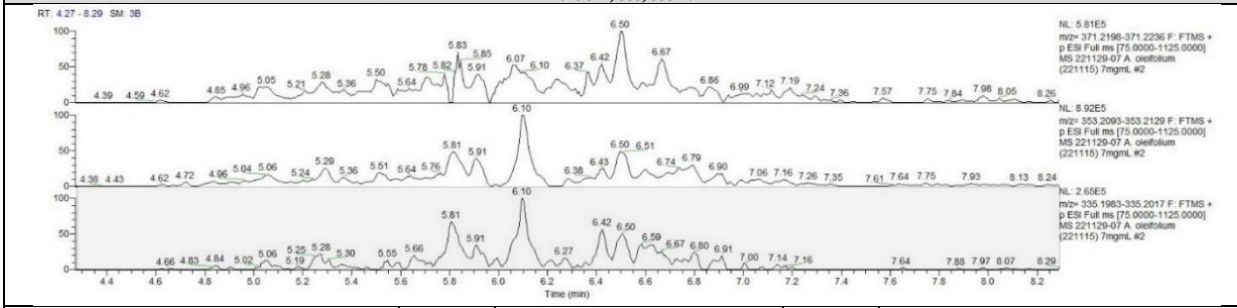

General Observations	RT	Observed Peaks	RT	Observed Peaks
Adequate abundances (≥E5) but poor peak shapes and noisy baseline.	5.80 – 5.82	Can appear as a major peak in all ions.	**6.09 – 6.11**	**Major peak. Most prominent in ions 353, 335.**
	5.90 – 5.92	Small peaks present in all ions.	6.49 – 6.51	Most prominent in ion 371.

Ions 373, 355, 337 *m/z*

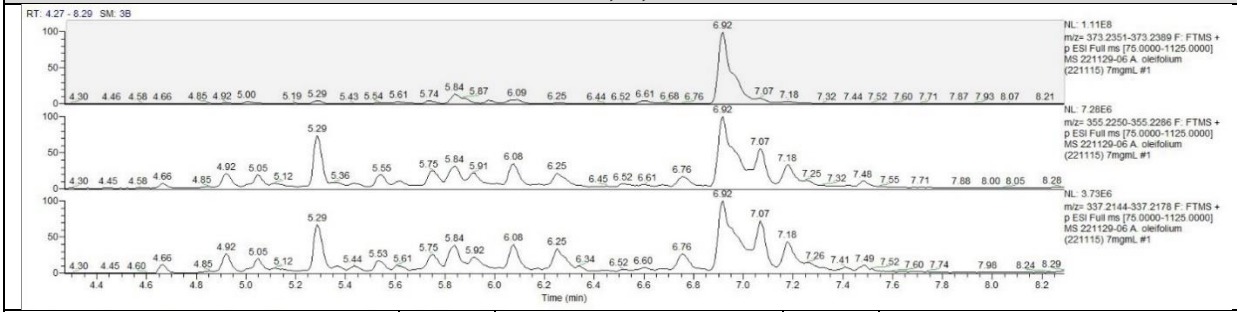

General Observations	RT	Observed Peaks	RT	Observed Peaks
Clean EICs with low baseline. Strong abundances (≥E6) for all ions. Consistent chromatograms across replicates.	4.89 – 4.91	Small peaks present in ions 355, 337.	5.72 – 5.92	Series of 3 peaks, most prominent in ions 355, 337.
	5.03 – 5.05	Small peaks present in ions 355, 337.	**6.91 – 6.93**	**Major peak in all ions.**
	5.26 – 5.28	**Major peak for ions 355, 337.**	7.04 – 7.06	May appear unresolved from 6.91 – 6.93 peak in ions 355, 337.
	5.58 – 5.60	Small peaks present in ions 355, 337.	7.17 – 7.19	Most prominent ion ions 355, 337.

Ions 375, 357, 339 *m/z*

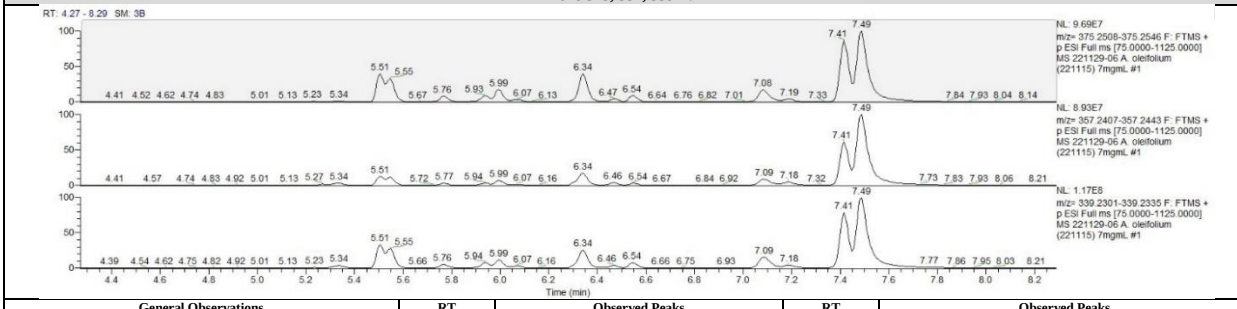

General Observations	RT	Observed Peaks	RT	Observed Peaks
Clean EICs and low baselines. Strong abundances (≥E6) and smooth peak shapes for all ions. Very consistent chromatograms across replicates.	5.50 – 5.52	Small peak present in all ions. May appear unresolved from 5.54 – 5.56 ion.	7.08 – 7.10	Small peak present in all ions.
	5.54 – 5.56	Small peak present in all ions. May appear unresolved from 5.50 – 5.52 peak.	**7.40 – 7.42**	**Major peak in all ions. May appear unresolved from 7.48 – 7.50 peak.**
	5.98 – 6.00	Small peak present in all ions.	**7.48 – 7.50**	**Major peak in all ions. May appear unresolved from 7.40 – 7.42 peak.**
	6.33 – 6.35	Medium peak present in all ions.		

Ions 433, 405, 391, 389, 375 *m/z* (genins)

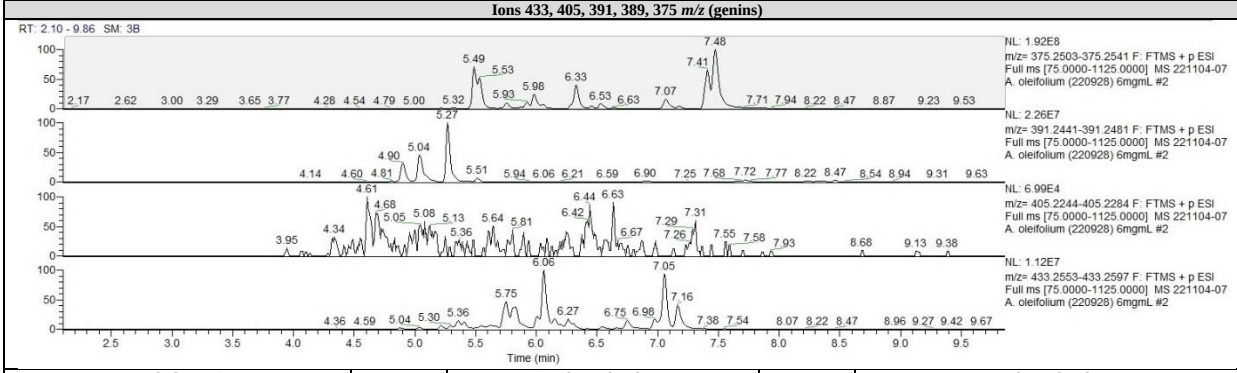

General Observations	RT	Observed Peaks	RT	Observed Peaks
Strong abundances (≥E6) for ions 375, 391, and 433. Poor (≥E4) abundance for ion 405. Very clean EIC for ion 391. Noisy EIC for ion 405, concentrated from around 4.00 to 7.55.	4.89 – 4.91	Present in ion 391.	6.26 – 6.28	Present in ion 433.
	5.03 – 5.05	**Present in ion 391.**	6.32 – 6.34	Present in ion 375.
	5.26 – 5.28	**Major peak in ion 391.**	7.04 – 7.06	Major peak in ion 433. May appear unresolved from 6.97 – 6.99 peak and 7.15 – 7.17 peak.
	5.48 -5.50	Present in ion 375. May appear unresolved from 5.52 – 5.54 peak.	7.04 – 7.06	Present in ion 375.
	5.42 – 5.54	Present in ion 375. May appear unresolved from 5.52 – 5.54.	7.15 – 7.17	Present in ion 433. May appear unresolved from 7.04 – 7.06 peak.
	5.74 – 5.76	Present in ion 433. May appear unresolved.	7.40 – 7.42	Major peak in ion 375. May appear unresolved from 7.47 – 7.49 peak.
	5.97 – 5.99	Present in ion 375.	7.47 – 7.49	Major peak in ion 375. May appear unresolved from 7.40 – 7.42 peak.
	6.05 – 6.07	Major peak in ion 433.		

3.2.4 *Adenium socotranum*

Ions 369, 351, 333 *m/z*

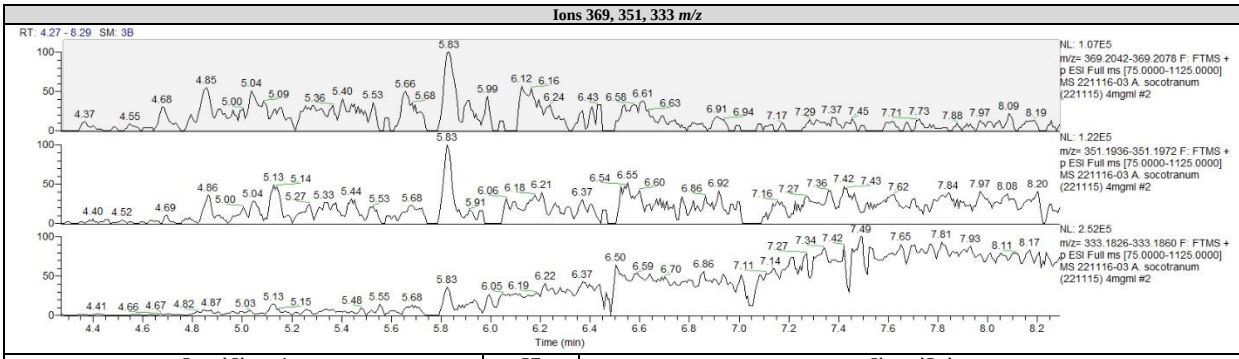

General Observations	RT	Observed Peaks
Poor chromatogram; poorly shaped peaks and noisy baseline. Inconsistent peaks across replicates. Inadequate abundances (E4 – E5) for all ions. Ions 369, 351, 333 do not appear to be present in *A. socotranum*, at least not in large amounts.	5.82 – 5.84	Most prominent in ions 369, 351, 333. Smallest peak in ion 333 compared to ions 369, 351.

Ions 371, 353, 335 *m/z*

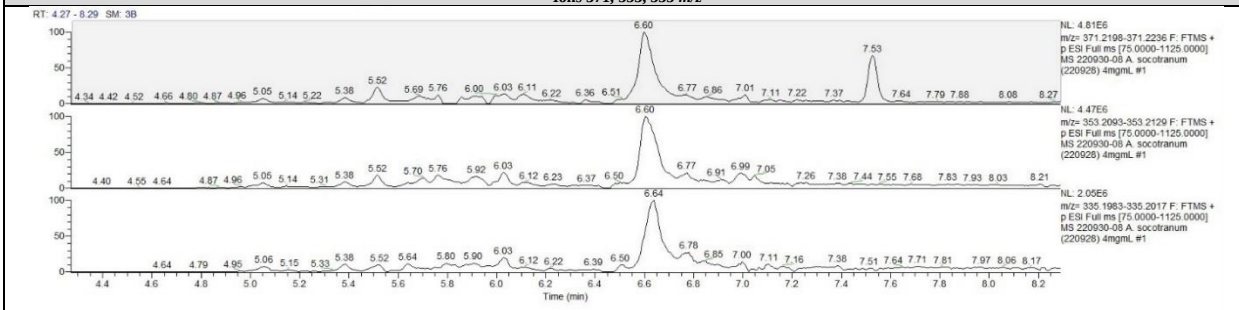

General Observations	RT	Observed Peaks	RT	Observed Peaks
Clean chromatogram and low baseline. Strong abundances (≥E6) and smooth peak shapes. Very consistent chromatograms across replicates.	5.52 – 5.53	Present in all ions. May appear as a major peak.	7.52 – 7.54	Most prominent in ion 371.
	6.59 – 6.61	Major peak for all ions		

Ions 373, 355, 337 m/z

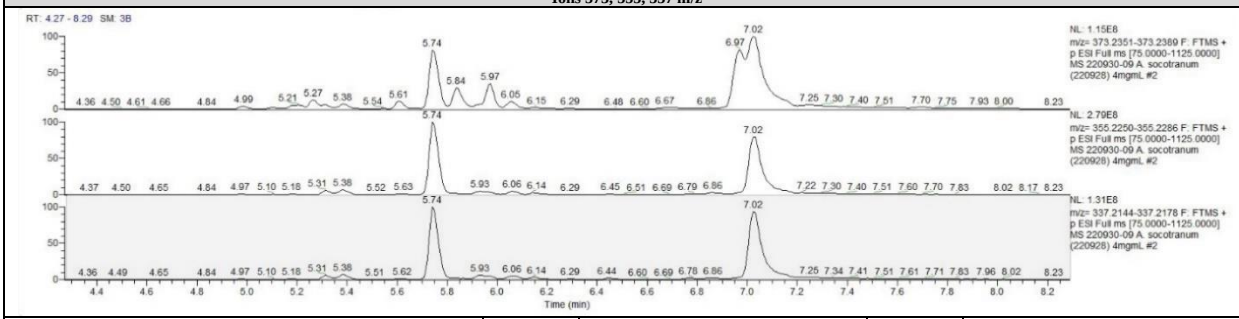

General Observations	RT	Observed Peaks	RT	Relevant Ions
Clean chromatogram and low baseline. Strong abundances (≥E6) and smooth peak shapes for all ions. Very consistent chromatograms across replicates.	**5.73 – 5.75**	**Major peak in all ions.**	6.96 – 6.98	Most prominent in ion 373. May appear unresolved from 7.01 – 7.03 peak.
	5.83 – 5.85	Small peak most prominent in ion 373.		
	5.96 – 5.98	Small peak most prominent in ion 373.	**7.01 – 7.03**	**Major peak in all ions.**

Ions 375, 357, 339 *m/z*

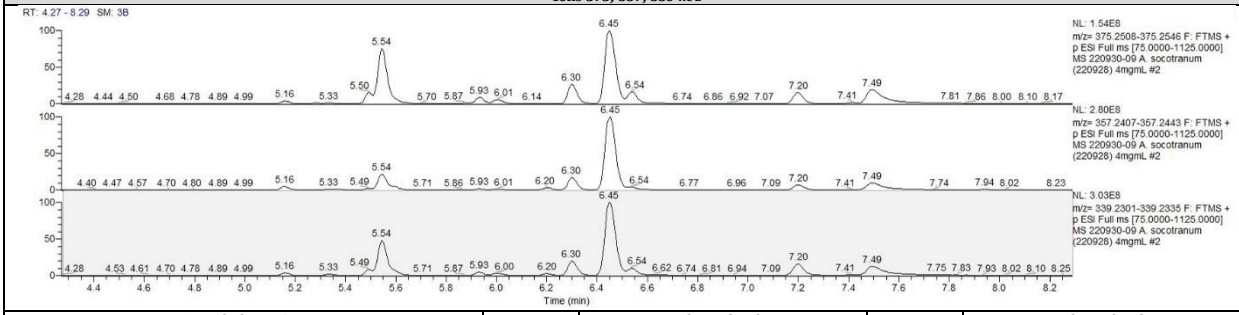

General Observations	RT	Observed Peaks	RT	Observed Peaks
Clean chromatogram and low baseline. Strong abundances (≥E6) and smooth peak shapes for all ions. Very consistent chromatograms across replicates.	**5.53 – 5.55**	**Medium peak in all ions. Most prominent in ion 375. May appear as a major peak.**	**6.44 – 6.46**	**Major peak for all ions.**
			7.19 – 7.21	Small peak present in all ions.
	6.29 – 6.31	Small peak present in all ions.	7.48 – 7.50	Small peak present in all ions

Ions 433, 405, 391, 389, 375 *m/z* (genins)

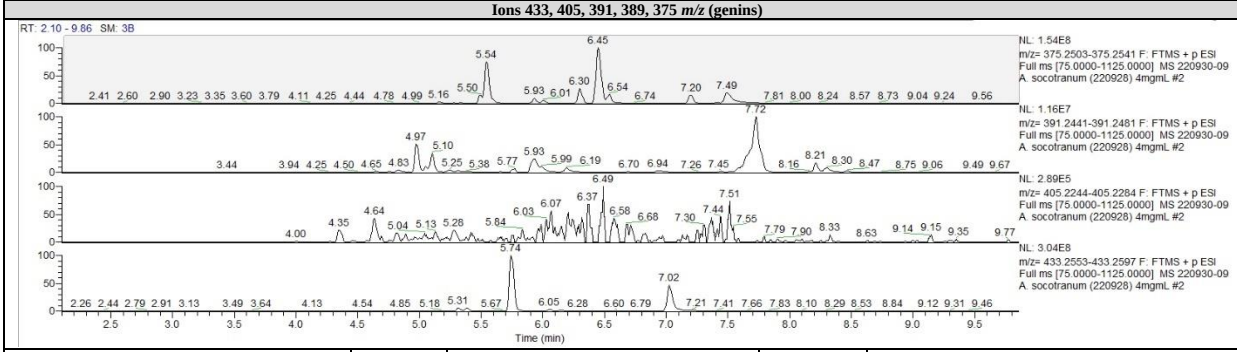

General Observations	RT	Observed Peaks	RT	Observed Peaks
Strong (≥E6) to adequate (≥E5) abundances for all ions. Noisy baseline in ion 405, concentrated around 5.84 to 7.56.	4.63 – 4.65	Present in ion 405.	6.02 – 6.69	Bunched peaks (noisy)
	4.96 – 4.98	Present in ion 391.	**6.44 – 6.46**	**Major peak in ion 375.**
	5.53 – 5.55	**Major peak in ion 375**	7.01 – 7.03	Present in ion 433.
	5.73 – 5.75	**Major peak in ion 433**	7.48 – 7.50	Present in ion 375.
	5.92 – 5.94	Present in ion 391.	**7.71 – 7.73**	**Major peak in ion 391.**

3.2.5 *Asclepias curassavica*

Ions 369, 351, 333 *m/z*

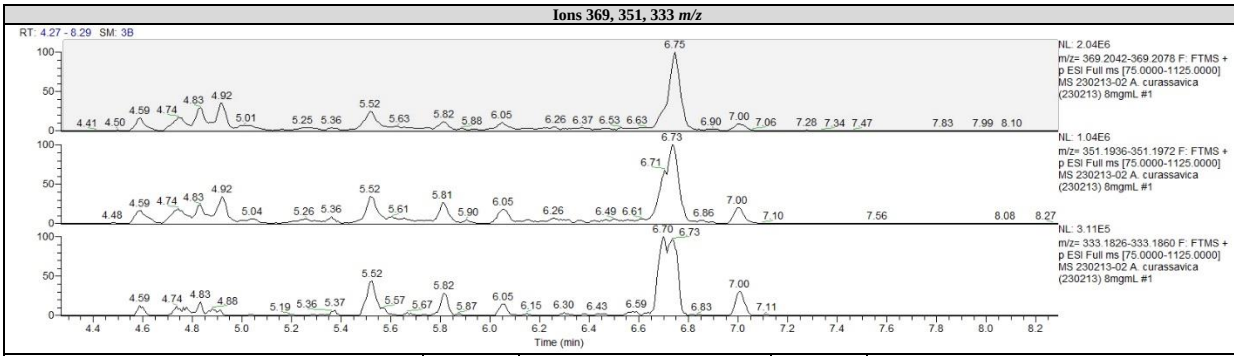

General Observations	RT	Observed Peaks	RT	Observed Peaks
Clean EICs and low baseline. Strong (≥E6) to adequate (≥E5) abundances for all ions. Very consistent chromatograms across replicates.	**4.58 – 4.93**	**Series of 4 peaks, with peak at 4.90 – 4.92 being tallest.**	6.04 – 6.06	Small peak present in all ions.
	5.50 – 5.52	Small peak present in all ions.	**6.74 – 6.76**	**Major peak in all ions.**
	5.80 – 5.82	Small peak present in all ions.	6.99 – 7.01	Small peak present in all ions.

Ions 371, 353, 335 *m/z*

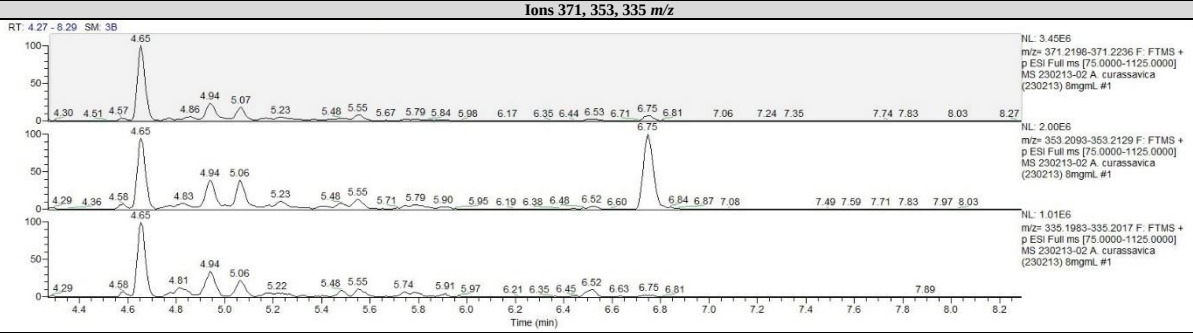

General Observations	RT	Observed Peaks	RT	Observed Peaks
Clean EICs with low baseline. Strong (≥E6) to adequate (≥E5) abundances for all ions. Very consistent peaks across replicates.	**4.64 – 4.66**	**Major peak in all ions.**	5.05 – 5.07	Peak present in all ions.
	4.93 – 4.95	Peak present in all ions.	**6.74 – 6.75**	**Major peak in ion 353 only.**

Ions 373, 355, 337 *m/z*

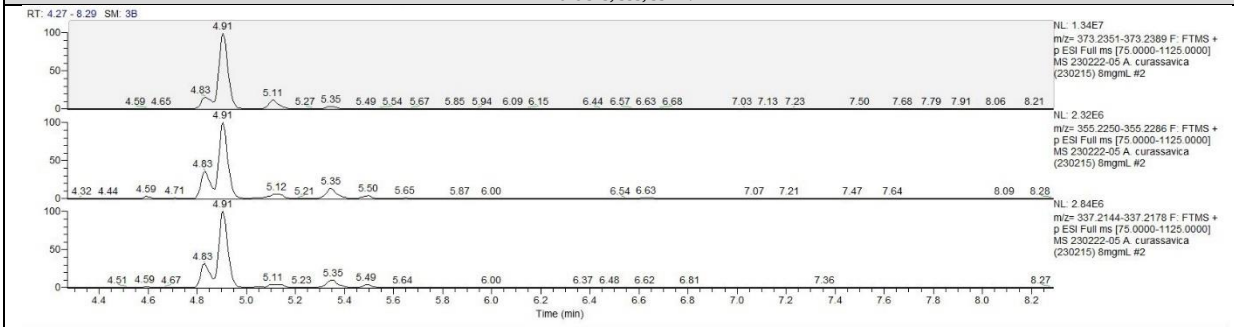

General Observations	RT	Observed Peaks	RT	Observed Peaks
Very clean EICs with very low baseline. Strong (≥E6) abundances for all ions. Very consistent across replicates.	4.82 – 4.84	Small peak present in all ions. May appear unresolved from 4.90 – 4.92 peak.	**4.90 – 4.92**	**Major peak for all ions.**
			5.34 – 5.36	Small peak present in all ions. Most prominent in ions 355, 337.

Ions 375, 357, 339 m/z

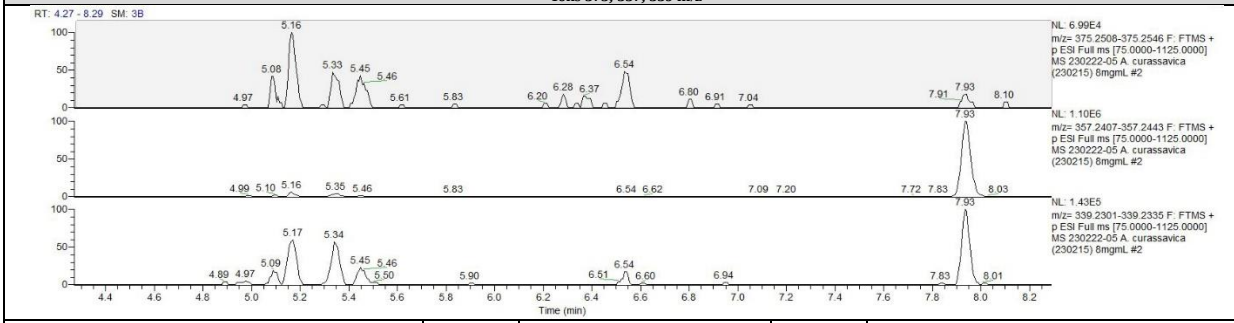

General Observations	RT	Observed Peaks	RT	Observed Peaks
Clean EICs with low baseline but poor, jagged, peak shapes for peaks in all ions, with the exception of 7.92 – 7.94 peak. Varying abundances from strong (≥E6), adequate(≥E5), to poor (≤E5). Still, chromatograms are quite consistent across replicates.	5.16 – 5.18	Major peak in ions 375, 339. More prominent in ion 375.	7.92 – 7.94	Major peak in ions 357, 339. Appears to be the only peak present for ion 357.
	6.53 – 6.55	Small peak in ions 375, 339. More prominent in ion 375.		

Ions 433, 405, 391, 389, 375 *m/z* (genins)

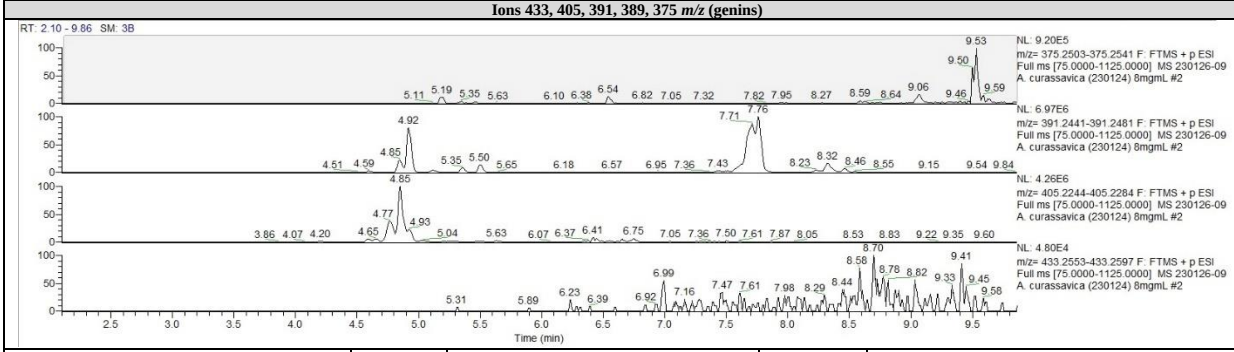

General Observations	RT	Observed Peaks	RT	Observed Peaks
Strong (≥E6) abundances for ions 391 and 405. Adequate (≥E5) abundance for ion 375. Poor (≥E4) abundance for ion 433. Noisy EIC for ion 433 concentrated around 6.22 to 9.60; no distinct peaks. "Fork" pattern around 4.64 to 5.06 in ion 405 (i.e. 3 peaks in succession).	4.76 – 4.78	Present in ion 405. May appear unresolved from 4.84 – 4.86 peak.	**7.70 – 7.72**	**Major peak in ion 391. May appear unresolved from 7.75 – 7.77 peak.**
	4.84 – 4.86	**Major peak in ion 405.** Present in ion 391.	**7.75 – 7.77**	**Major peak in ion 391. May appear unresolved from 7.70 – 7.72.**
	4.91 – 4.93	**Major peak in ion 391.**	8.31 – 8.33	Present in ion 391.
	4.92 – 4.94	Present in ion 405. May appear unresolved from 4.84 – 4.86 peak.	**9.49 – 9.51, 9.52 – 9.54**	**Major peak in ion 375. May appear unresolved from each other. Appears to be commonality between *Asclepias* samples.**

3.2.6 *Asclepias fascicularis*

Ions 39, 351, 333 *m/z*

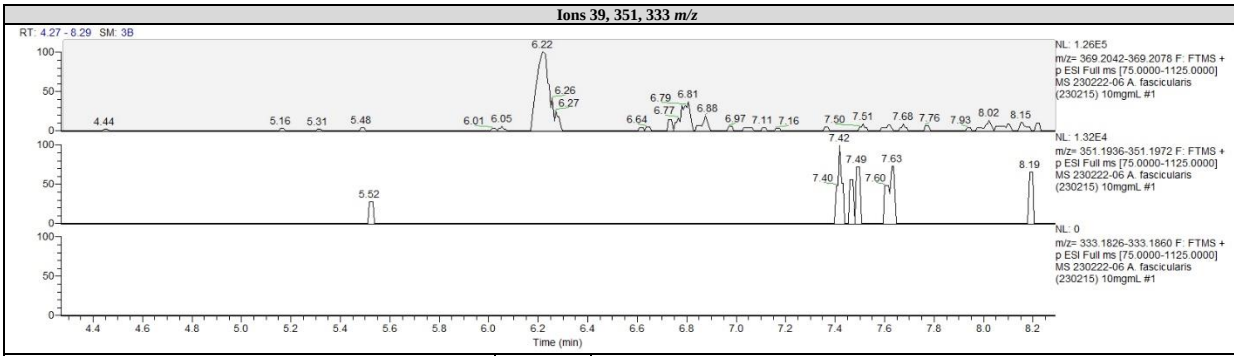

General Observations	RT	Relevant Ions
Very poor signal. Inconsistent peaks with the exception of 6.21 – 6.23 in ion 369. Poor abundances (≤E5) for all ions. No signal for ion 333. Ions 369, 351, and 333 do not appear to be present in *A. fascicularis*.	6.21 – 6.23	Potential major peak for ion 369. However, given the low abundance and poor peak shape, its reliability should be scrutinized.

Ions 371, 353, 335 *m/z*

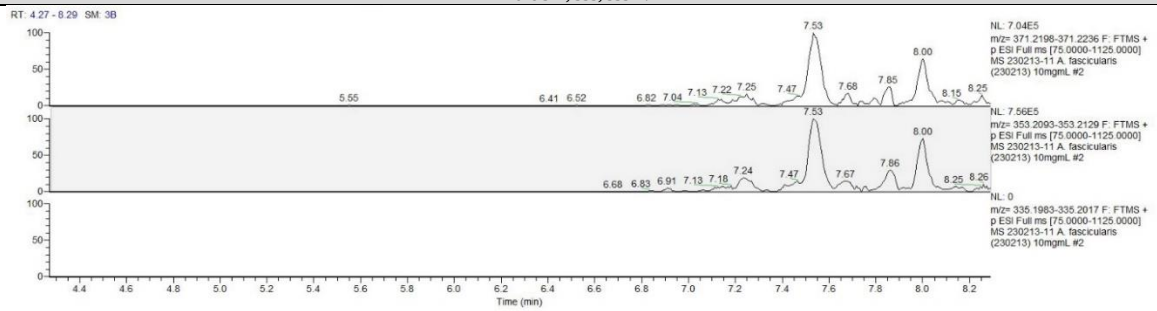

General Observations	RT	Observed Peaks	RT	Observed Peaks
Adequate abundances (≥E5) for ions 371, 353 but poor abundance for ion 335. Low baseline for ions 371, 353. Smooth peak shape for ions 371, 353. No signal for ion 335. Ion 335 does not appear to be present in *A. fascicularis*. Consistent chromatograms across replicates.	7.52 – 7.54	Major peak in ions 371, 353.	7.99 – 8.01	Medium/Major peak in ions 371, 353.
	7.84 – 7.86	Small peak in ions 371, 353.		

Ions 373, 355, 337 *m/z*

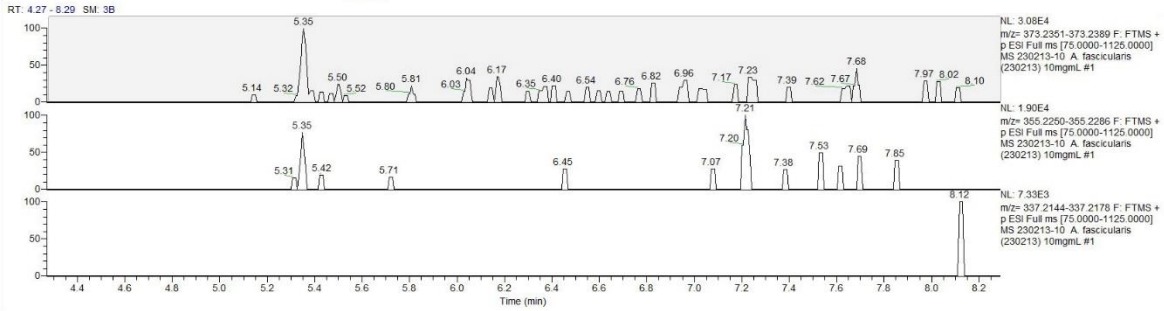

General Observations	RT	Observed Peaks
Very poor signal for all ions, with abundances (≤E5) for all ions. Poor peak shape for the few peaks present. Inconsistent chromatograms across replicates. Ions 373, 355, and 337 do not appear to be present in *A. fascicularis*.	5.34 – 5.36	Only peak that consistently shows up across replicates. However, given the low abundance and poor peak shape, its reliability should be scrutinized.

Ions 375, 357, 339 *m/z*

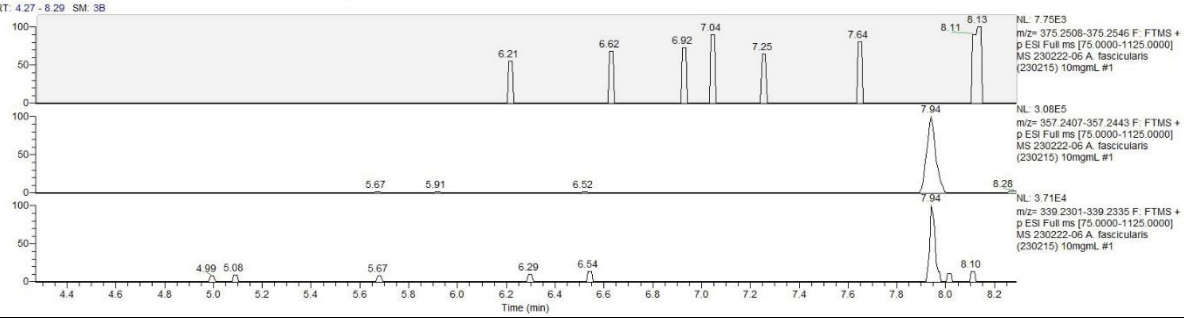

General Observations	RT	Observed Peaks
Very poor signal for all ions, with abundances adequate to poor (≤E5) for all ions. Poor peak shape for the few peaks present. Ions 357 and 339 do not appear to be present in *A. fascicularis* in large amounts. Ion 375 does not appear to be present in *A. fascicularis*.	7.93 – 7.95	Only peak that appears consistently across replicates. Major peak for ion 357 only.

Ions 433, 405, 391, 389, 375 *m/z* (genins)

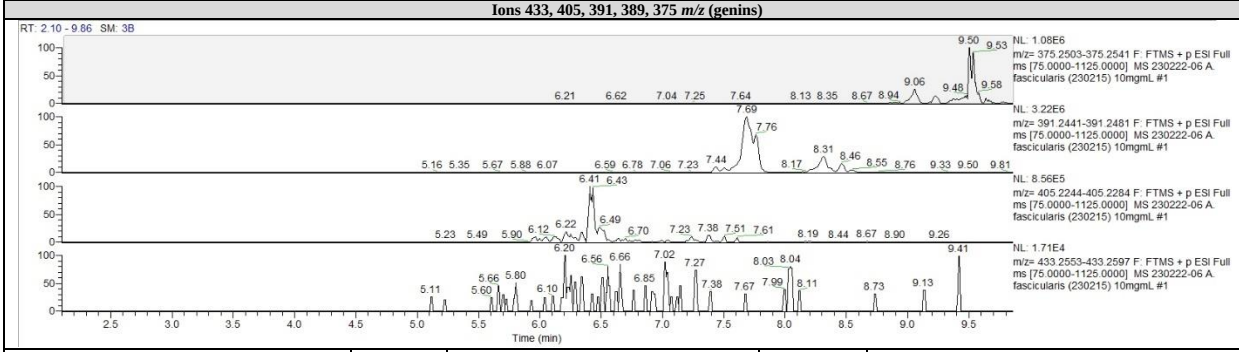

General Observations	RT	Observed Peaks	RT	Observed Peaks
Strong (≥E6) abundances for ions 375 and 391. Adequate abundance (≥E5) for ion 405 but can be variable. Poor abundance (≥E4) for ion 433. Noisy EIC for ion 433 concentrated around 5.60 to 8.0; no distinct peaks.	6.40 – 6.42	**Major peak in ion 405. May appear unresolved from 6.48 – 6.50 peak.**	**8.30 – 8.32**	**Present in ion 391**
	6.48 – 5.50	Present in ion 405. May appear unresolved from 6.40 – 6.42 peak.	9.05 – 9.07	Present in ion 375.
	7.68 – 7.70	**Major peak in ion 391. May appear unresolved from 7.75 – 7.77 peak.**	**9.49 – 9.51, 9.52 – 9.54**	**Major peak in ion 375. May appear unresolved from each other. Appears to be commonality between *Asclepias* samples.**
	7.75 – 7.77	**Major peak in ion 391. May appear unresolved from 7.68 – 7.70 peak.**		

3.2.7 *Asclepias speciosa*

Ions 369, 351, 333 *m/z*

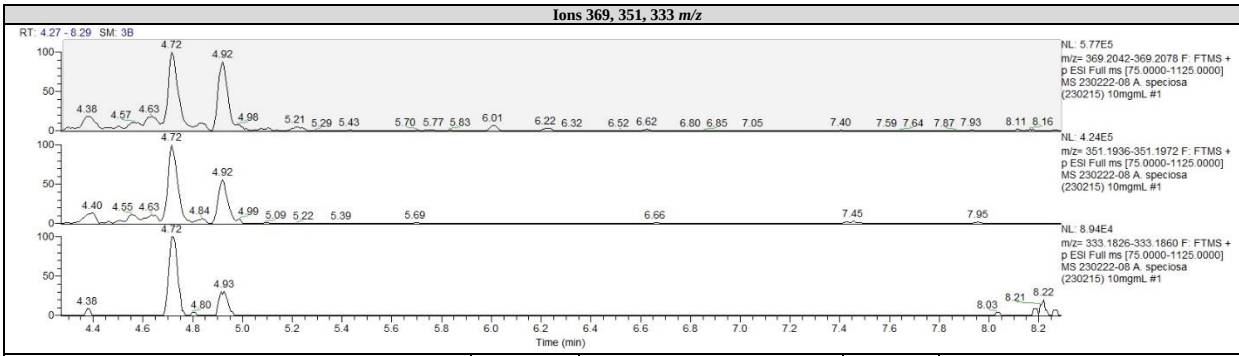

General Observations	RT	Observed Peaks	RT	Observed Peaks
Adequate (≥E5) abundances for ions 369, 351. Poor (≥E4) abundance for ion 333. Clean EICs with low baseline. Consistent chromatograms across replicates.	**4.38 – 4.40**	**Major peak in all ions.**	**4.72 – 4.74**	**Major peak in all ions.**
	4.64 – 4.66	Small peak present in ions 369, 351.	**4.92 – 4.94**	**Major peak in all ions.**

Ions 371, 353, 335 *m/z*

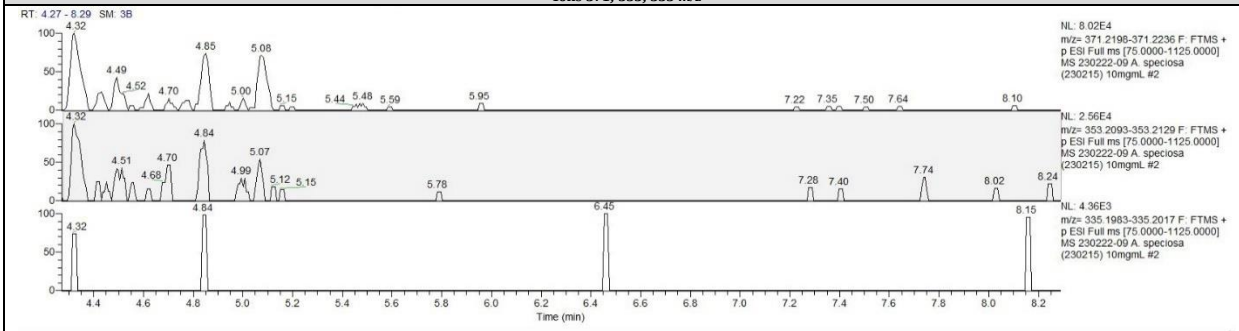

General Observations	RT	Observed Peaks	RT	Observed Peaks
Poor signal/abundances (≤E4). Poor (jagged) peak shape for the few peaks present. Consistent chromatograms across replicates. Ions 371, 353, and 335 do not appear to be present in *A. speciosa*, at least not in large amounts.	4.30 – 4.32	Peak present in all ions.	4.84 – 4.86	Peak present in all ions.

Ions 373, 355, 337 *m/z*

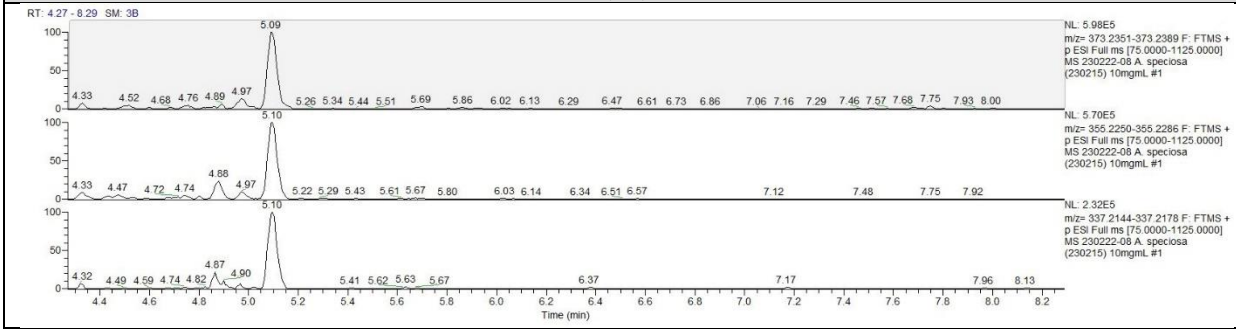

General Observations	RT	Observed Peaks
Clean EICs with low baseline. Adequate (≥E5) abundances for ions 373, 355 and poor (≤E5) abundance for ion 337. Consistent chromatograms across replicates.	**4.48 – 4.50**	**Present in all ions. May appear as a major peak.**
	4.96 – 4.98	Present in all ions. Most prominent in ion 373.
	5.09 – 5.11	**Major peak in all ions.**

Ions 375, 357, 339 *m/z*

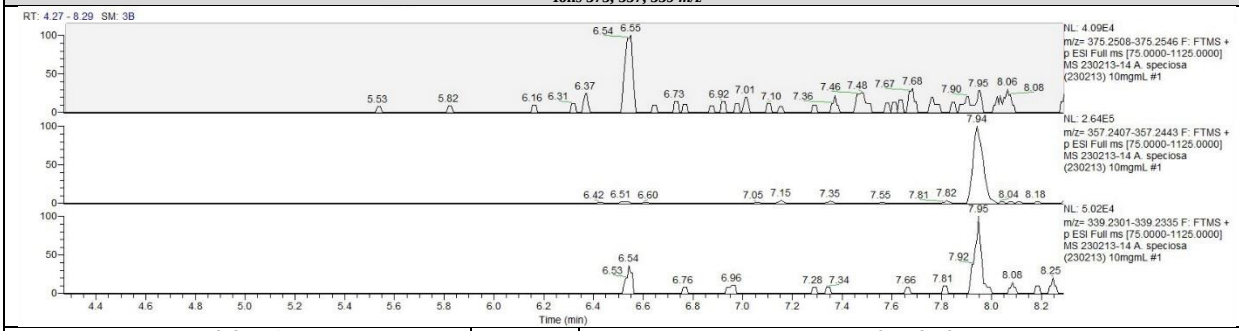

General Observations	RT	Observed Peaks
Poor abundances (≤E5) for all ions. Consistent chromatograms across replicates. Poor peak shape for the few peaks present.	**6.54 – 6.56**	**Present in all ions. Major peak and most prominent in ion 375.**
	7.93 – 7.95	**Present in all ions. Major peak and most prominent in ions 357, 339.**

Ions 433, 405, 391, 389, 375 *m/z* (genins)

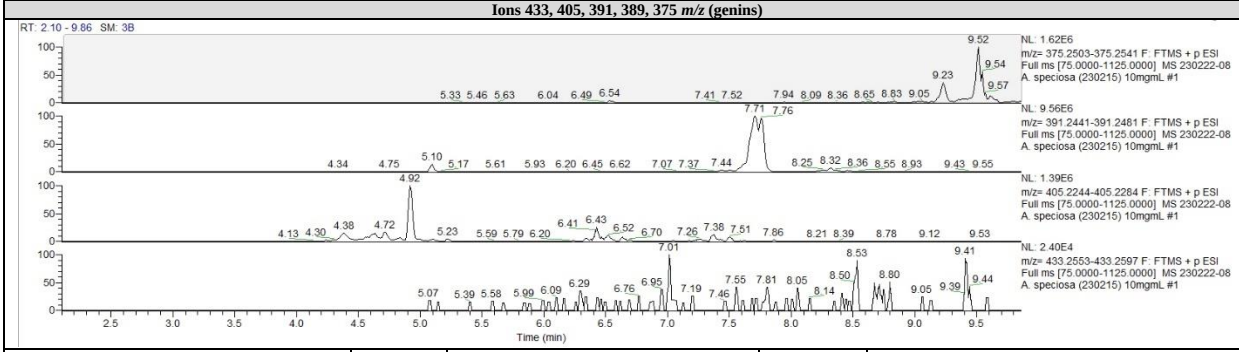

General Observations	RT	Observed Peaks	RT	Observed Peaks
Strong (≥E6) abundances for ions 375, 391, and 405. Poor (≥E4) abundance for ion 433. Noisy EIC for ion 433. Clean EICs for other ions.	**4.91 – 4.93**	**Major peak in ion 405.**	**9.22 – 9.24**	**Present in 375.**
	6.42 – 6.44	Present in ion 405.	9.49 – 9.51, 9.52 – 9.54	**Major peak in ion 375.** May appear unresolved from each other. Appears to be commonality between *Asclepias* samples.
	7.70 – 7.72, 7.75 – 7.77	Major peaks in ion 391. May appear unresolved from each other.		

3.2.8 *Carissa macrocarpa*

Ions 369, 351, 333 *m/z*

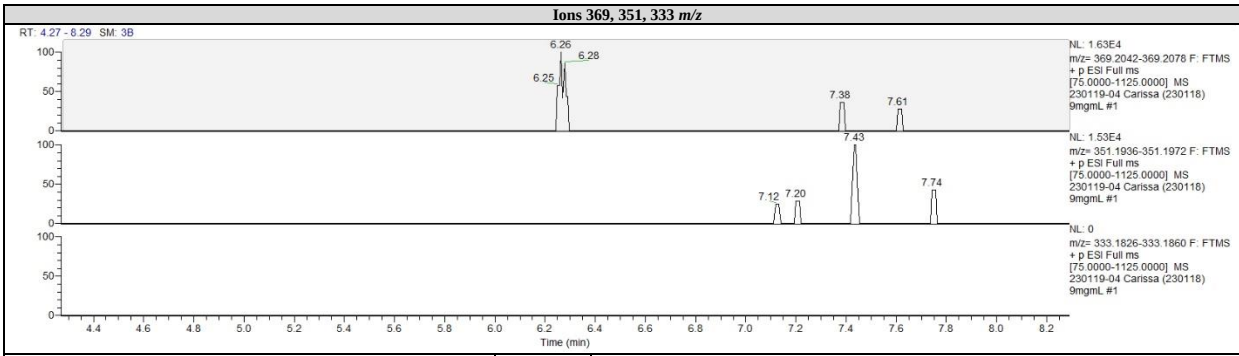

General Observations	RT	Observed Peaks
Poor signal/abundances (≤E4) for all ions. Ions 369, 351, and 333 do not appear to be present in *C. macrocarpa*. Inconsistent chromatograms across replicates.	-	-

Ions 371, 353, 335 *m/z*

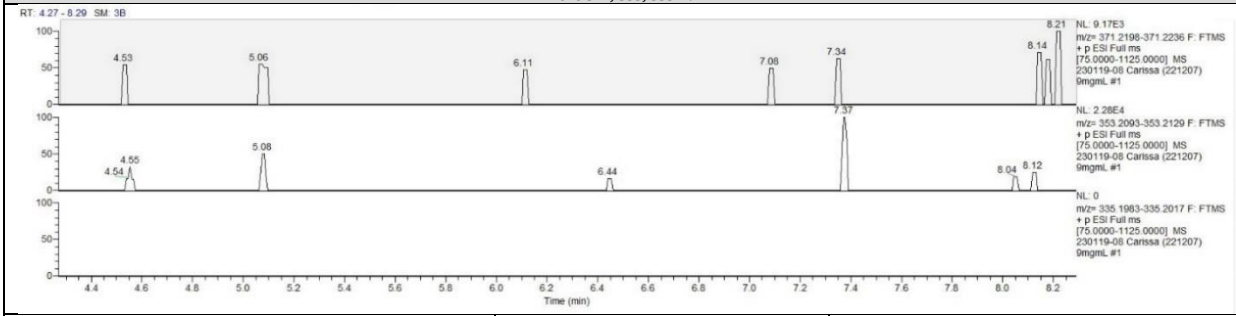

General Observations	RT	Observed Peaks
Poor signal/abundances (≤E4) for all ions. Ions 387, 369, 351, and 333 do not appear to be present in *C. macrocarpa*. Inconsistent chromatograms across replicates.	-	-

Ions 373, 355, 337 *m/z*

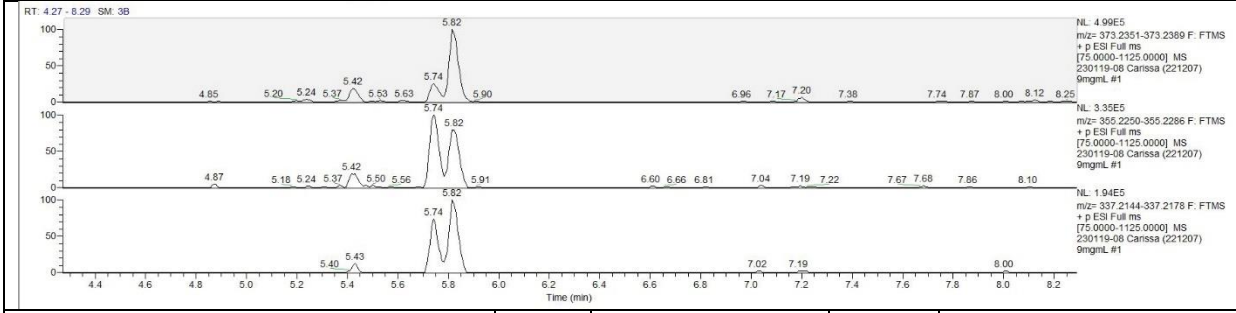

General Observations	RT	Observed Peaks	RT	Observed Peaks
Clean EICs with very low baseline. Adequate abundances (≥E5). Smooth peak shapes for all ions. Consistent chromatograms across replicates.	5.41 – 5.43	Small peak present in all ions.	**5.81 – 5.85**	**Major peak in all ions.**
	5.73 – 5.75	**Major peak in all ions.**		

Ions 375, 357, 339 *m/z*

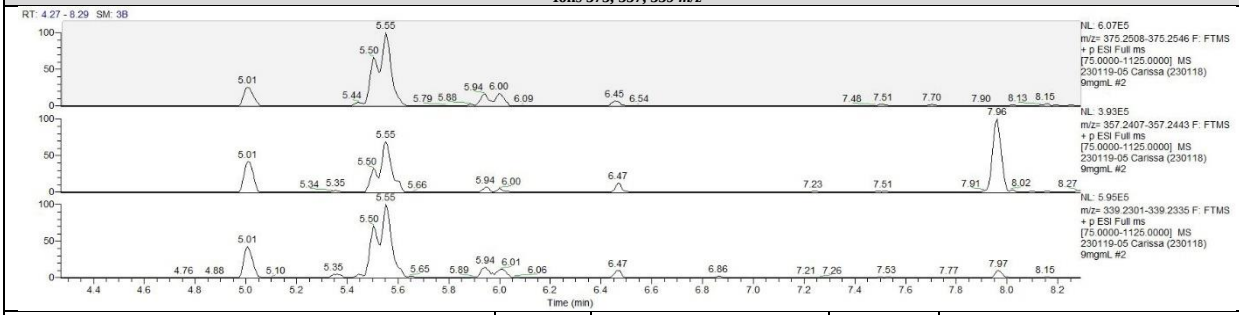

General Observations	RT	Observed Peaks	RT	Observed Peaks
Clean EICs with low baseline. Adequate abundances (≥E5). Smooth peak shapes for all ions. Consistent chromatograms across replicates.	5.00 – 5.02	Medium peak present in all ions.	5.93 – 5.95	Small peak present in all ions.
	5.49 – 5.51	Medium peak present in all ions. May appear unresolved from 5.54 – 5.56 peak.	5.99 – 6.01	Small peak present in all ions.
			6.46 – 6.48	Small peak present in all ions.
	5.54 – 5.56	**Major peak in all ions**	**7.95 – 7.97**	**Major peak for ion 357.**

Ions 433, 405, 391, 389, 375 *m/z* (genins)

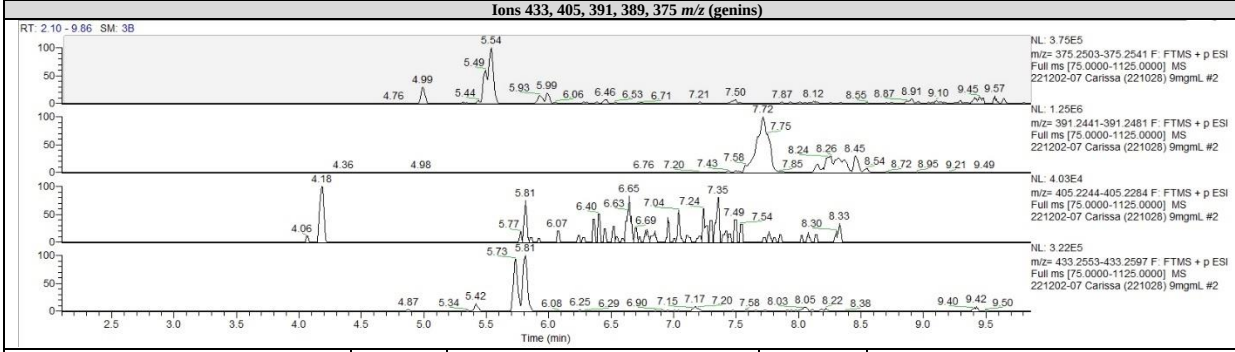

General Observations	RT	Observed Peaks	RT	Observed Peaks
Strong(≥E6) abundance for ion 391. Adequate (≥E5) abundances for ions 375 and 433. Poor (≥E5) abundance for ion 405. Noisy EIC for ion 405, concentrated around 6.06 to 8.00.	4.98 – 5.00	Present in ion 375.	**5.72 – 5.73, 5.80 – 5.82**	**Major peaks in ion 433. May appear unresolved from each other.**
	5.48 – 5.50, 5.53 – 5.55	**Major peaks in ion 365. May appear unresolved from each other.**	**7.71 – 7.73, 7.74 – 7.75**	**Major peaks in ion 391. May appear unresolved from each other.**

3.2.9 *Cerbera odollam*

Ions 369, 351, 333 *m/z*

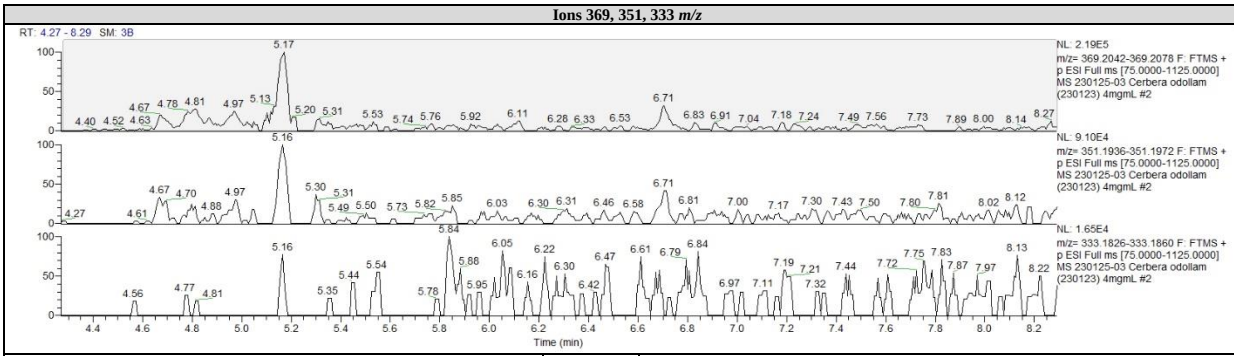

General Observations	RT	Observed Peaks
Poor chromatogram, noisy, poor signal/abundances (≤E5) in all ions. Poor peak shapes (jagged) in any peaks present. Consistent chromatograms across replicates.	5.15 – 5.17	Peak present in all ions.

Ions 371, 353, 335 *m/z*

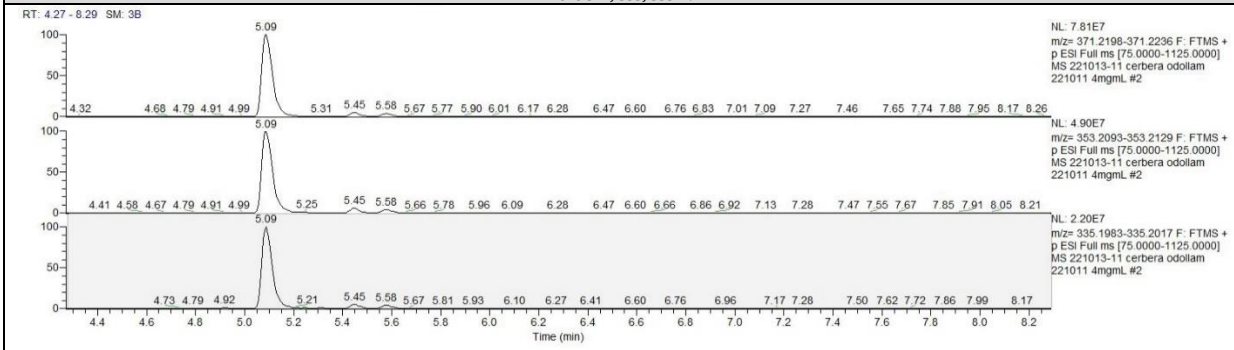

General Observations	RT	Observed Peaks
Extremely clean EICs with very low baseline. Strong abundances (≥E6) and smooth peak shapes. Extremely consistent chromatograms across replicates.	5.08 – 5.10	Major and only peak in chromatogram.

Ions 373, 355, 337 *m/z*

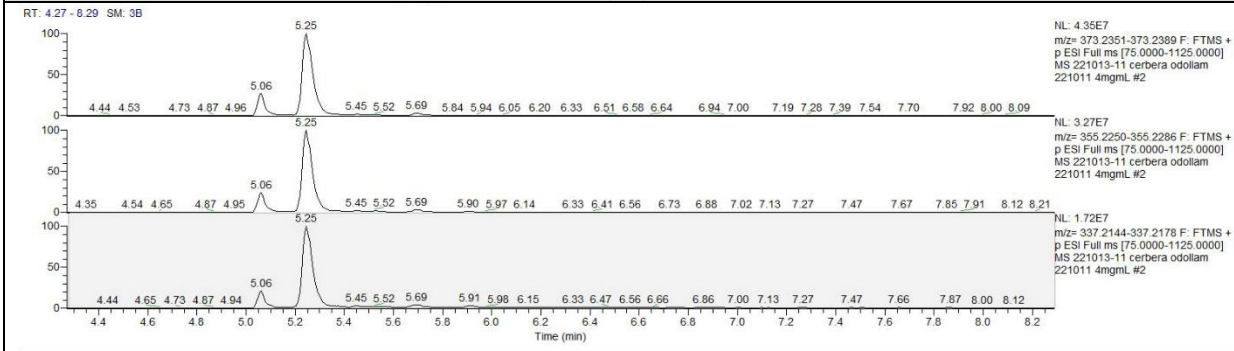

General Observations	RT	Observed Peaks
Extremely clean EICs with very low baseline. Strong abundances (≥E5) and smooth peak shapes. Extremely consistent chromatograms across replicates.	5.05 – 5.07	Peak present in all ions. 1 of 2 peaks in chromatogram.
	5.24 – 5.26	Peak present in all ions. 1 of 2 peaks in chromatogram.

Ions 375, 357, 339 *m/z*

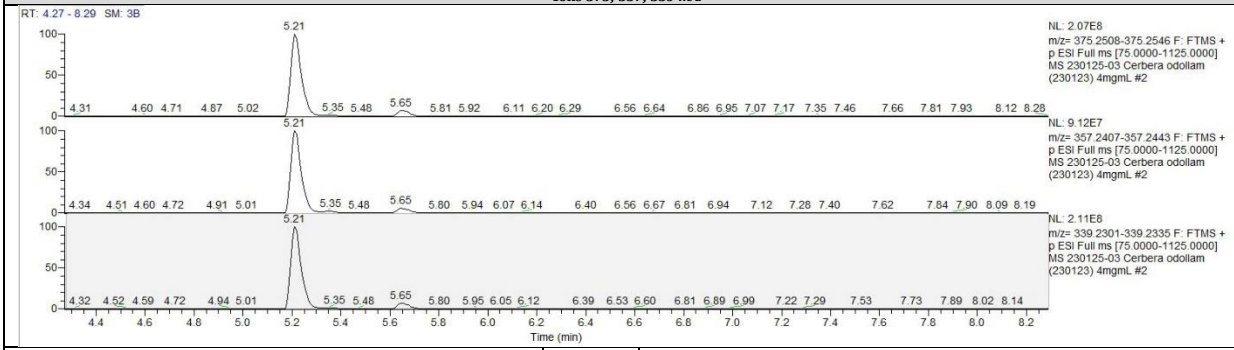

General Observations	RT	Observed Peaks
Extremely clean EICs with very low baseline. Strong abundances (≥E5) and smooth peak shapes. Extremely consistent chromatograms across replicates.	**5.20 – 5.22**	**Major peak in all ions.**
	5.64 – 5.66	Small peak present in all ions.

Ions 433, 405, 391, 389, 375 *m/z* (genins)

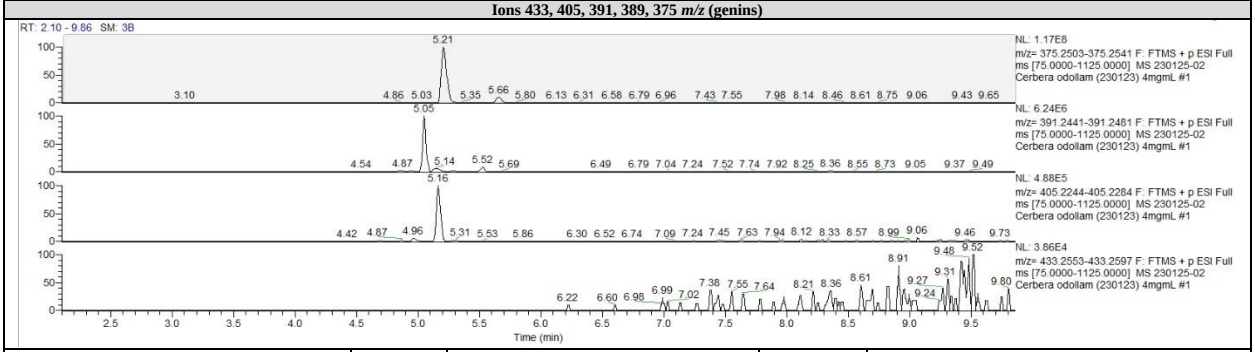

General Observations	RT	Observed Peaks	RT	Observed Peaks
Strong (≥E6) abundances for ions 375 and 391. Adequate (≥E5) for ion 405. Poor abundance (≥E4) for ion 433. Noisy EIC for ion 433, concentrated around 7.00 to 9.53. Very clean EICs for other ions.	5.04 – 5.06	**Major peak in ion 391.** Main peak in ion 391; different from other plants as it does not have peaks at 7.71 -7.75 region.	5.15 – 5.16	**Major peak in ion 405.**
			5.20 – 5.22	**Major peak in ion 375.**

3.2.10 *Convallaria majalis*

Ions 369, 351, 333 *m/z*

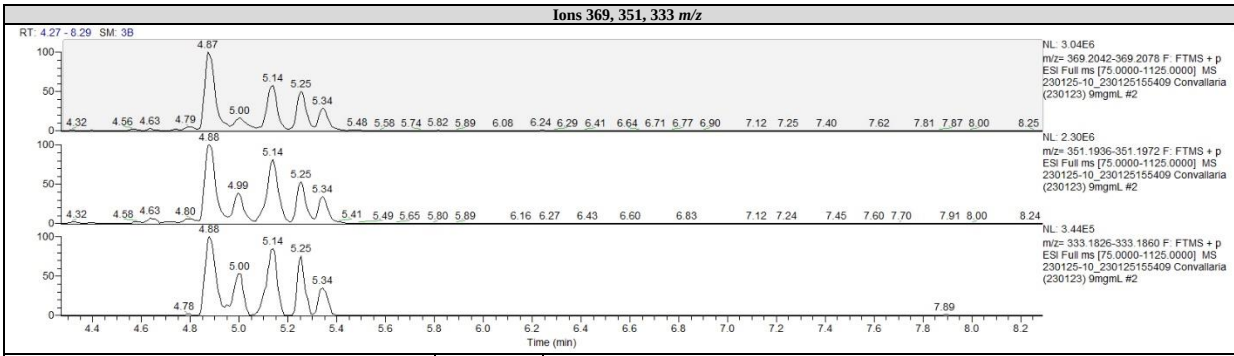

General Observations	RT	Observed Peaks
Very clean EICs with very low baseline. Strong (≥E6) to adequate (≥E5) abundances for all ions. Very consistent chromatograms across replicates.	4.78 – 5.36	Series of 5 peaks at 4.86 – 4.88, 4.99 – 5.01, 5.13 – 5.15, 5.24 – 5.26, and 5.33 – 5.35. Present in all ions. Main peaks that appear in chromatogram at ions 369, 351, 333.

Ions 371, 353, 335 *m/z*

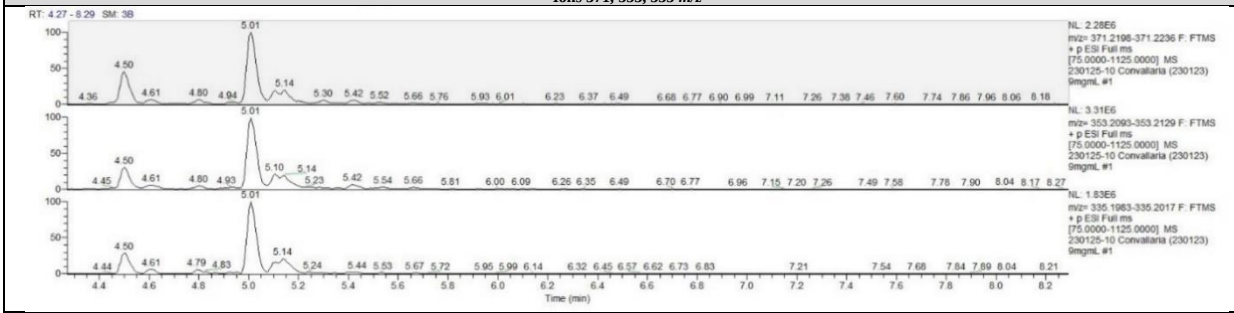

General Observations	RT	Observed Peaks	RT	Observed Peaks
Very clean EICs with very low baseline. Strong (≥E6) abundances for all ions. Very consistent chromatograms across replicates.	**4.49 – 4.51**	**Medium peak present in all ions.**	**5.00 – 5.02**	**Major peak in all ions.**
	4.60 – 4.64	Small peak present in all ions.	5.09 – 5.11	Present in all ions.
	4.79 – 4.81	Small peak present in all ions.		

Ions 373, 355, 337 *m/z*

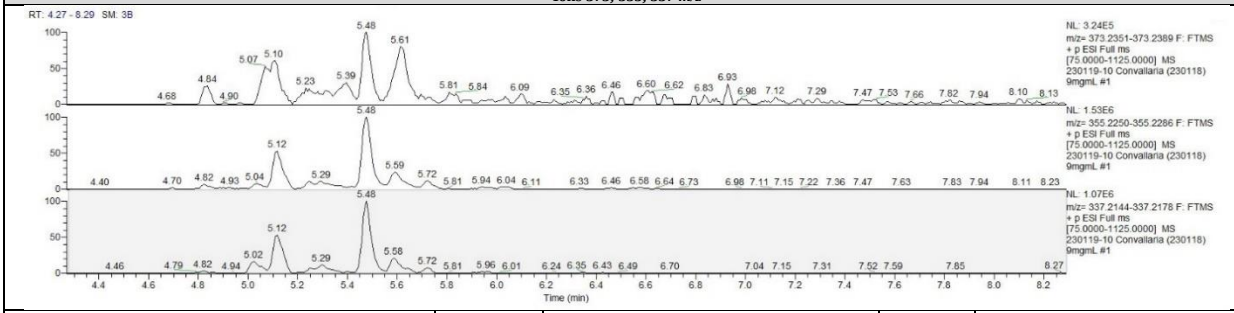

General Observations	RT	Observed Peaks	RT	Observed Peaks
Strong (≥E6) to adequate (≥E5) abundances for all ions. Higher/noisier baseline. Consistent chromatograms across replicates.	4.84 – 4.85	Small peak present in all ions. Most prominent in ion 373.	**5.47 – 5.49**	**Major peak for all ions.**
	5.11 – 5.13	**Major peak for all ions. Most prominent in ions 355, 337.**	5.60 – 5.62	Most prominent in ion 373.

Ions 375, 357, 339 *m/z*

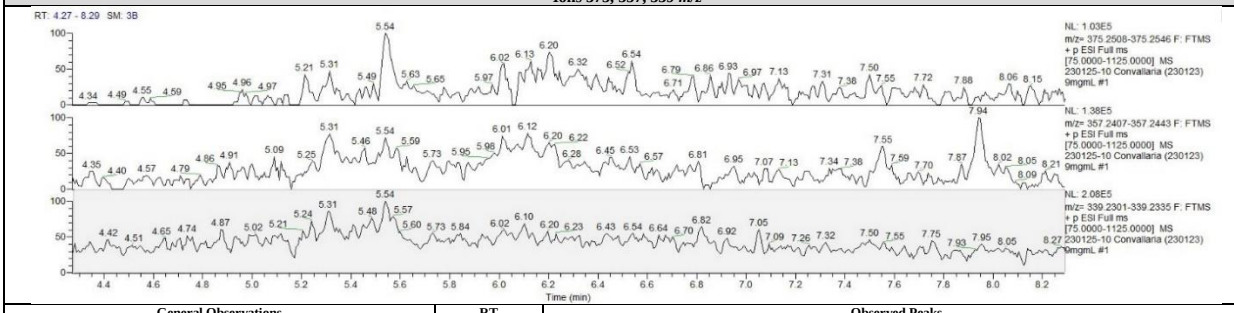

General Observations	RT	Observed Peaks
Adequate abundances (≥E5) but poor/noisy chromatogram with high/noisy baseline. Inconsistent chromatograms across replicates.	**5.30 – 5.32**	Peak that seems to consistently show up across replicates for all ions. However, given the high noise and poor peak shape, its reliability should be scrutinized.
	5.53 – 5.55	Peak that seems to consistently show up across replicates for all ions. However, given the high noise and poor peak shape, its reliability should be scrutinized.

Ions 433, 405, 391, 389, 375 *m/z* (genins)

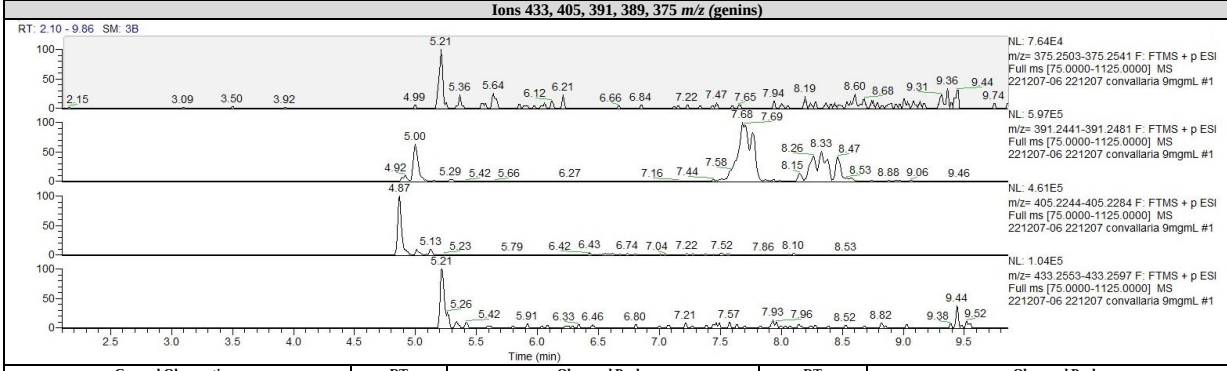

General Observations	RT	Observed Peaks	RT	Observed Peaks
Adequate (≥E5) abundances for ions 391, 405, and 433. Poor (≥E4) abundance for ion 375. Clean EICs.	**4.86 – 4.88**	**Major peak in ion 405.**	7.67 – 7.69, 7.68 – 7.70	Major peaks in ion 391. May appear unresolved from each other.
	4.99 – 5.01	**Major peak in ion 391.**	8.14 – 8.54	Series/group of peaks in ion 391.
	5.20 – 5.21	**Major peak in ion 375.** **Major peak in ion 433.**		

3.2.11 *Digitalis purpurea*

Ions 369, 351, 333 *m/z*

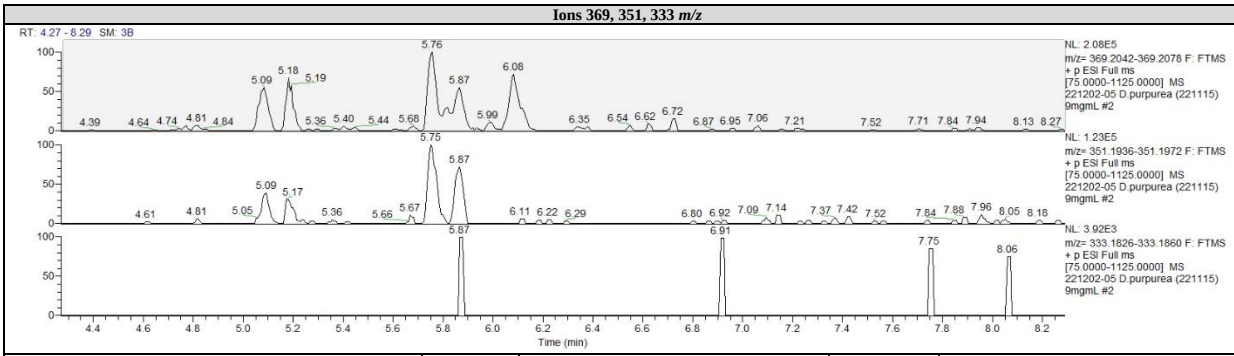

General Observations	RT	Observed Peaks	RT	Observed Peaks
Adequate (≥E5) abundances for ions 387, 369, 351. Poor abundance (≤E4) for ion 333. Ion 333 does not appear to be present in *D. purpurea*.	**5.08 – 5.10**	**Major peak in ions 369, 351.**	5.86 – 5.88	Present in ions 387, 369, 351.inn
	5.18 – 5.20	**Major peak in ions 369, 351**	**6.07 – 6.09**	**Major peak in ion 369.**
	5.75 – 5.77	**Major peak in ions 369, 351.**		

Ions 371, 353, 335 *m/z*

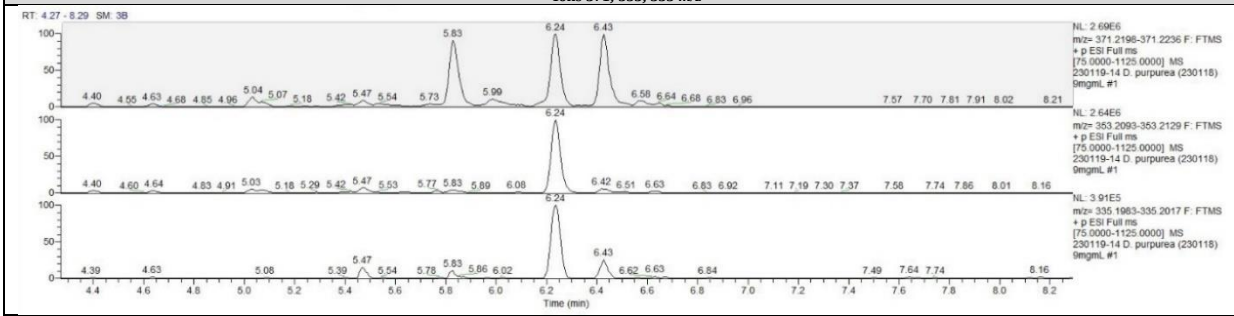

General Observations	RT	Observed Peaks	RT	Observed Peaks
Strong (≥E6) to adequate (≥E5) abundances for all ions. Clean EICs with low baseline/noisy. Smooth peak shapes. Very consistent chromatograms across replicates.	5.03 – 5.05	Present in all ions. May be a major peak in all ions.	**6.23 – 6.25**	**Major peak in all ions.**
	5.82 – 5.84	**Major peak in ion 371.**	**6.42 – 6.44**	**Major peak in ion 371. May be a major peak in ion 335.**

Ions 373, 355, 337 *m/z*

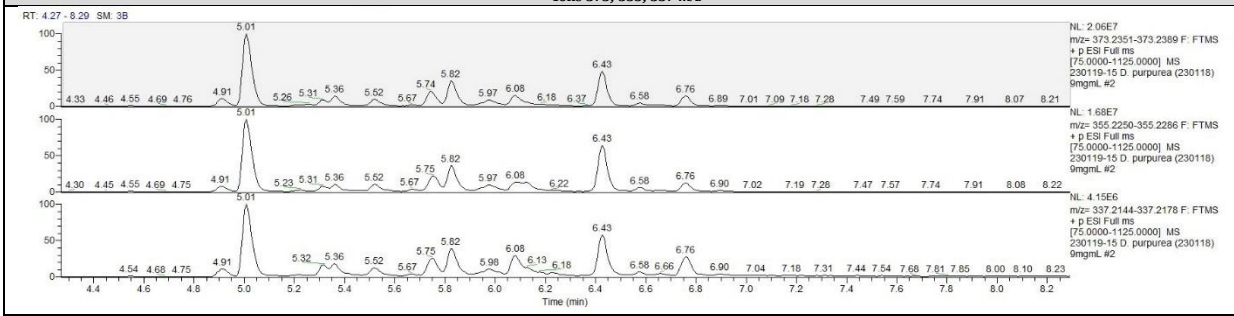

General Observations	RT	Observed Peaks	RT	Observed Peaks
Strong (≥E6) abundances for all ions. Clean EICs with low baseline/noisy. Smooth peak shapes. Very consistent chromatograms across replicates.	**5.00 – 5.02**	**Major peak ions all ions.**	6.07 – 6.09	Present in all ions.
	5.34- 5.36	Small to Medium peak present in all ions.	**6.42 – 6.44**	**Major peak in all ions.**
	5.73 – 5.75	Present in all ions.	6.75 – 6.77	Present in all ions.
	5.81 – 5.83	Present in all ions. May be a major peak in all ions.		

Ions 375, 357, 339 *m/z*

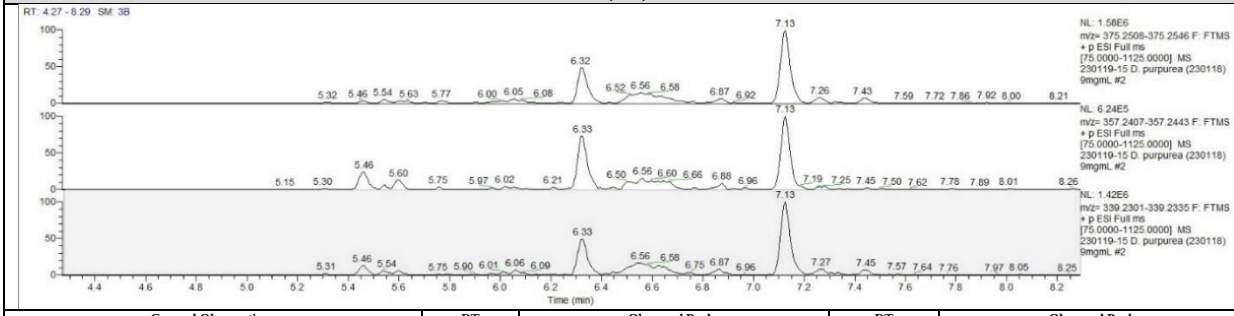

General Observations	RT	Observed Peaks	RT	Observed Peaks
Strong (≥E6) to adequate (≥E5) abundances for all ions. Clean EICs with low baseline/noise. Smooth peak shapes. Very consistent chromatograms across replicates.	5.45 – 5.47	Small to medium peak present in all ions.	6.50 – 6.90	May appear as a series of small peaks.
	6.32 – 6.34	**Major peak for all ions**	**7.12 – 7.14**	**Major peak in all ions.**

Ions 433, 405, 391, 389, 375 *m/z* (genins)

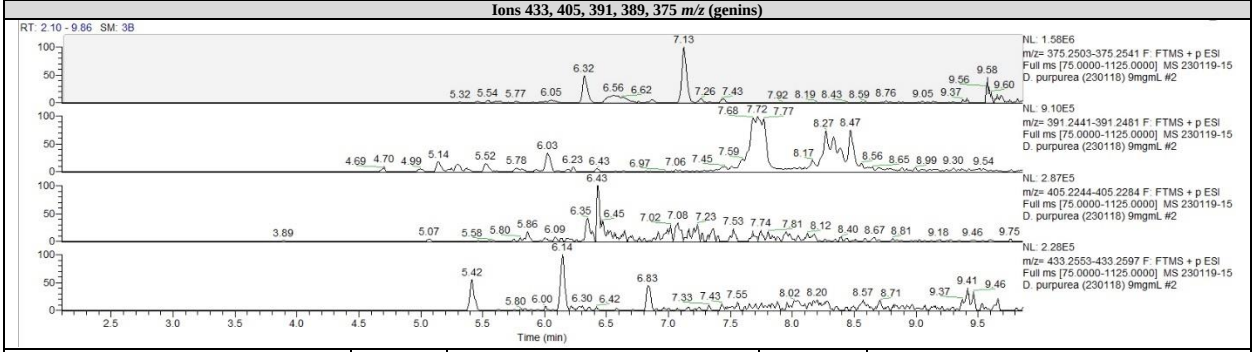

General Observations	RT	Observed Peaks	RT	Observed Peaks
Strong (≥E6) to adequate (≥E5) abundances for all ions. Noisy EIC for ion 405, concentrated around 5.57 to 8.12.	5.41 – 5.43	Present in ion 433.	6.82 – 6.84	Present in ion 433.
	6.02 – 6.04	Present in ion 391.	**7.12 -7.14**	**Major peak in ion 375.**
	6.13 – 6.15	**Major peak in ion 433.**	**7.69 – 7.71, 7.71 – 7.73, 7.76 – 7.78**	**Major peak in ion 391. May appear unresolved from each other.**
	6.31 – 6.33	Present in ion 375.	8.16 – 8.48	Series/group of peaks in ion 405.
	6.42 – 6.44	**Major peak in ion 405.**		

3.2.12 *Nerium oleander*

Ions 387, 369, 351, 333 *m/z*

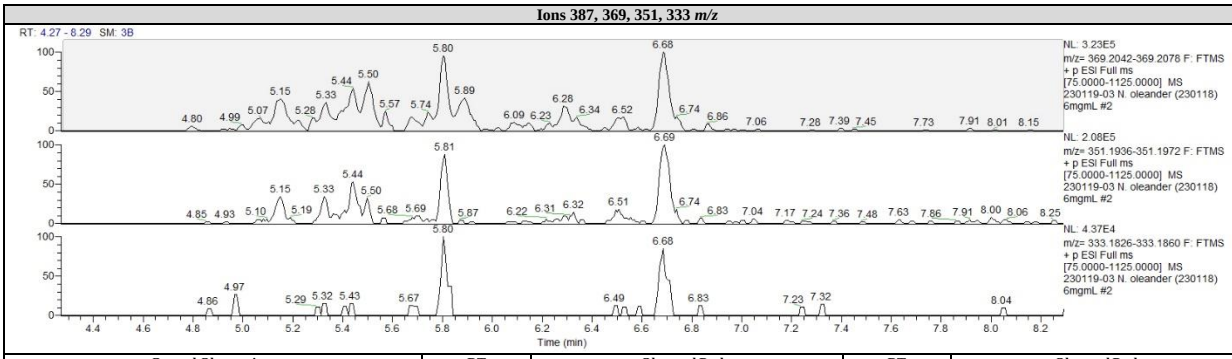

General Observations	RT	Observed Peaks	RT	Observed Peaks
Adequate (≥E5) abundances for ions 369, 351. Poor (≥E4) abundance for ion 333. Some noise for ions 369, 35, group of peaks concentrated around 5.08 – 5.58.	5.32 – 5.34	Present in all ions.	6.49 – 6.51	Present in all ions.
	5.79 – 5.81	Present in all ions.	**6.67 – 6.69**	**Major peak in all ions.**

Ions 371, 353, 335 *m/z*

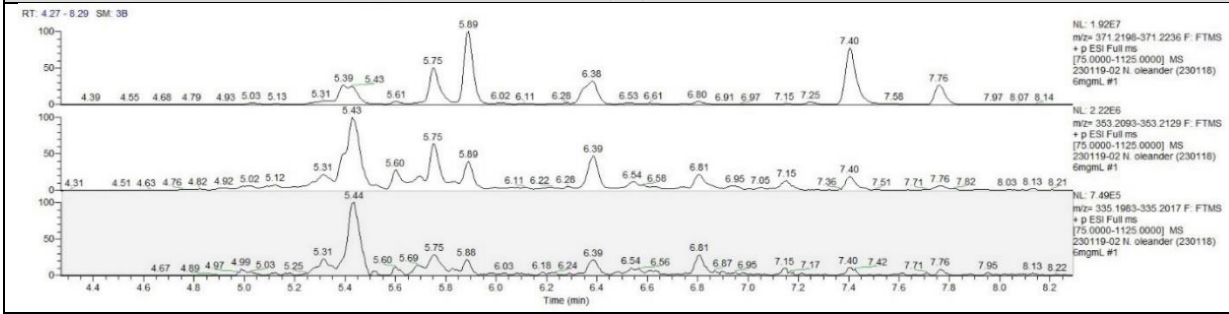

General Observations	RT	Observed Peaks	RT	Observed Peaks
Strong (≥E6) abundances for ions 371, 353, adequate (≥E5) abundance for ion 335. Little noise and low baseline.	**5.42 – 5.44**	**Major peak in ions 353, 335. Present in ion 371.**	6.37 – 6.39	Present in all ions. Most prominent in ions 371, 353.
	5.59 – 5.61	Small peak present in all ions.	6.79 – 6.81	Present in all ions.
	5.74 – 5.76	Present in all ions. Most prominent in ions 353, 335.	**7.39 – 7.41**	**Major peak in ion 371. Present in ions 353, 335.**
	5.88 – 5.90	**Major peak in ion 371. Present in ions 353, 335.**	7.75 – 7.77	Present in all ions. Most prominent in ion 371.

Ions 373, 355, 337 *m/z*

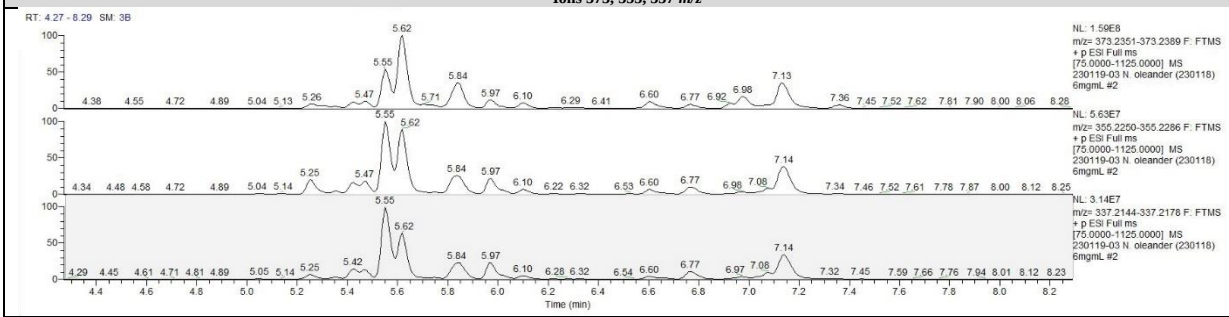

General Observations	RT	Observed Peaks	RT	Observed Peaks
Strong (≥E6) abundances for all ions. Clean chromatogram with low baseline/noise. Smooth peak shapes. Very consistent chromatograms across replicates.	5.24 – 5.26	Small peak present in all ions. Most prominent in ion 355.	5.83 – 5.85	Small to Medium peak present in all ions.
	5.54 – 5.56	**Major peak for all ions**	5.96 – 5.98	Small to Medium peak present in all ions.
	5.61 – 5.63	**Major peak for all ions**	7.12 – 7.14	**Major peak in all ions.**

Ions 375, 357, 339 *m/z*

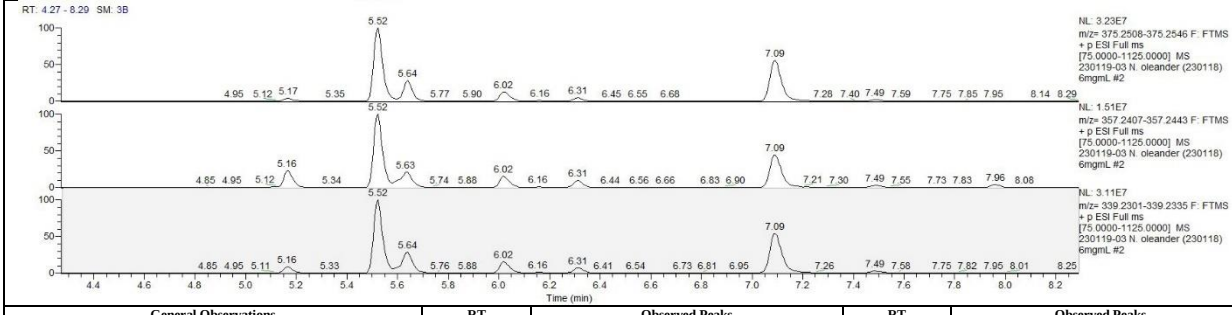

General Observations	RT	Observed Peaks	RT	Observed Peaks
Strong (≥E6) abundances for all ions. Clean chromatogram with low baseline/noise. Smooth peak shapes. Very consistent chromatograms across replicates.	**5.51 – 5.53**	**Major peak in all ions.**	6.30 – 6.32	Small peak present in all ions.
	5.63 – 5.65	Small peak present in all ions.	**7.08 – 7.10**	**Major peak in all ions.**
	6.01 – 6.03	Small peak present in all ions.		

Ions 433, 405, 391, 389, 375 *m/z* (genins)

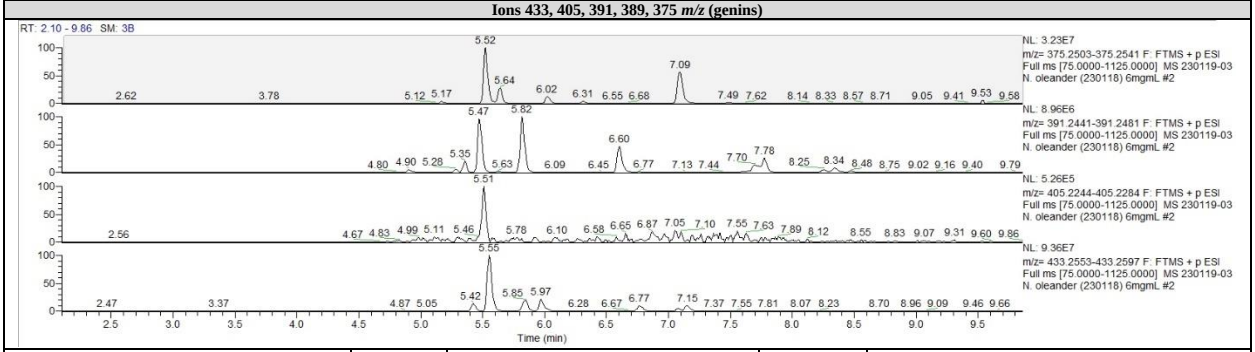

General Observations	RT	Observed Peaks	RT	Observed Peaks
Strong (≥E6) to adequate (≥E5) abundances for all ions. Clean EICs across all ions.	5.34 – 5.36	Present in ion 391.	5.84 – 5.86	Present in ion 433
	5.46 – 5.48	**Major peak in ion 391.**	5.96 – 5.98	Present in ion 433.
	5.50 – 5.52	**Major peak in ion 405.**	6.01 – 6.03	Present in ion 375.
	5.51 – 5.53	**Major peak in ion 375.**	**6.59 – 6.61**	**Major peak in ion 391.**
	5.54 – 5.56	**Major peak in ion 433.**	**7.08 – 7.10**	**Major peak in ion 375**
	5.63 – 5.65	Present in ion 375.	7.69 – 7.71, 7.77 – 7.79	Present in ion 391. May appear unresolved from each other.
	5.81 – 5.83	**Major peak in ion 391.**		

3.2.13 *Ornithogalum fimbrimarginatum*

Ions 387, 369, 351, 333 *m/z*

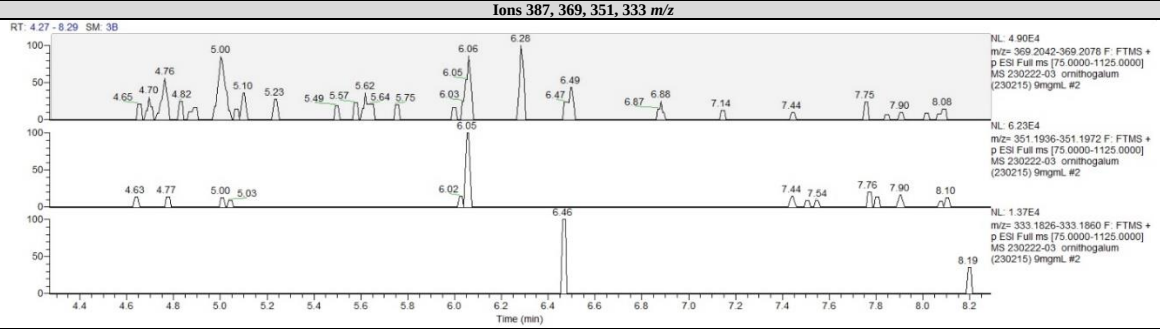

General Observations	RT	Observed Peaks
Poor chromatogram, noisy, poor signal/abundances (≤E4) in all ions. It appears that ions 369, 351, and 333 are not present in *O. fimbrimarginatum*.	-	-

Ions 371, 353, 335 *m/z*

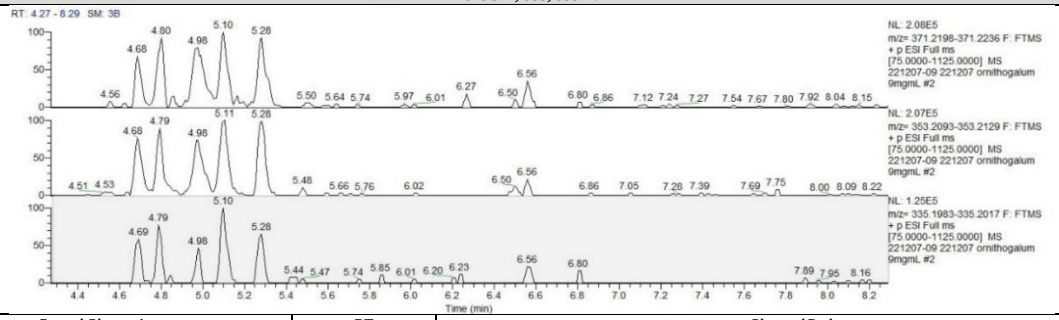

General Observations	RT	Observed Peaks
Adequate (≥E5) abundances for all ions. Low baseline/noise. Consistent chromatograms across replicates.	**4.55 – 5.30**	**Series of 5 peaks at 4.67 – 4.69, 4.79 – 4.81, 4.97 – 4.99, 5.09 – 5.11, and 5.27 – 5.29. Present in all ions.**
	6.55 – 6.57	Small peak present in all ions.

Ions 373, 355, 337 *m/z*

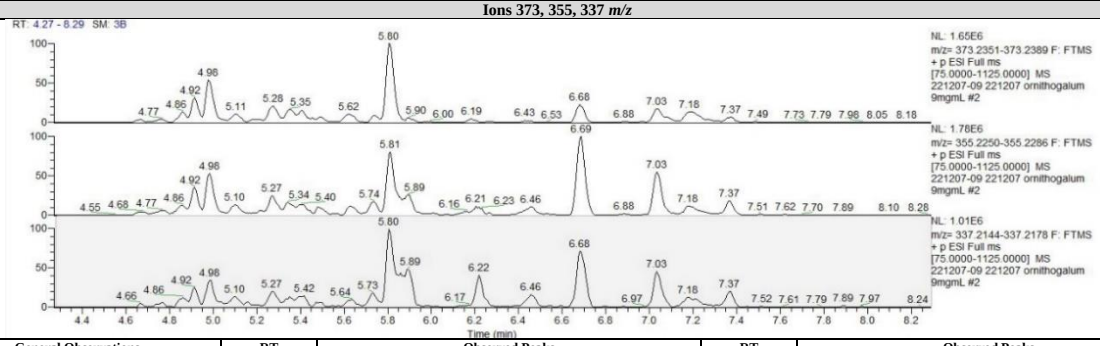

General Observations	RT	Observed Peaks	RT	Observed Peaks
Strong (≥E6) abundances for all ions. Low baseline but slightly noisy for 5.08 – 5.74. Consistent chromatograms across replicates.	4.91 – 4.99	Two peaks at 4.91 – 4.93 and 4.97 – 4.99. Present in all ions.	6.45 – 6.47	Small peak present in all ions.
	5.27 – 5.29	Small peak present in all ions.	**6.68 – 6.70**	**Major peak in all ions. Most prominent in ions 355, 337.**
	5.73 – 5.75	Present in all ions. May appear unresolved from 5.79 – 5.81 peak.	**7.02 – 7.04**	**Major peak present in all ions. Most prominent in ions 355, 337.**
	5.79 – 5.81	**Major peak in all ions.**	7.17 – 7.19	Small peak present in all ions.
	6.21 – 6.23	Present in all ions. Most prominent in ion 337.	7.36 -7.38	Present in all ions.

Ions 375, 357, 339 *m/z*

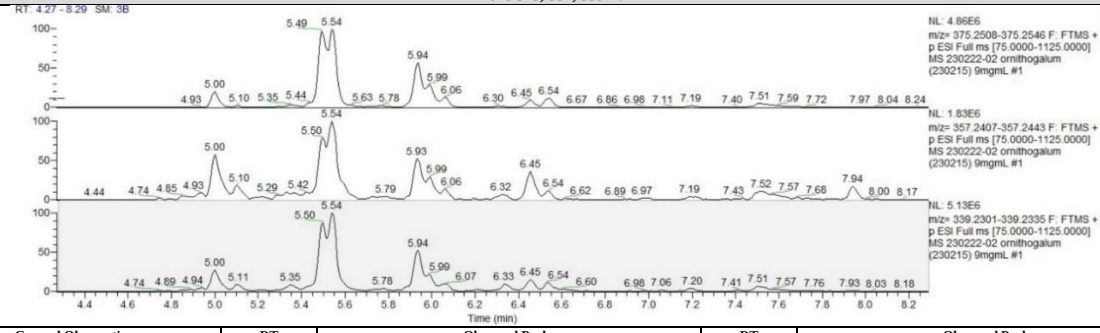

General Observations	RT	Observed Peaks	RT	Observed Peaks
Strong (≥E6) abundances for all ions. Low baseline and little noise. Consistent chromatograms across replicates.	4.99 – 5.01	Present in all ions.	5.93 – 5.95	Major peak in all ions.
	5.49 – 5.51	**Major peak in all ions. May appear unresolved from 5.53 – 5.55 peak.**	6.44 – 6.46	Major peak 357. Present in ions 375, 339.
	5.53 – 5.55	Major peak in all ions. May appear unresolved from 5.49 – 5.51 peak.		

Ions 433, 405, 391, 389, 375 *m/z* (genins)

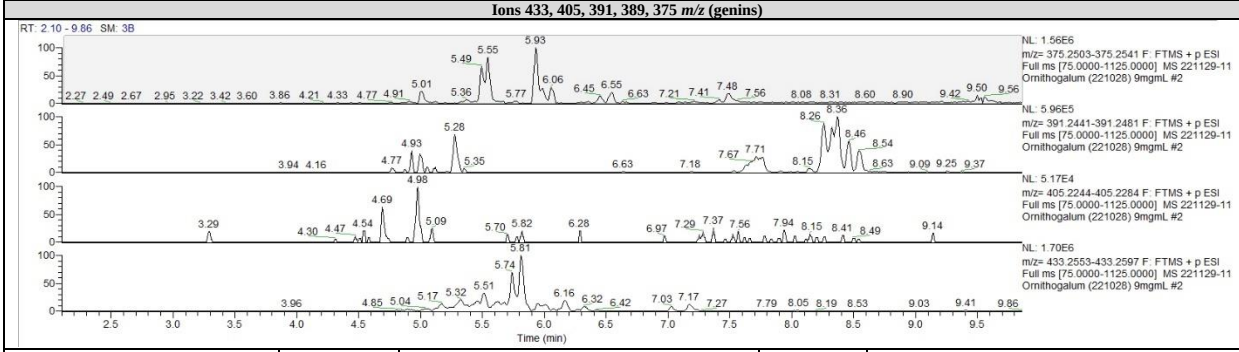

General Observations	RT	Observed Peaks	RT	Observed Peaks
Strong (≥E6) to adequate (≥E5) abundances for ions 375, 391, and 433. Poor (≥E4) for ion 405.	4.68 – 4.70	Present in ion 405.	5.48 – 5.50, 5.54 – 5.56	**Major peaks in ion 375. May appear unresolved from each other.**
	4.92 – 4.94	Present in ion 391.	**5.73 – 5.75, 5.80 – 5.82**	**Major peaks in ion 433. May appear unresolved from each other.**
	4.97 – 4.99	Majorpeak in ion 405.	5.92 – 5.94	**Major peak in ion 375.**
	5.00 – 5.02	Present in ion 375	**7.66 – 7.68, 7.70 – 7.72**	**Short peaks in ion 391, may appear unresolved from each other.**
	5.27 – 5.29	Present in ion 391.	**8.25 – 8.64**	**Series/group of peaks in ion 391.**

3.2.14 *Thevetia peruviana*

Ions 369, 351, 333 *m/z*

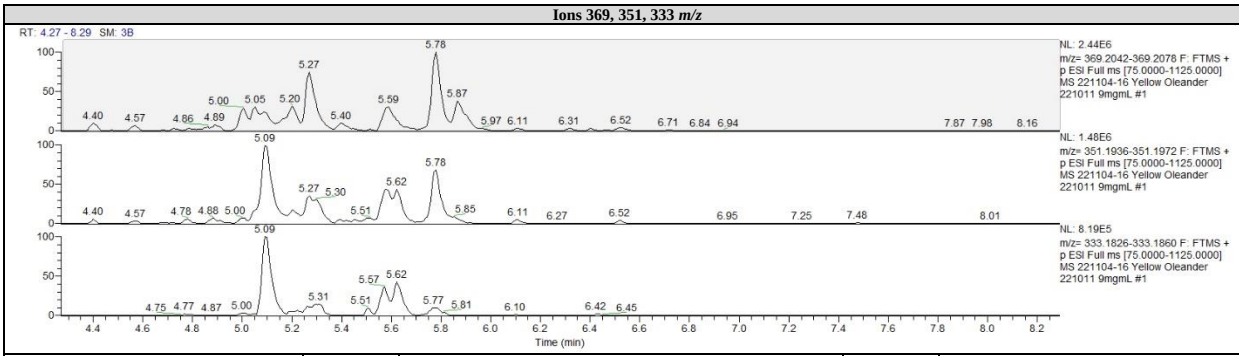

General Observations	RT	Observed Peaks	RT	Observed Peaks
Strong (≥E6) abundances for all ions. Low baseline and little noise. Consistent chromatograms across replicates.	4.56 – 4.58	Present in all ions.	5.58 – 5.60	Present in all ions.
	5.08 – 5.10	**Major peak present in all ions. Most prominent in ion 351, 333.**	**5.77 – 5.79**	**Major peak in ions 369, 351. Present in ion 333.**
	5.26 – 5.28	Present in all ions. Most prominent in ions 369, 351.	5.85 – 5.88	Most prominent in ions 369.

Ions 371, 353, 335 *m/z*

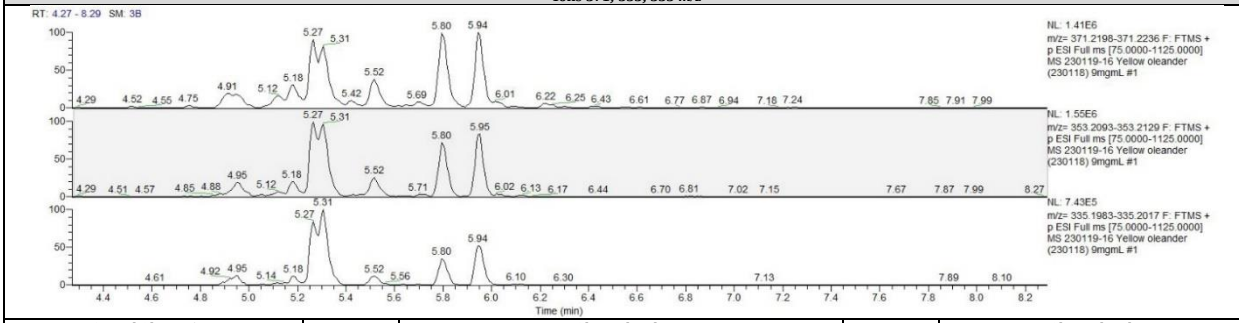

General Observations	RT	Observed Peaks	RT	Observed Peaks
Strong (≥E6) abundances for ions 371 and 353. Adequate (≥E6) abundance for ion 335. Low baseline and little noise. Very consistent chromatograms across replicates.	4.93 – 4.95	Present in all ions.	5.51- 5.53	Present in all ions.
	5.26 – 5.28	**Major peak in all ions. May appear unresolved from 5.30 – 5.32 peak.**	**5.79 – 5.81**	**Major peak in all ions.**
	5.30 – 5.32	**Major peak in all ions. May appear unresolved from 5.26 – 5.28 peak.**	**5.94 – 5.96**	**Major peak in all ions.**

Ions 373, 355, 337 *m/z*

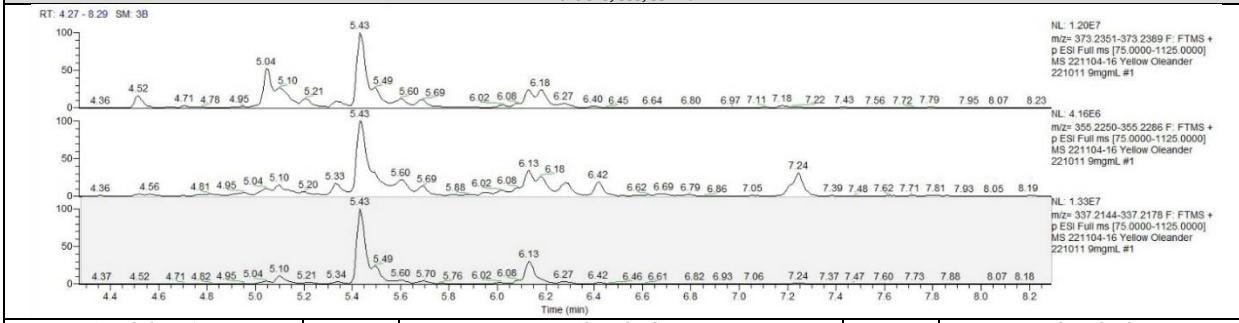

General Observations	RT	Observed Peaks	RT	Observed Peaks
Strong (≥E6) abundances for all ions. Low baseline and little noise. Consistent chromatograms across replicates.	4.51 – 4.53	Present in all ions. Most prominent in ion 373.	6.12 – 6.14	Present in all ions.
	5.03 – 5.05	**Present in all ions. Major peak in in ion 373.**	6.17 – 6.19	Present in all ions. May appear unresolved from 6.12 – 6.14 peak.
	5.33 – 5.35	Present in all ions.	6.41 – 6.43	Most prominent in ion 355.
	5.42 -5.44	**Major peak in all ions.**	**7.23 – 7.26**	**Major peak in ion 355.**

Ions 375, 357, 339 *m/z*

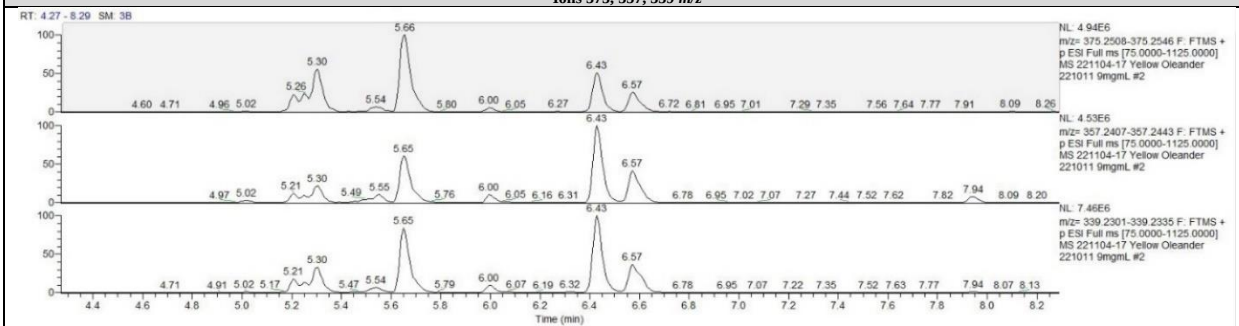

General Observations	RT	Observed Peaks	RT	Observed Peaks
Strong (≥E6) abundances for all ions. Very low baseline and little noise. Consistent chromatograms across replicates.	5.25 – 5.27	Present in all ions.	5.99 – 6.01	Present in all ions.
	5.29 – 5.31	Present in all ions. Most prominent in ion 375.	**6.42 – 6.44**	**Major peak in all ions.**
	5.65 – 5.67	**Major peak in all ions.**	**6.56 – 6.58**	**Major peak in all ions.**

Ions 433, 405, 391, 389, 375 *m/z* (genins)

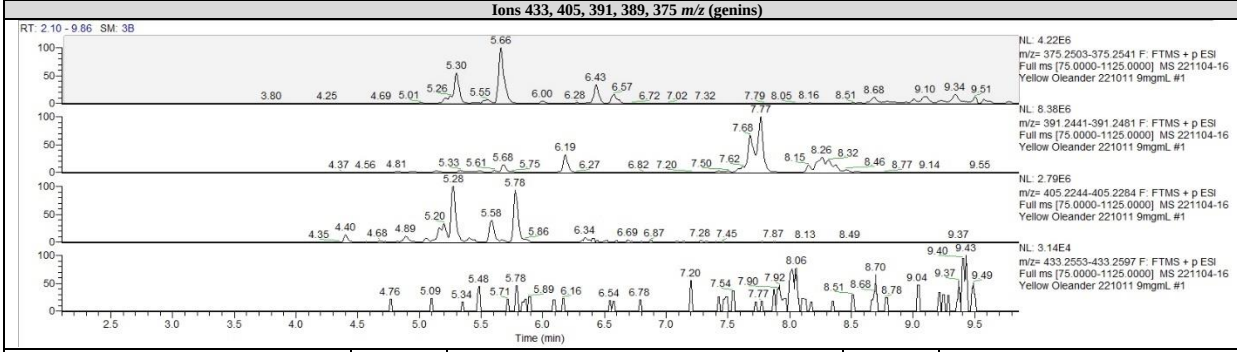

General Observations	RT	Observed Peaks	RT	Observed Peaks
Strong (≥E6) abundances for ions 375, 391, and 405. Poor (≥E4) abundance for ion 433. Noisy EIC for ion 433 without distinct peaks. Clean EICs for other ions.	5.19 – 5.21	Present in ion 405. May appear unresolved from 5.27 – 5.29 peak.	**5.65 – 5.67**	**Major peak in ion 375.**
	5.25 – 5.27	Present in ion 375. May appear unresolved from 5.29 – 5.31	**5.77 – 5.79**	**Major peak in ion 405.**
	5.27 – 5.29	**Major peak in ion 405.**	6.18 – 6.20	Present in ion 391.
	5.29 – 5.31	Present in ion 375.	**7.68 – 7.70, 7.76 – 7.78**	**Major peaks in ion 391. May appear unresolved from each other.**
	5.57 – 5.59	Present in ion 405.	8.14 – 8.47	Series/group of small peaks in ion 391.

3.2.15 *Heteromeles arbitufolia*

Ions 369, 351, 333 *m/z*

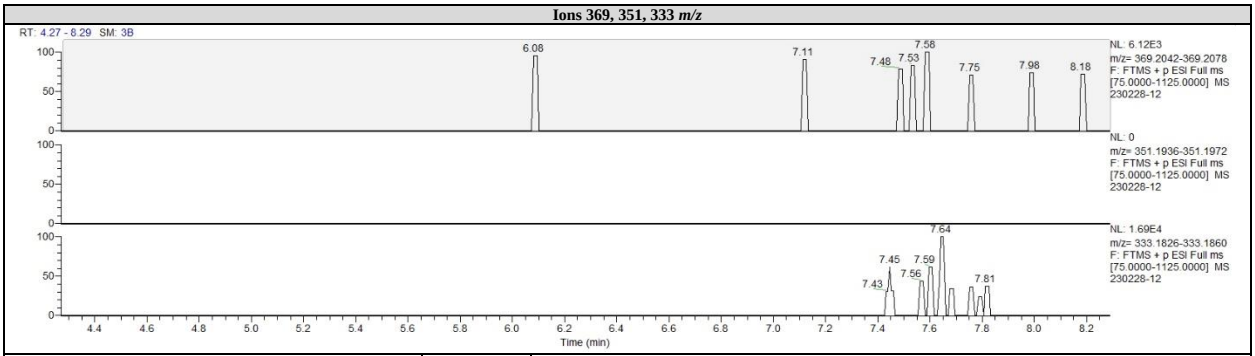

General Observations	RT	Observed Peaks
Very bare EICs. Low abundances for all ions (≤E4) and no clear signs of peaks.	-	-

Ions 371, 353, 335 *m/z*

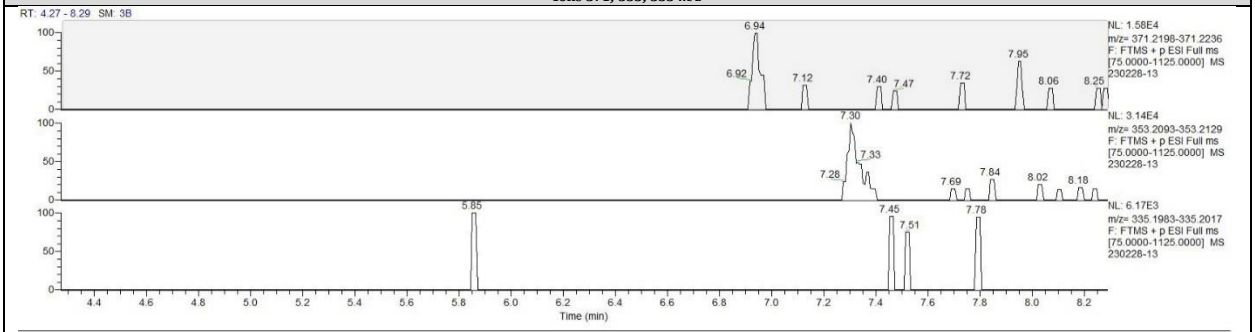

General Observations	RT	Observed Peaks
Very bare EICs. Low abundances (≤E4) for all ions. No clear signs of peaks; any peaks that appear to be present lack distinction.	6.92 – 6.94, 7.29 – 7.31	May appear to have peaks, but poor peak shape, low abundances, and lack of peaks at the same RT in all three ions makes it unlikely that this is from a CG. A CG would exhibit the same pattern across all 3 ions, due to the loss of 18 fragmentation pattern discussed earlier.

Ions 373, 355, 337 *m/z*

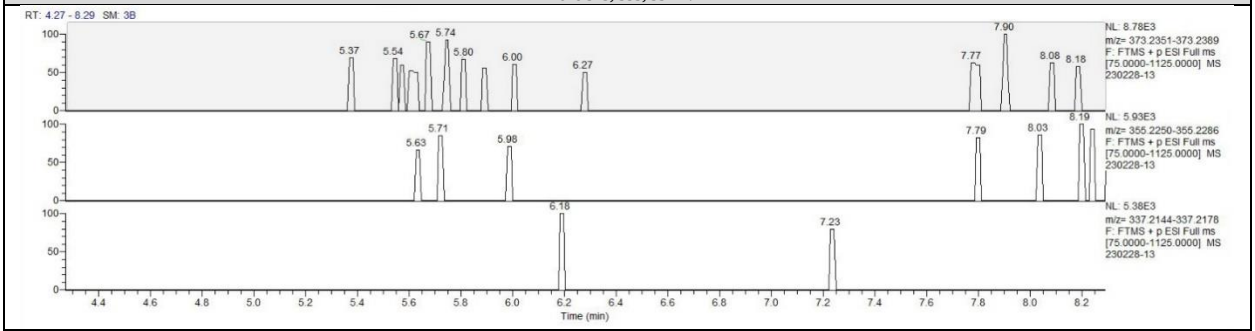

General Observations	RT	Observed Peaks
Very bare EICs. Low abundances (≤E4) for all ions. No clear signs of peaks.	-	-

Ions 375, 357, 339 *m/z*

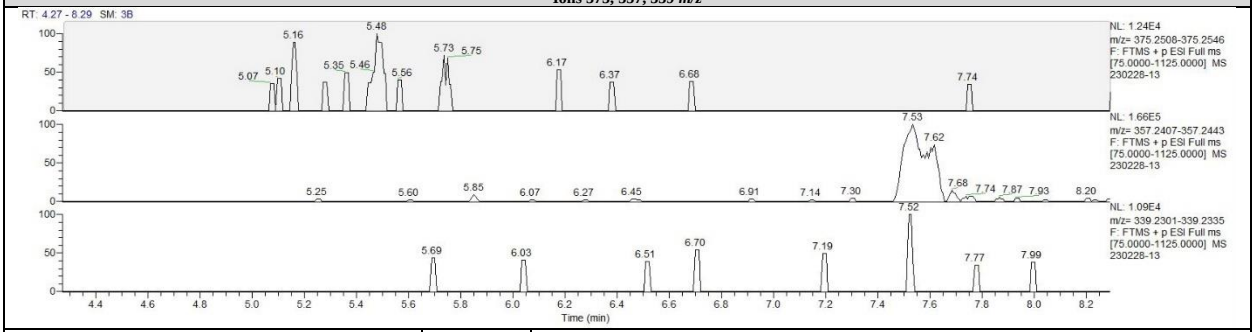

General Observations	RT	Observed Peaks
Very bare EICs. Low abundances (≤E4) for ions 375 and 339. No clear signs of peaks; any peaks that appear to be present lack distinction.	5.47 – 5.49, 7.52 – 7.54	May appear to have peaks, but poor peak shape and lack of peaks at the same RT in all three ions makes it unlikely that this is from a CG.

Ions 433, 405, 391, 389, 375 *m/z* (genins)

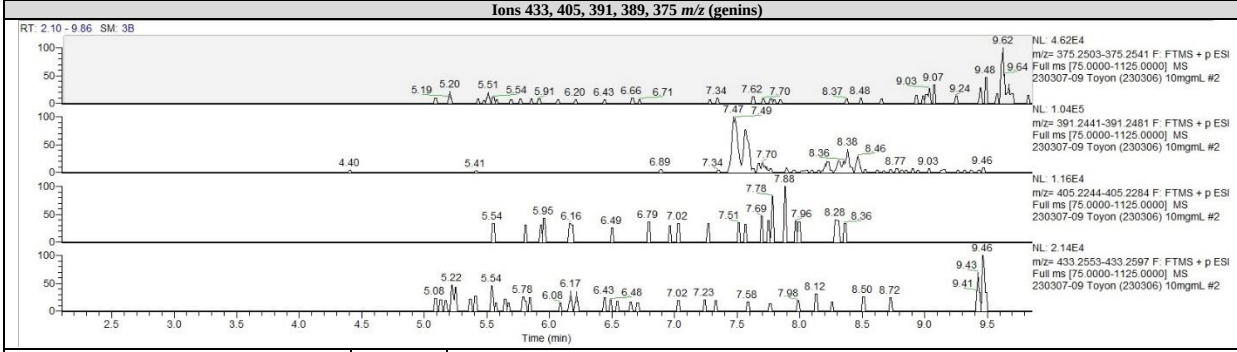

General Observations	RT	Observed Peaks
Adequate (≥E5) to poor (≥E4) abundances for all ions. No clear signs of peaks in EIC of ion 405.	7.46 – 7.48, 7.48 – 7.50	Present in ion 391.
	8.35 – 8.47	Group/series of small peaks in ion 391.

3.2.16 *Taxus baccata*

Ions 387, 369, 351, 333 *m/z*

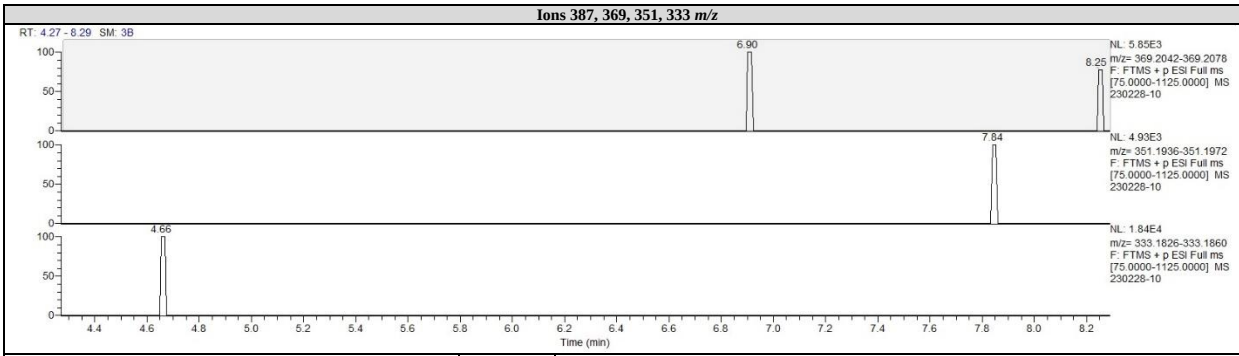

General Observations	RT	Observed Peaks
Very bare EICs. Low abundances for all ions (≤E4) and no clear signs of peaks	-	-

Ions 371, 353, 335 *m/z*

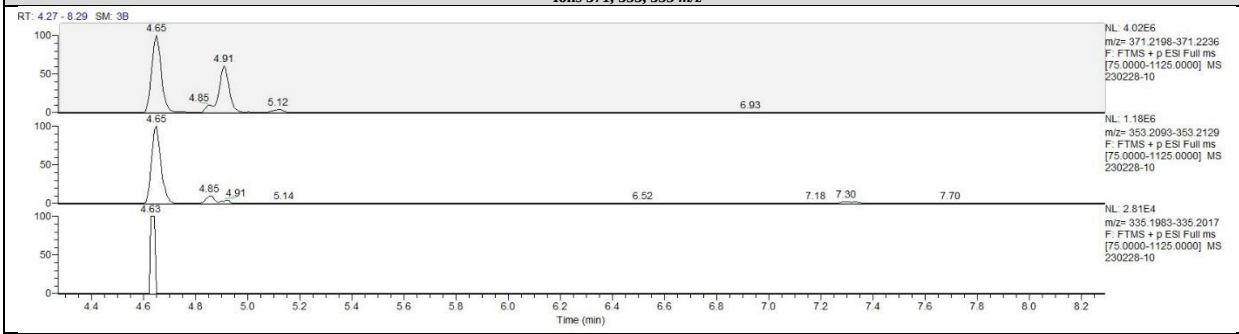

General Observations	RT	Observed Peaks
Very bare EICs. Low abundance (≤E4) for ion 335. Strong abundance (≥E6) for ions 371 and 353.	4.66 – 4.56, 4.84 – 4.86, 4.90 – 4.92	Appears to have a major peak for ions 371 and 353 at 4.64 - 4.66. However, the peak is poorly shaped with a low abundance in ion 335. Similarly, the 4.84 – 4.86 and 4.90 – 4.92 peaks are not present in ion 335.

Ions 373, 355, 337 *m/z*

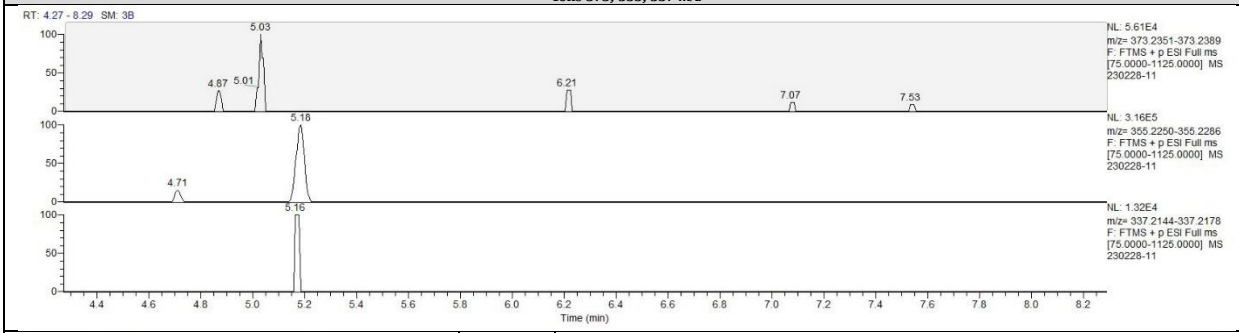

General Observations	RT	Observed Peaks
Very bare EICs. Low abundances for all ions (≤E4) and no clear signs of peaks	5.16 – 5.18	May appear to have a peak for ions 355 and 337. However, the peak is not present for ion 373. Typically, for CGs, if peaks in the lower mass (330s, 350s m/z) ions are present, it should be present in the highest mass (370s m/z) ion as well.

Ions 375, 357, 339 *m/z*

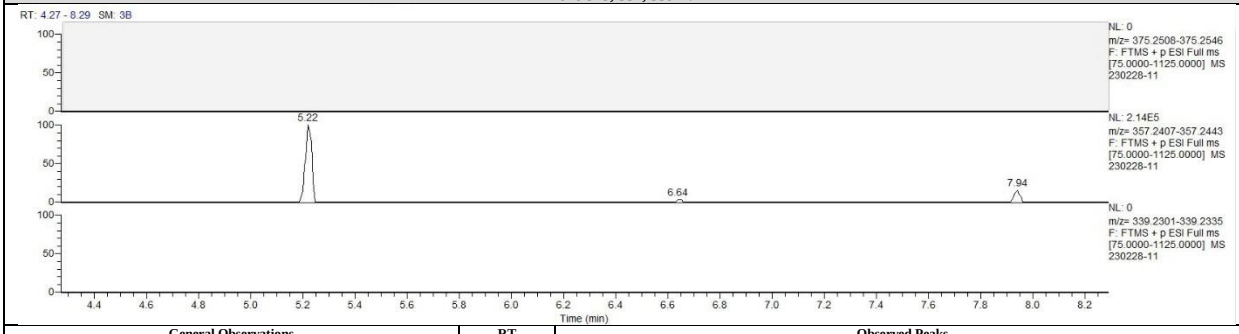

General Observations	RT	Observed Peaks
Very bare EICs. Low abundances for all ions (≤E4) and no clear signs of peaks	-	-

Ions 433, 405, 391, 389, 375 *m/z* (genins)

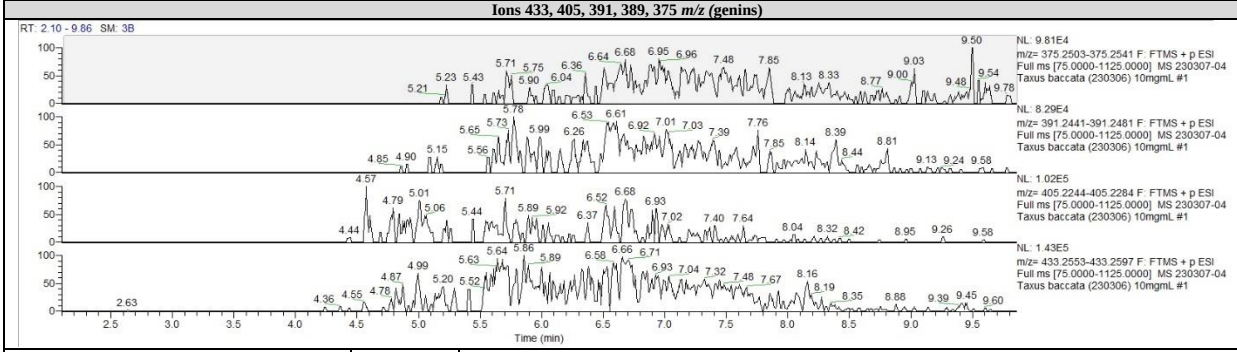

General Observations	RT	Observed Peaks
Adequate(≥E5) abundances for ions 405 and 433. Low abundances (≤E4) for ions 375 and 391. Very noisy EICs for all ions. No distinct peaks.	-	-

3.2.17 *Prunus laurocerasus*

Ions 369, 351, 333 *m/z*

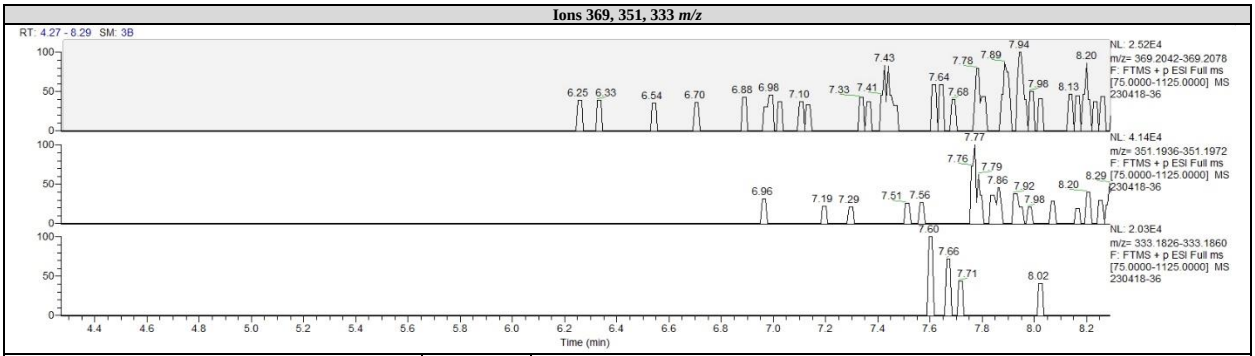

General Observations	RT	Observed Peaks
Low abundances for all ions (≤E4) and no clear signs of peaks	-	-

Ions 371, 353, 335 *m/z*

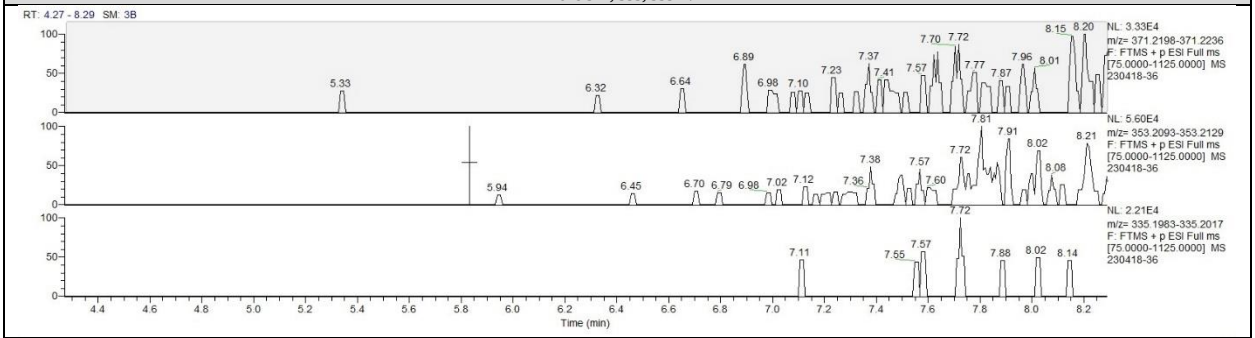

General Observations	RT	Observed Peaks
Low abundances for all ions (≤E4) and no clear signs of peaks	-	-

Ions 373, 355, 337 *m/z*

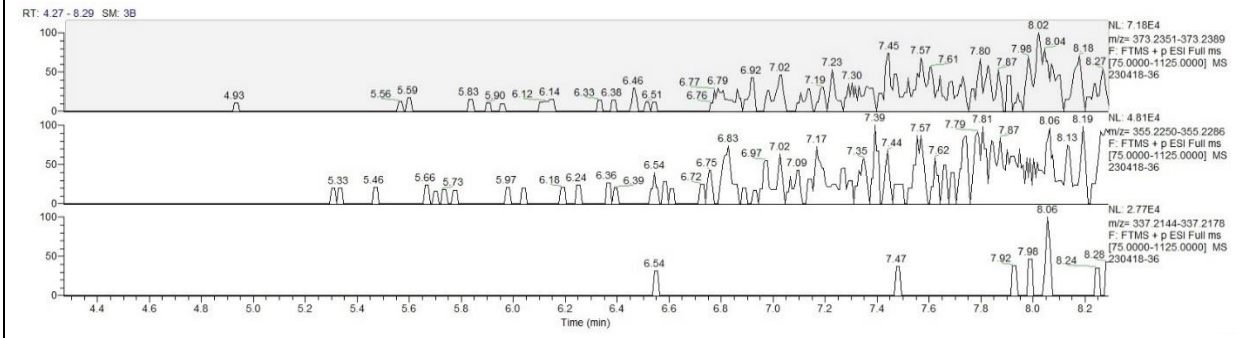

General Observations	RT	Observed Peaks
Low abundances for all ions (≤E4) and no clear signs of peaks	-	-

Ions 375, 357, 339 *m/z*

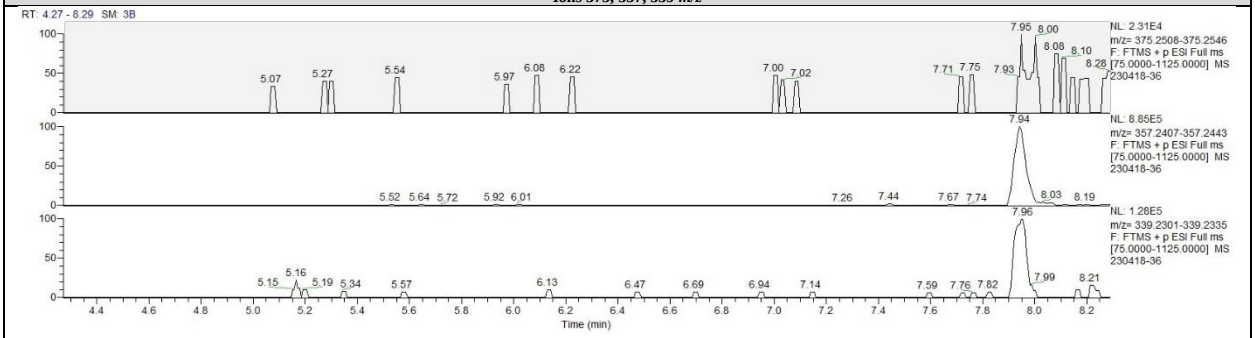

General Observations	RT	Observed Peaks
Very bare chromatogram. Low abundances for all ions (≤E4) and no clear signs of peaks	7.93 – 7.95	Appears to have peak here for ions 375, 357, 339. However, low abundance for ion 375 and poor peak shape compared to ions 357 and 339. Typically for CGs, peaks for highest mass ion (e.g. ion 375 here) show the highest abundance.

Ions 433, 405, 391, 389, 375 *m/z* (genins)

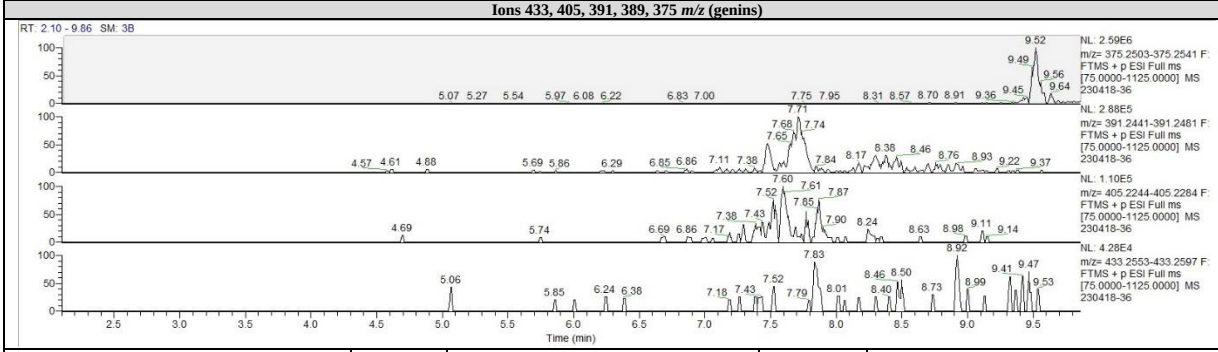

General Observations	RT	Observed Peaks	RT	Observed Peaks
Strong (≥E6) to adequate (≥E5) to poor (≥E4) abundances for ions. Lack of distinct peaks.	**7.64 – 7.66, 7.70 – 7.72**	**Major peaks in ion 391.**	**9.51 – 9.53**	**Major peak in ion 375.**
	7.42 – 7.91	Group/series of peaks in ion 405.		

3.3 Blind Test 1: Identification of Cardenolide-containing Plants

3.3.1 Using “High” Ion Grouping

	Cardenolide-containing (True)	Non-cardenolide-containing (True)	Proposed Total
Cardenolide-containing (Proposed)	16	0	16
Non-cardenolide-containing (Proposed)	0	16	16
True Total	16	16	32

Individual Test			**Overall Test**
CC Plants	**16/16 = 1.00**	**1.00 > 0.500**	**32/32 = 1.00** **1.00 > 0.50**
Non-CC Plants	**16/16 = 1.00**	**1.00 > 0.500**	

3.3.2 Using “Medium” Ion Grouping

	Cardenolide-containing (True)	Non-cardenolide-containing (True)	Proposed Total
Cardenolide-containing (Proposed)	16	0	16
Non-cardenolide-containing (Proposed)	0	16	16
True Total	16	16	32

Individual Test			**Overall Test**
CC Plants	**16/16 = 1.00**	**1.00 > 0.500**	**32/32 = 1.00** **1.00 > 0.50**
Non-CC Plants	**16/16 = 1.00**	**1.00 > 0.500**	

3.3.3 Using “Low” Ion Grouping

	Cardenolide-containing (True)	Non-cardenolide-containing (True)	Proposed Total
Cardenolide-containing (Proposed)	16	0	16
Non-cardenolide-containing (Proposed)	0	16	16
True Total	16	16	32

Individual Test			**Overall Test**
CC Plants	**16/16 = 1.00**	**1.00 > 0.500**	**32/32 = 1.00** **1.00 > 0.50**
Non-CC Plants	**16/16 = 1.00**	**1.00 > 0.500**	

3.3.4 Using “Genin” Ion Grouping

	Cardenolide-containing (True)	Non-cardenolide-containing (True)	Proposed Total
Cardenolide-containing (Proposed)	16	0	16
Non-cardenolide-containing (Proposed)	0	16	16
True Total	16	16	32

Individual Test			**Overall Test**
CC Plants	**16/16 = 1.00**	**1.00 > 0.500**	**32/32 = 1.00** **1.00 > 0.50**
Non-CC Plants	**16/16 = 1.00**	**1.00 > 0.500**	

3.4 Blind Test 2: Individual Plant Classifications

3.4.1 Using "High" Ion Grouping

		True ID														
		A. boe	***A. obe***	***A. ole***	***A. soc***	***A. cur***	***A. fas***	***A. spe***	***C. mac***	***C. odo***	***C. maj***	***D. pur***	***N. ole***	***O. fim***	***T. per***	**Proposed Total**
Proposed ID	***A. boe***	**8**	0	0	0	0	0	0	0	0	0	0	0	0	0	**8**
	A. obe	0	**8**	0	0	0	0	0	0	0	0	0	0	0	0	**8**
	A. ole	0	0	**7**	0	0	0	0	0	0	0	0	0	0	0	**7**
	A. soc	0	0	0	**8**	0	0	0	0	0	0	0	0	0	0	**8**
	A. cur	0	0	0	0	**7**	0	0	0	0	0	0	0	0	0	**7**
	A. fas	0	0	0	0	0	**8**	0	0	0	0	0	0	0	0	**8**
	A. spe	0	0	0	0	0	0	**7**	0	0	0	0	0	0	0	**7**
	C. mac	0	0	0	0	0	0	0	**7**	0	0	0	0	0	0	**7**
	C. odo	0	0	0	0	0	0	0	0	**8**	0	0	0	0	0	**8**
	C. maj	0	0	0	0	0	0	0	0	0	**7**	0	0	0	0	**7**
	D. pur	0	0	0	0	0	0	0	0	0	0	**8**		0	0	**8**
	N. ole	0	0	0	0	0	0	0	0	0	0		**8**	0	0	**8**
	O. fim	0	0	0	0	0	0	0	0	0	0	0	0	**7**	0	**7**
	T. per	0	0	0	0	0	0	0	0	0	0	0	0	0	**7**	**7**
	True Total	**8**	**8**	**7**	**8**	**7**	**8**	**7**	**7**	**8**	**7**	**8**	**8**	**7**	**7**	**105**

Individual Test			**Overall Test**
A. boehmianum	8/8 = 1.00	1.00 > 0.0714	105/105 = 1.00 1.00 > 0.0714
A. obesum	8/8 = 1.00	1.00 > 0.0714	
A. oleifolium	7/7 = 1.00	1.00 > 0.0714	
A. socotranum	8/8 = 1.00	1.00 > 0.0714	
A. curassavica	7/7 = 1.00	1.00 > 0.0714	
A. fascicularis	8/8 = 1.00	1.00 > 0.0714	
A. speciosa	7/7 = 1.00	1.00 > 0.0714	
C. macrocarpa	7/7 = 1.00	1.00 > 0.0714	
C. odollam	8/8 = 1.00	1.00 > 0.0714	
C. majalis	7/7 = 1.00	1.00 > 0.0714	
D. purpurea	8/8 = 1.00	1.00 > 0.0714	
N. oleander	8/8 = 1.00	1.00 > 0.0714	
O. fimbrimarginatum	7/7 = 1.00	1.00 > 0.0714	
T. peruviana	7/7 = 1.00	1.00 > 0.0714	

3.4.2 Using "Medium" Ion Grouping

		True ID														
		A. boe	***A. obe***	***A. ole***	***A. soc***	***A. cur***	***A. fas***	***A. spe***	***C. mac***	***C. odo***	***C. maj***	***D. pur***	***N. ole***	***O. fim***	***T. per***	**Proposed Total**
Proposed ID	***A. boe***	8	0	0	0	0	0	0	0	0	0	0	0	0	0	**8**
	A. obe	0	8	0	0	0	0	0	0	0	0	0	0	0	0	**8**
	A. ole	0	0	7	0	0	0	0	0	0	0	0	0	0	0	**7**
	A. soc	0	0	0	8	0	0	0	0	0	0	0	0	0	0	**8**
	A. cur	0	0	0	0	7	0	0	0	0	0	0	0	0	0	**7**
	A. fas	0	0	0	0	0	8	0	0	0	0	0	0	0	0	**8**
	A. spe	0	0	0	0	0	0	7	0	0	0	0	0	0	0	**0**
	C. mac	0	0	0	0	0	0	0	7	0	0	0	0	0	0	**7**
	C. odo	0	0	0	0	0	0	0	0	8	0	0	0	0	0	**8**
	C. maj	0	0	0	0	0	0	0	0	0	7	0	0	0	0	**7**
	D. pur	0	0	0	0	0	0	0	0	0	0	8	0	0	0	**8**
	N. ole	0	0	0	0	0	0	0	0	0	0	0	8	0	0	**8**
	O. fim	0	0	0	0	0	0	0	0	0	0	0	0	7	0	**7**
	T. per	0	0	0	0	0	0	0	0	0	0	0	0	0	7	**7**
	True Total	**8**	**8**	**7**	**8**	**7**	**8**	**7**	**7**	**8**	**7**	**8**	**8**	**7**	**7**	**105**

Individual Test			**Overall Test**
A. boehmianum	8/8 = 1.00	1.00 > 0.0714	105/105 = 1.00 1.00 > 0.0714
A. obesum	8/8 = 1.00	1.00 > 0.0714	
A. oleifolium	7/7 = 1.00	1.00 > 0.0714	
A. socotranum	8/8 = 1.00	1.00 > 0.0714	
A. curassavica	7/7 = 1.00	1.00 > 0.0714	
A. fascicularis	8/8 = 1.00	1.00 > 0.0714	
A. speciosa	7/7 = 1.00	1.00 > 0.0714	
C. macrocarpa	7/7 = 1.00	1.00 > 0.0714	
C. odollam	8/8 = 1.00	1.00 > 0.0714	
C. majalis	7/7 = 1.00	1.00 > 0.0714	
D. purpurea	8/8 = 1.00	1.00 > 0.0714	
N. oleander	8/8 = 1.00	1.00 > 0.0714	
O. fimbrimarginatum	7/7 = 1.00	1.00 > 0.0714	
T. peruviana	7/7 = 1.00	1.00 > 0.0714	

3.4.3 Using "Low" Ion Grouping

		True ID														
		A. boe	***A. obe***	***A. ole***	***A. soc***	***A. cur***	***A. fas***	***A. spe***	***C. mac***	***C. odo***	***C. maj***	***D. pur***	***N. ole***	***O. fim***	***T. per***	**Proposed Total**
Proposed ID	***A. boe***	**8**	0	0	0	0	0	0	0	0	0	0	0	0	0	**8**
	A. obe	0	**8**	0	0	0	0	0	0	0	0	0	0	0	0	**8**
	A. ole	0	0	**7**	0	0	0	0	0	0	0	0	0	0	0	**7**
	A. soc	0	0	0	**8**	0	0	0	0	0	0	0	0	0	0	**8**
	A. cur	0	0	0	0	**7**	0	0	0	0	0	0	0	0	0	**7**
	A. fas	0	0	0	0	0	**7**	0	0	0	0	0	0	0	0	**7**
	A. spe	0	0	0	0	0	**1**	**7**	0	0	0	0	0	0	0	**8**
	C. mac	0	0	0	0	0	0	0	**7**	0	0	0	0	0	0	**7**
	C. odo	0	0	0	0	0	0	0	0	**8**	0	0	0	0	0	**8**
	C. maj	0	0	0	0	0	0	0	0	0	**7**	0	0	0	0	**7**
	D. pur	0	0	0	0	0	0	0	0	0	0	**8**	0	0	0	**8**
	N. ole	0	0	0	0	0	0	0	0	0	0	0	**8**	0	0	**8**
	O. fim	0	0	0	0	0	0	0	0	0	0	0	0	**7**	0	**7**
	T. per	0	0	0	0	0	0	0	0	0	0	0	0	0	**7**	**7**
	True Total	**8**	**8**	**7**	**8**	**7**	**8**	**7**	**7**	**8**	**7**	**8**	**8**	**7**	**7**	**105**

Individual Test			**Overall Test**
A. boehmianum	8/8 = 1.00	1.00 > 0.0714	104/105 = 0.990 0.990 > 0.0714
A. obesum	8/8 = 1.00	1.00 > 0.0714	
A. oleifolium	7/7 = 1.00	1.00 > 0.0714	
A. socotranum	8/8 = 1.00	1.00 > 0.0714	
A. curassavica	7/7 = 1.00	1.00 > 0.0714	
A. fascicularis	**7/8 = 0.875**	**0.875 > 0.0714**	
A. speciosa	7/7 = 1.00	1.00 > 0.0714	
C. macrocarpa	7/7 = 1.00	1.00 > 0.0714	
C. odollam	8/8 = 1.00	1.00 > 0.0714	
C. majalis	7/7 = 1.00	1.00 > 0.0714	
D. purpurea	8/8 = 1.00	1.00 > 0.0714	
N. oleander	8/8 = 1.00	1.00 > 0.0714	
O. fimbrimarginatum	7/7 = 1.00	1.00 > 0.0714	
T. peruviana	7/7 = 1.00	1.00 > 0.0714	

3.4.4 Using "Genins" Ion Grouping

		True ID														
		A. boe	***A. obe***	***A. ole***	***A. soc***	***A. cur***	***A. fas***	***A. spe***	***C. mac***	***C. odo***	***C. maj***	***D. pur***	***N. ole***	***O. fim***	***T. per***	**Proposed Total**
Proposed ID	***A. boe***	**8**	0	0	0	0	0	0	**1**	0	0	0	0	0	0	9
	A. obe	0	**8**	0	0	0	0	0	0	0	0	0	0	0	0	8
	A. ole	0	0	**7**	0	0	0	0	0	0	0	0	0	0	0	7
	A. soc	0	0	0	**8**	0	0	0	0	0	0	0	0	0	0	8
	A. cur	0	0	0	0	**7**	0	0	0	0	0	0	0	0	0	7
	A. fas	0	0	0	0	0	**8**	0	0	0	0	0	0	0	0	8
	A. spe	0	0	0	0	0	0	**7**	0	0	0	0	0	0	0	7
	C. mac	0	0	0	0	0	0	0	6	0	0	0	0	0	0	6
	C. odo	0	0	0	0	0	0	0	0	**8**	0	0	0	0	0	8
	C. maj	0	0	0	0	0	0	0	0	0	**7**	0	0	0	0	7
	D. pur	0	0	0	0	0	0	0	0	0	0	**8**	0	0	0	8
	N. ole	0	0	0	0	0	0	0	0	0	0	0	**8**	0	0	8
	O. fim	0	0	0	0	0	0	0	0	0	0	0	0	**7**	0	7
	T. per	0	0	0	0	0	0	0	0	0	0	0	0	0	**7**	7
	True Total	8	8	7	8	7	8	7	7	8	7	8	8	7	7	105

Individual Test			**Overall Test**
A. boehmianum	8/8 = 1.00	1.00 > 0.0714	104/105 = 0.990 0.990 > 0.0714
A. obesum	8/8 = 1.00	1.00 > 0.0714	
A. oleifolium	7/7 = 1.00	1.00 > 0.0714	
A. socotranum	8/8 = 1.00	1.00 > 0.0714	
A. curassavica	7/7 = 1.00	1.00 > 0.0714	
A. fascicularis	8/8 = 1.00	1.00 > 0.0714	
A. speciosa	7/7 = 1.00	1.00 > 0.0714	
C. macrocarpa	**6/7 = 0.857**	**0.857 > 0.0714**	
C. odollam	8/8 = 1.00	1.00 > 0.0714	
C. majalis	7/7 = 1.00	1.00 > 0.0714	
D. purpurea	8/8 = 1.00	1.00 > 0.0714	
N. oleander	8/8 = 1.00	1.00 > 0.0714	
O. fimbrimarginatum	7/7 = 1.00	1.00 > 0.0714	
T. peruviana	7/7 = 1.00	1.00 > 0.0714	

4. Discussion

4.1 Extracted Ion Chromatograms of Standards

Ions present in the Full MS^2 (AIF) scans of the standards were used to determine the exact masses of the ions of interest. Digitoxigenin, digitoxin, cerberin, and neriifolin exhibited the "trio of ions" pattern at ions 375, 357, and 339 *m/z* in the Full MS^2 scan, which is characteristic to digitoxigenin. Digoxigenin, digoxin, and gitoxin had an ion pattern of 373, 355, and 337 *m/z* in the Full MS^2 scan, which is characteristic for digoxigenin. Convallotoxin and cymarin had an ion pattern of 369, 351, and 333 *m/z* in the Full MS^2 scan, which is characteristic for strophanthidin or calotropagenin.

Ions 375 and 373 were not appearing in the Full MS^2 scan for cerberin and gitoxin, respectively, and only appeared in the Full MS scan. The observed *m/z* for ions 375, 357, and 339 were taken from the ions seen in the Full MS^2 scans for digitoxigenin and digitoxin, rather than cerberin. Similarly, the observed m/z for ions 373, 355, and 337 were taken from digoxigenin and digoxin, rather than gitoxin.

4.2 Extracted Ion Chromatograms of Plants and Blind Test Identification

The Full MS^2 (AIF) mass spectra and chromatograms were primarily used for evaluating the ions of interest in the standards. These samples were clean, consisting purely of the standard and the diluent, methanol. On the other hand, the actual plant leaves contain many extraneous compounds, such as waxes, pigments, carbohydrates. Full MS scan was used instead because AIF would fragment these compounds, in addition to the cardenolides of interest, resulting in a noisy spectrum which makes it difficult to discern any characteristic peaks. Furthermore,

fragments of the ions of interest are still present in Full MS scan due to inherent in-source fragmentation during ionization.

A. curassavica, C. odollam, C. majalis, D. purpurea, N. oleander, and *T. peruviana* were among the plants expected to contain high amounts of cardenolides. Indeed, their ions had consistently strong abundances and many distinct chromatographic peaks for ions 375, 357, 339; 373, 355, 337; 371, 353, 335; 369, 351, 333, and genins 433, 405, 391, 389, and 375. Thus, the unknown samples of these plants were easily recognizable. *C. odollam* contained the highest amount of cardenolides by far, exhibiting the same magnitude of abundances if not higher (E6 – E8) at 4mg/mL as *N. oleander* at 6mg/mL, *A. curassavica* at 8mg/mL, and *C. majalis, D. purpurea,* and *T. peruviana* at 9mg/mL.

A. obesum exhibited strong abundances and chromatographic peaks at the selected ions as expected. *A. boehmianum, A. oleifolium,* and *A. socotranum,* which have a scarce amount of literature on their cardenolide content, also exhibited strong abundances. *A. socotranum* appeared to have the highest cardenolide content of the four *Adenium* species. Only 4mg/mL of *A. socotranum* was needed to yield E6 abundances, which is comparable to *C. odollam*. Meanwhile, *A. boehmianum, A. obesum,* and *A. oleifolium* showed strong abundances only at 6-7 mg/mL. Ions 387, 369, 351, and 333 were not particularly useful for *A. oleifolium* and *A. socotranum* identification as the EICs contained considerable noise. Similarly, ion 405 contained considerable noise and a lack of distinct peaks for all *Adenium* sp. Ions 375, 357, 339; 373, 355, 337; 371, 353, 335; and 433 provided the best EICs for *Adenium* sp.

C. macrocarpa surprisingly had peaks present at the selected ions. This was unexpected because although it was hypothesized to contain cardenolides, the bulk of the literature on *C. macrocarpa* discusses its antioxidant properties while its cardenolide content remains largely

undiscussed. However, it took the most attempts during validation to evaluate it due to the peaks being inconsistent for ions 369, 351, 333 and ions 371, 353, 335. Ions 375, 357, 339 and 373, 355, 337 provided the best EICs for *C. macrocarpa.*

Similar to the *Adenium* plants, literature on cardenolides in *Ornithogalum* focused on species other than *O. fimbrimarginatum* but *O. fimbrimarginatum* was hypothesized to contain cardenolides as well. Indeed, *O. fimbrimarginatum* had peaks present for all of the ions of interest. In particular, ions 371, 353, and 335 were the most characteristic for *O. fimbrimarginatum* as it consistently showed a series of five peaks between 4.65 to 5.30 minutes, which was very useful in its identification.

A. fascicularis and *A. speciosa* are known to have low cardenolide contents. As expected, the abundances were low for *A. fascicularis* and *A. speciosa*, to an extent. The two plants required the highest optimal concentration of all the plants, at 10 mg/mL, for discernible and consistent chromatographic peaks to be observed. *A. fascicularis* did not have many characteristic peaks, and the few peaks observed were not always consistently present throughout every replicate. *A. speciosa* was expected to also have a low cardenolide content, but it had EICs with distinct peaks and adequate abundances, particularly in ions 369, 351, 333 and 373, 355, 337.

4.3 Blind Test Ion Performance

4.3.1 Blind Test 1

There were no issues in discerning between a CC plant and a NCC plant. The difference between *N. oleander* and *T. peruviana*, compared to *H. arbitufolia* and *P. laurocerasus* were obvious. *N. oleander* and *T. peruviana*, which contain cardenolides, will show distinct peaks in

all EICs at all ions. Meanwhile, *H. arbitufolia* and *P. laurocerasus* would exhibit EICs with low abundances ($\leq$ E4) with the absence of any distinct peaks.

4.3.2 Blind Test 2

Ion 375 *m/z* was useful for identifying all plants, as every plant's EICs had peaks present for this ion. In the 391 *m/z* EIC, there were peaks present at retention times (RTs) 7.70 to 7.74 and 8.20 to 8.40 for every plant; these peaks were not particularly useful in identifying the CC plants. However, the presence of additional peaks in the 391 *m/z* EICs of *A. socotranum, A. oleifolium, N. oleander, O. fimbrimarginatum, C. majalis,* and *C. odollam* aided plant identification. As expected, ion 405 *m/z* was most useful for identifying *C. majalis* and the *Asclepias* plants, as it is the mass for strophanthidin and calotropagenin, which have been found in these genera of plants. However, it also aided the identification of *N. oleander, T. peruviana, C. odollam,* and *O. fimbrimarginatum.* As expected, ion 433 *m/z* was useful for identifying *N. oleander* since it is the mass for oleandrigenin. It was surprisingly helpful for *O. fimbrimarginatum, D. purpurea, C. majalis, C. macrocarpa,* and the *Adenium spp.* as well. *N. oleander, C. odollam, C. majalis, T. peruviana,* and *D. purpurea* provided EICs with low noise and sharp, tall peaks at consistent RTs for all ion groupings, so there was little issue in identifying their unknowns.

The identification of *A. fascicularis* was difficult due to its inherently low cardenolide-content. As a result, it often had ambiguous EICs with either the lack of peaks or inconsistent peaks. This was exacerbated for the "low" ion grouping. The EICs for ion 357 *m/z* are remarkably similar in *A. fascicularis* and *A. speciosa,* but peaks present in the EICs of other ions in the "medium" ion grouping (i.e. 351, 353, 355 *m/z*) aided in discerning between the two. *C. macrocarpa* also provided inconsistent EICs, in particular for 371, 353, 335 *m/z* and 369, 351,

and 333 *m/z*, but the presence of the other ions in their respective groupings (i.e. 375, 357, 339 *m/z* and 373, 355, 337 *m/z*) aided its identification.

O. fimbrimarginatum was initially mistaken for *C. macrocarpa.* Both have a peak at RT 5.49 – 5.51, as well as several peaks in the range of RTs 5.94 – 6.00 in the 375, 357, 339 *m/z* EICs. Both also had EICs with minimal peaks for 369, 351, and 333 *m/z*. This made it difficult to distinguish between the two, and the lower the ion groupings used (medium, low), the more difficult it became to tell them apart. As discussed earlier, *O. fimbrimarginatum* has a very distinct pattern of peaks for ions 371, 353, and 335 *m/z*. These ions were the distinguishing feature of *O. fimbrimarginatum* that differentiated it from *C. macrocarpa.*

It was obvious to identify when the unknown EICs were from an *Adenium* plant. However, as expected, the *Adenium* EICs were very similar to each other across all ions as they share the same genus. Still, there was enough variation in the RTs of characteristic peaks between the different species to discern them. *A. obesum, A. oleifolium,* and *A. socotranum* have noisy EICs for 369, 351, 333 *m/z* while there are distinct peaks and little noise for *A. boehmianum*. *A. obesum* and *A. oleifolium* have noisy EICs for 371, 353, and 335 *m/z* while these EICs are less noisy and exhibit distinct peaks for *A. boehmianum* and *A. socotranum*. For the 373, 355, and 337 *m/z* EICs, *A. socotranum* typically exhibited unresolved peaks at RTs 6.94 – 6.96 and 7.01 – 7.03 while *A. oleifolium* exhibits a single peak at RT 6.90 – 6.92. While this peak is also present for *A. obesum*, it is much smaller in *A. obesum* than in *A. oleifolium.* These similarities with subtle differences meant it was important to be more vigilant in the identification of *Adenium* samples.

There was one false identification when using the “low” ions grouping, where *A. fascicularis* was mistaken for *A. speciosa.* As discussed earlier, at lower *m/z*, it is difficult to see

any distinct peaks in the EICs for *A. fascicularis* given how few are normally present. Similarly, many of *A. speciosa's* defining peaks are absent at the lower *m/z* EICs. One of *A. speciosa's* defining peaks is at RT 5.09 – 5.11 in the 373, 355, 337 *m/z* EICs. Using the low ion groupings EIC, this is the only useful peak that is present; there are no other peaks as distinct in the other EICs (i.e. 339, 335, or 333 *m/z*). In the *A. fascicularis* unknown sample, this peak was present at a low intensity (Figure 19). Thus, it was misidentified as *A. speciosa* instead.

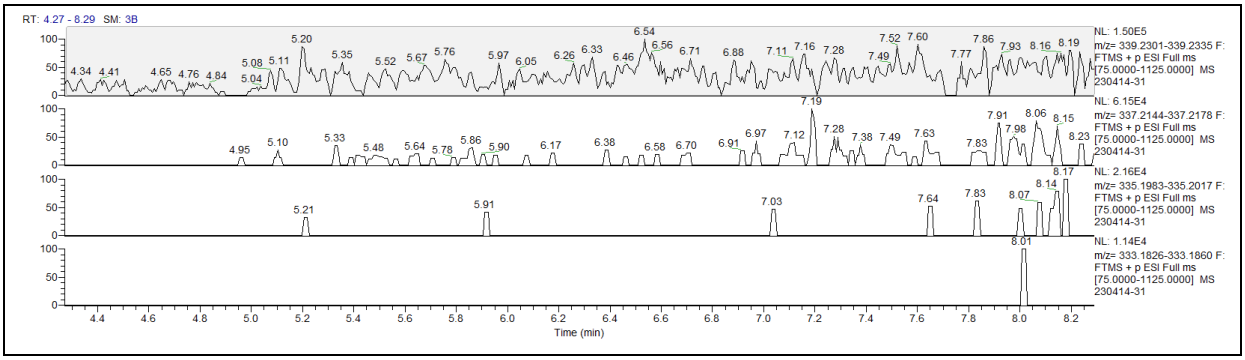

Figure 19. *"Low" ions grouping EIC for A. fascicularis unknown (Blind Test 2, Sample 65).*

There was also one false identification when using the "genin" ion grouping, where *C. macrocarpa* was mistaken for *A. boehmianum.* The genin EICs for *C. macrocarpa* and *A. boehmianum* are remarkably similar, with the only discernible difference being the presence of a peak at RT 7.48 – 7.50 in the 375 *m/z* EIC for *A. boehmianum* but not for *C. macrocarpa* (Figure 20). While this peak was not seen in any of the other *C. macrocarpa* unknowns nor the *C. macrocarpa* validation samples, the peak is present in *A. boehmianum* at varying intensities. The misidentification of only one out of seven *C. macrocarpa* unknowns does not indicate an association between the misidentification of *C. macrocarpa* and *A. boehmianum.*

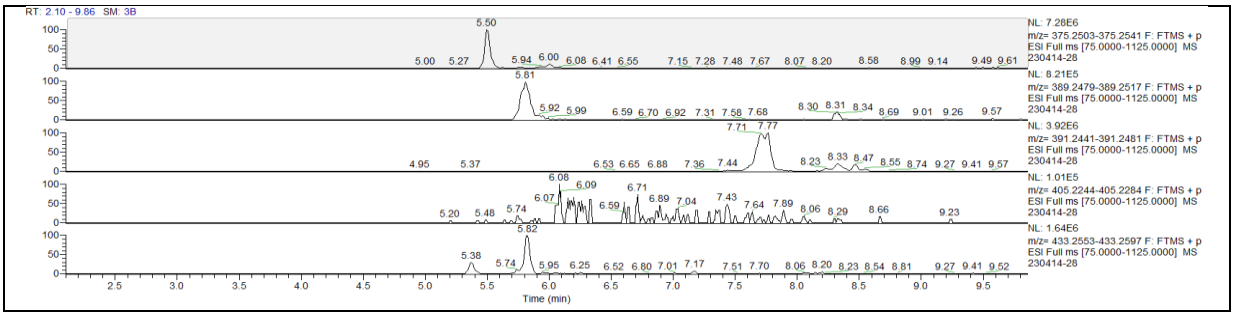

Figure 20. *"Genin" ions grouping EIC for C. macrocarpa unknown (Blind Test 2, Sample 27).*

The identifications made using the "high" and "medium" ion groupings were most successful, likely due to the stability of larger ions. With larger ions there is also a smaller pool of compounds with similar higher masses. Therefore, there is a lower probability of extraneous compounds appearing instead when looking at that particular compound. Conversely, with smaller ions there is a larger pool of compounds that have similar masses. This heightens the probability of extraneous smaller compounds interfering with identification.

This is not to say that low ion and genin ion patterns cannot be used for identification. The low and genin ion groupings still showed a remarkably high rate of success in identification. The strength of this method is certainly having a combination of different ions to use for identification. Often, different unknowns might exhibit similar EICs for a particular ion so they might appear to be the same plant, but this is easily resolved when the EICs of another ion are considered.

4.4 Blind Test Issues

Identifications using the “high”, “medium”, “low”, and “genin” ion groupings were all made on the same set of unknown samples. The intent was to ensure that any differences in identifications were due to the ion groupings used, since the set of unknown samples remained constant.

However, a potential problem arises from the fact that only one individual performed the identifications using the “high”, “medium”, “low”, and “genin” ions grouping. Despite the high volume of samples for a single individual to identify (32 for Blind Test 1 and 105 for Blind Test 2), and measures to mitigate potential bias, there is still a possibility that the analyst remembers what they answered from one ion grouping to another for some of the unknowns.

Another issue was the analyst’s prior knowledge of the species of plants included in the unknown. As discussed earlier, *A. fascicularis* contains low cardenolide content. Peaks were not present in the EICs at lower mass ions (i.e., 339, 337, 335, and 333 *m/z*) (Figure 21). Had the analyst performing the identification been blinded that *A. fascicularis* was an option, *A. fascicularis* could have easily been incorrectly deemed as a NCC plant.

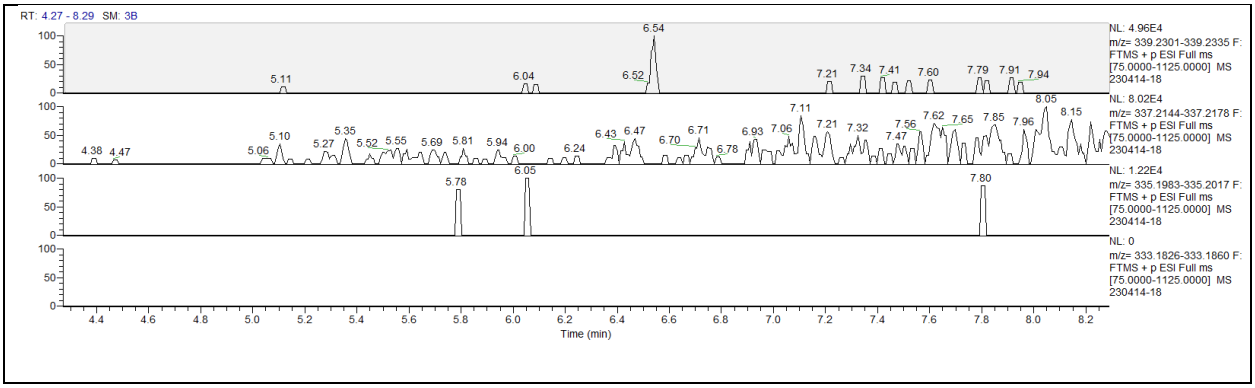

Figure 21. *“Low ions grouping” EIC for A. fascicularis unknown (Blind Test 2, Sample 52).*

4.5 Future Endeavors

4.5.1 Additional Plants and Ions

Now that we have a method, it would be worthwhile to analyze more plants, especially ones that are common causes of toxicosis in humans and animals, such as *D.* lanata. *D. lanata* contains cardenolides such as verodoxin, glucoverodoxin, glucolanadoxin, and lanatoside E which are derivatives of gitaloxigenin and diginatigenin (Ravi et al. 2020b). Other plants worth looking into are *Calotropis gigantea*, which contains corotoxigenin, and *Digitalis canariensis*, which contains xysmalogenin and canarigenin (Sun et al., 2017; Schaller and Kreis, 2006). This will lead to the discovery of more potential ions of interest from other genins in the 300 to 400 *m/z* region exhibiting the "loss of 18 *m/z*" pattern. Including a broader variety of CC plants provides insight in the fragmentation of genins beyond the digoxigenin, digitoxigenin, strophanthidin, and Δ16Adynerigenin that were the focus of this present study.

A considerable number of milkweed cardenolides appear to exhibit fragments at ion 387 rather than at ion 333 (Kanojiya et al. 2012). Ion 387 should have been included in this study as it may have been more distinct for milkweeds than ion 333, therefore aiding identification . In the standards prepared, ion 387 appears to only be present in the Full MS scan of convallotoxin. Similarly, ion 387 appears to be present in cymarin at a high abundance (E6) in Full MS scan but at a lower abundance in Full MS2 scan (E4). The exact mass of ion 387 could have been determined from cymarin and used in the blind tests.

4.5.2 Blind Test Changes

Changes to the experimental design can be made to prevent potential bias next time. There should be a different set of unknowns for each ion grouping that the individual uses to perform identifications. Alternatively, there can be multiple individuals performing identifications on the same set of unknown samples, with a different individual using a different ion grouping. It would also be worthwhile to have the individual unaware of the possible plants that were sampled when they perform the identification of the unknowns.

4.5.3 Other Matrices

A glaring issue of this present study is that the samples were simply plant material extracted in methanol. This resulted in a very simple matrix and is not representative of the more complex biological matrices that cardenolides are often found in following intoxications in humans or animals, such as blood, serum, vomitus, or even urine. These matrices require significant cleanup, more so than leaves in methanol. This method of identification should be attempted on extractions of cardenolides from such complex matrices and any differences in abundances, peak shapes, and retention times, or noise noted . It would be worth investigating if these ions and the EIC patterns are still observed in such more complex matrices, and how well the ions found in this present study perform for the identification of the plants .

5. Conclusion

This present study shows a promising start in using select ion chromatographic finger prints as a means of qualitative identification of cardenolide-containing plants. There is a strong potential for the EIC finger prints of these select ions to be used as a screening tool for identification of cardenolide-containing plants. Not only could this method be an alternative to one that depends on expensive and unavailable standards, but it may also be a valuable tool for forensic and veterinary diagnostic laboratories. In particular, it could be an effective general approach of CC plant identification in situations lacking exposure history or when the type of plant ingested is unclear from vomitus or stomach contents. This method can certainly be expanded upon, by including a larger variety of CC plants, including more ions that are part of the "loss of 18 *m/z*" pattern, having different individuals conduct the identifications in blind tests, and to explore different matrices, to truly assess the usefulness of the approach. With further research and improvements, it has the potential to become a powerful diagnostic tool.

References

Abe, F., Yamauchi, T., Yahara, S., & Nohara, T. (1994). Glycosides of 19-formylthevetiogenin and 5 alpha-thevetiogenin from Thevetia neriifolia. *Phytochemistry, 37(5),* 1429–1432. https://doi.org/10.1016/s0031-9422(00)90426-6

Agrawal, A. A., Böröczky, K., Haribal, M., Hastings, A. P., White, R. A., Jiang, R. W., & Duplais, C. (2021). Cardenolides, toxicity, and the costs of sequestration in the coevolutionary interaction between monarchs and milkweeds. *Proceedings of the National Academy of Sciences of the United States of America, 118(16),* e2024463118. https://doi.org/10.1073/pnas.2024463118

Agrawal, A. A., Petschenka, G., Bingham, R. A., Weber, M. G., & Rasmann, S. (2012). Toxic cardenolides: chemical ecology and coevolution of specialized plant-herbivore interactions. *The New Phytologist, 194(1),* 28–45. https://doi.org/10.1111/j.1469-8137.2011.04049.x

Akinmoladun, A. C., Olaleye, M. T., & Farombi, E. O. (2014). 13 – Cardiotoxicity and cardioprotective effects of African medicinal plants. In *V. Kuete (Ed.), Toxicological Survey of African Medicinal Plants* (pp. 395–421). Elsevier. https://doi.org/10.1016/B978-0-12-800018-2.00013-3

Alzabib, A. A., Abobakr, Y., Al-Sarar, A. S., Hussein, H. I., Basudan, O. A., El-Gamal, A. A., Abdel-Kader, M. S., & El Komy, M. H. (2019). Molluscicidal activity of cardiac glycosides isolated from Adenium obesum. *Pest Management Science, 75(10),* 2770–2775. https://doi.org/10.1002/ps.5388

Arai, M. A., Tateno, C., Koyano, T., Kowithayakorn, T., Kawabe, S., & Ishibashi, M. (2011). New hedgehog/GLI-signaling inhibitors from Adenium obesum. *Organic & Biomolecular Chemistry, 9(4),* 1133–1139. https://doi.org/10.1039/c0ob00677g

Bavendiek, U., Aguirre Davila, L., Koch, A., & Bauersachs, J. (2017). Assumption versus evidence: the case of digoxin in atrial fibrillation and heart failure. *European Heart Journal, 38(27),* 2095–2099. https://doi.org/10.1093/eurheartj/ehw577

Begum, S., Siddiqui, B. S., Sultana, R., Zia, A., & Suria, A. (1999). Bio-active cardenolides from the leaves of Nerium oleander. *Phytochemistry, 50(3),* 435–438. https://doi.org/10.1016/s0031-9422(98)00523-8

Berny, P., Caloni, F., Croubels, S., Sachana, M., Vandenbroucke, V., Davanzo, F., & Guitart, R. (2010). Animal poisoning in Europe. Part 2: Companion animals. *Veterinary Journal, 183(3),* 255–259. https://doi.org/10.1016/j.tvjl.2009.03.034

Brower, L. P., Seiber, J. N., Nelson, C. J., Lynch, S. P., & Holland, M. M. (1984). Plant-determined variation in the cardenolide content, thin-layer chromatography profiles, and emetic potency of monarch butterflies, Danaus plexippus L. reared on milkweed plants in California: 2. Asclepias speciosa. *Journal of Chemical Ecology, 10(4),* 601–639. https://doi.org/10.1007/BF00994224

Brower, L. P., van Brower, J., & Corvino, J. M. (1967). Plant poisons in a terrestrial food chain. *Proceedings of the National Academy of Sciences of the United States of America, 57(4),* 893–898. https://doi.org/10.1073/pnas.57.4.893

Carullo, N., Fabiano, G., D'Agostino, M., Zicarelli, M. T., Musolino, M., Presta, P., Michael, A., Andreucci, M., Bolignano, D., & Coppolino, G. (2023). New insights on the role of marinobufagenin from bench to bedside in cardiovascular and kidney diseases.

International Journal of Molecular Sciences, 24(13), 11186. https://doi.org/10.3390/ijms241311186

Cheenpracha, S., Karalai, C., Rat-A-Pa, Y., Ponglimanont, C., & Chantrapromma, K. (2004). New cytotoxic cardenolide glycoside from the seeds of Cerbera manghas. *Chemical & Pharmaceutical Bulletin, 52(8),* 1023–1025. https://doi.org/10.1248/cpb.52.1023

Chen, K. K., & Kovaríková, A. (1967). Pharmacology and toxicology of toad venom. *Journal of Pharmaceutical Sciences, 56(12),* 1535–1541. https://doi.org/10.1002/jps.2600561202

Cheung, H. T. A., Nelson, C. J., & Watson, T. R. (1988). New glucoside conjugates and other cardenolide glycosides from the monarch butterfly reared on Asclepias fruticosa L. *Journal of the Chemical Society, Perkin Transactions 1, 7,* 1851–1857. https://doi.org/10.1039/P19880001851

Cheung, Y. Y., Chen, K. C., Chen, H., Seng, E. K., & Chu, J. J. (2014). Antiviral activity of lanatoside C against dengue virus infection. *Antiviral Research, 111,* 93–99. https://doi.org/10.1016/j.antiviral.2014.09.007

Dement, W. A., & Mooney, H. A. (1974). Seasonal variation in the production of tannins and cyanogenic glucosides in the chaparral shrub, Heteromeles arbutifolia. *Oecologia, 15(1),* 65–76. https://doi.org/10.1007/BF00345228

Dmitrieva, R. I., Bagrov, A. Y., Lalli, E., Sassone-Corsi, P., Stocco, D. M., & Doris, P. A. (2000). Mammalian bufadienolide is synthesized from cholesterol in the adrenal cortex by a pathway that is independent of cholesterol side-chain cleavage. *Hypertension, 36(3),* 442–448. https://doi.org/10.1161/01.hyp.36.3.442

Duffey, S. S., & Scudder, G. G. E. (1972). Cardiac glycosides in North American Asclepiadaceae, a basis for unpalatability in brightly coloured Hemiptera and Coleoptera.

Journal of Insect Physiology, *18(1)*, 63–78. https://doi.org/10.1016/0022-1910(72)90065-0

Eddleston, M., Ariaratnam, C. A., Meyer, W. P., Perera, G., Kularatne, A. M., Attapattu, S., Sheriff, M. H., & Warrell, D. A. (1999). Epidemic of self-poisoning with seeds of the yellow oleander tree (Thevetia peruviana) in northern Sri Lanka. *Tropical Medicine & International Health, 4(4),* 266–273. https://doi.org/10.1046/j.1365-3156.1999.00397.x

Eisner, T., Wiemer, D. F., Haynes, L. W., & Meinwald, J. (1978). Lucibufagins: Defensive steroids from the fireflies Photinus ignitus and P. marginellus (Coleoptera: Lampyridae). *Proceedings of the National Academy of Sciences of the United States of America, 75(2),* 905–908. https://doi.org/10.1073/pnas.75.2.905

Evans, F. J., & Cowley, P. S. (1972). Cardenolides and spirostanols in Digitalis purpurea at various stages of development. *Phytochemistry, 11(10)*, 2971–2975. https://doi.org/10.1016/0031-9422(72)80087-6

Fauchier, L., Laborie, G., Clementy, N., & Babuty, D. (2016). Beta-blockers or Digoxin for Atrial Fibrillation and Heart Failure? *Cardiac Failure Review, 2(1)*, 35–39. https://doi.org/10.15420/cfr.2015:28:2

Ferth, R., & Kopp, B. (1992). Cardenolides from Ornithogalum umbellatum L. *Pharmazie, 47*, 626–629.

Ferth, R., Baumann, A., Mayer, K., Robien, W. & Kopp, B. (1992). Cardenolide aus Ornithogalum nutans (2 n = 30), 2. Mitteilung+ [Cardenolides from Ornithogalum nutans (2 n = 30), Part 2+]. *Zeitschrift für Naturforschung B, 47(10),* 1459-1468. https://doi.org/10.1515/znb-1992-1018

Fujii, Y., Ikeda, Y., & Yamazaki, M. (1989). High-performance liquid chromatographic determination of secondary cardiac glycosides in Digitalis purpurea leaves. *Journal of Chromatography, 479(2),* 319–325. https://doi.org/10.1016/s0021-9673(01)83346-x

Galey, F. D., Holstege, D. M., Plumlee, K. H., Tor, E., Johnson, B., Anderson, M. L., Blanchard, P. C., & Brown, F. (1996). Diagnosis of oleander poisoning in livestock. *Journal of Veterinary Diagnostic Investigation : Official Publication of the American Association of Veterinary Laboratory Diagnosticians, Inc, 8(3),* 358–364. https://doi.org/10.1177/104063879600800314

Gao, H., Popescu, R., Kopp, B., & Wang, Z. (2011). Bufadienolides and their antitumor activity. *Natural Product Reports, 28(5),* 953–969. https://doi.org/10.1039/c0np00032a

Gault, G., Berny, P., & Lorgue, G. (1995). Plantes toxiques pour les animaux de compagnie. *Recueil de Médecine Vétérinaire, 171,* 171–176.

Ghannamy, U., Kopp, B., Robien, W., & Kubelka, W. (1987). Cardenolides from Ornithogalum boucheanum. *Planta Medica, 53(2),* 172–178. https://doi.org/10.1055/s-2006-962666

Groen, S. C., & Whiteman, N. K. (2021). Convergent evolution of cardiac-glycoside resistance in predators and parasites of milkweed herbivores. *Current Biology, 31(22),* R1465–R1466. https://doi.org/10.1016/j.cub.2021.10.025

Guerrero, A., Herranz, N., Sun, B., Wagner, V., Gallage, S., Guiho, R., Wolter, K., Pombo, J., Irvine, E. E., Innes, A. J., Birch, J., Glegola, J., Manshaei, S., Heide, D., Dharmalingam, G., Harbig, J., Olona, A., Behmoaras, J., Dauch, D., Uren, A. G., … Gil, J. (2019). Cardiac glycosides are broad-spectrum senolytics. *Nature Metabolism, 1(11),* 1074–1088. https://doi.org/10.1038/s42255-019-0122-z

Gummin, D. D., Mowry, J. B., Beuhler, M. C., Spyker, D. A., Rivers, L. J., Feldman, R., Brown, K., Nathaniel, P. T. P., Bronstein, A. C., & Weber, J. A. (2022). 2021 Annual report of the National Poison Data System© (NPDS) from America's poison centers: 39th annual report. *Clinical Toxicology, 60(12),* 1381–1643. https://doi.org/10.1080/15563650.2022.2132768

Higano, T., Kuroda, M., Sakagami, H., & Mimaki, Y. (2007). Convallasaponin A, a new 5beta-spirostanol triglycoside from the rhizomes of Convallaria majalis. *Chemical & Pharmaceutical Bulletin, 55(2),* 337–339. https://doi.org/10.1248/cpb.55.337

Hilton, P. J., White, R. W., Lord, G. A., Garner, G. V., Gordon, D. B., Hilton, M. J., Forni, L. G., McKinnon, W., Ismail, F. M., Keenan, M., Jones, K., & Morden, W. E. (1996). An inhibitor of the sodium pump obtained from human placenta. *Lancet, 348(9023),* 303–305. https://doi.org/10.1016/s0140-6736(96)02257-x

Hoffmann, J. J., & Cole, J. R. (1977). Phytochemical investigation of Adenium obesum Forskal (Apocynaceae): isolation and identification of cytotoxic agents. *Journal of Pharmaceutical Sciences, 66(9),* 1336–1338. https://doi.org/10.1002/jps.2600660935

Hutchinson, D. A., Mori, A., Savitzky, A. H., Burghardt, G. M., Wu, X., Meinwald, J., & Schroeder, F. C. (2007). Dietary sequestration of defensive steroids in nuchal glands of the Asian snake Rhabdophis tigrinus. *Proceedings of the National Academy of Sciences of the United States of America, 104(7),* 2265–2270. https://doi.org/10.1073/pnas.0610785104

Jacobs, C. M., Wagmann, L., & Meyer, M. R. (2023). Analytical toxicology of yew constituents in human blood and urine by liquid chromatography-high-resolution tandem mass

spectrometry. *Drug Testing and Analysis, 15(1),* 123–127. https://doi.org/10.1002/dta.3360

Jin, Y. H., Jeon, S., Lee, J., Kim, S., Jang, M. S., Park, C. M., Song, J. H., Kim, H. R., & Kwon, S. (2021). Broad spectrum antiviral properties of cardiotonic steroids used as potential therapeutics for emerging coronavirus infections. *Pharmaceutics, 13(11),* 1839. https://doi.org/10.3390/pharmaceutics13111839

Kanojiya, S., & Madhusudanan, K. P. (2012). Rapid identification of calotropagenin glycosides using high-performance liquid chromatography electrospray ionization tandem mass spectrometry. *Phytochemical Analysis, 23(2),* 117–125. https://doi.org/10.1002/pca.1332

Kaunda, J. S., Qin, X. J., Yang, X. Z., Mwitari, P. G., Zhu, H. T., Wang, D., & Zhang, Y. J. (2020). Ten new glycosides, carissaedulosides A-J from the root barks of Carissa edulis and their cytotoxicities. *Bioorganic Chemistry, 102,* 104097. https://doi.org/10.1016/j.bioorg.2020.104097

Kopp, B., & Kubelka, W. (1982). Neue Cardenolide aus Convallaria majalis [New cardenolides from Convallaria majalis]. *Planta Medica, 45(4),* 195–202. https://doi.org/10.1055/s-2007-971372

Kopp, B., Krenn, L., Kubelka, E., & Kubelka, W. (1992). Cardenolides from Adonis aestivalis. Phytochemistry, 31(9), 3195–3198. https://doi.org/10.1016/0031-9422(92)83473-c

Kozikowski, T. A., Magdesian, K. G., & Puschner, B. (2009). Oleander intoxication in New World camelids: 12 cases (1995-2006). *Journal of the American Veterinary Medical Association, 235*(3), 305–310. https://doi.org/10.2460/javma.235.3.305

Kreis, W., & Müller-Uri , F. (2010). Biochemistry of Sterols, Cardiac Glycosides, Brassinosteroids, Phytoecdysteroids and Steroid saponins. *Annual Plant Reviews, 40,* 304–363. https://doi.org/10.1002/9781444320503.ch6

Kwon, H. J., Sim, H. J., Lee, S. I., Lee, Y. M., Park, Y. D., & Hong, S. P. (2011). HPLC method validation for Digitalis and its analogue by pulsed amperometric detection. *Journal of Pharmaceutical and Biomedical Analysis, 54(1),* 217–221. https://doi.org/10.1016/j.jpba.2010.07.037

Laird, G. M., Eisele, E. E., Rabi, S. A., Nikolaeva, D., & Siliciano, R. F. (2014). A novel cell-based high-throughput screen for inhibitors of HIV-1 gene expression and budding identifies the cardiac glycosides. *The Journal of Antimicrobial Chemotherapy, 69(4),* 988–994. https://doi.org/10.1093/jac/dkt471

Langford, S. D., & Boor, P. J. (1996). Oleander toxicity: an examination of human and animal toxic exposures. *Toxicology, 109(1),* 1–13.https://doi.org/10.1016/0300-483x(95)03296-r

Laphookhieo, S., Cheenpracha, S., Karalai, C., Chantrapromma, S., Rat-a-Pa, Y., Ponglimanont, C., & Chantrapromma, K. (2004). Cytotoxic cardenolide glycoside from the seeds of Cerbera odollam. *Phytochemistry, 65(4),* 507–510. https://doi.org/10.1016/j.phytochem.2003.10.019

Luckner, M., & Wichtl, M. (2000). Digitalis. Stuttgart, Germany: *Wissenschaftliche Verlagsgesellschaft mbH*.

Malaspina, P., Betuzzi, F., Ingegneri, M., Smeriglio, A., Cornara, L., & Trombetta, D. (2022). Risk of Poisoning from Garden Plants: Misidentification between Laurel and Cherry Laurel. *Toxins, 14(11),* 726. https://doi.org/10.3390/toxins14110726

Miyagawa, T., Ohtsuki, T., Koyano, T., Kowithayakorn, T., & Ishibashi, M. (2009). Cardenolide glycosides of Thevetia peruviana and triterpenoid saponins of Sapindus emarginatus as TRAIL resistance-overcoming compounds. *Journal of Natural Products, 72(8),* 1507–1511. https://doi.org/10.1021/np900202n

Nelson, C. J., Seiber, J. N., & Brower, L. P. (1981). Seasonal and intraplant variation of cardenolide content in the California milkweed, Asclepias eriocarpa, and implications for plant defense. *Journal of Chemical Ecology, 7(6),* 981–1010. https://doi.org/10.1007/BF00987622

Osterloh, J., Herold, S., & Pond, S. (1982). Oleander interference in the digoxin radioimmunoassay in a fatal ingestion. *JAMA, 247(11),* 1596–1597.

Pan, L., Zhang, Y., Zhao, W., Zhou, X., Wang, C., & Deng, F. (2017). The cardiac glycoside oleandrin induces apoptosis in human colon cancer cells via the mitochondrial pathway. *Cancer Chemotherapy and Pharmacology, 80(1),* 91–100. https://doi.org/10.1007/s00280-017-3337-2

Papi, L., Luciani, A. B., Forni, D., & Giusiani, M. (2012). Unexpected double lethal oleander poisoning. *The American Journal of Forensic Medicine and Pathology, 33(1),* 93–97. https://doi.org/10.1097/PAF.0b013e31822d33d4

Petschenka, G., Fei, C. S., Araya, J. J., Schröder, S., Timmermann, B. N., & Agrawal, A. A. (2018). Relative selectivity of plant cardenolides for Na+/K+-ATPases from the monarch butterfly and non-resistant insects. *Frontiers in Plant Science, 9,* 1424. https://doi.org/10.3389/fpls.2018.01424

Pokharel, P., Sippel, M., Vilcinskas, A., & Petschenka, G. (2020). Defense of milkweed bugs (Heteroptera: Lygaeinae) against predatory lacewing larvae depends on structural

differences of sequestered cardenolides. *Insects, 11(8*), 485. https://doi.org/10.3390/insects11080485

Rahnama-Moghadam, S., Hillis, L. D., & Lange, R. A. (2015). Chapter 3 – Environmental Toxins and the Heart. In *M. Ramachandran (Ed.), Heart and Toxins* (pp. 75–132). Academic Press. https://doi.org/10.1016/B978-0-12-416595-3.00003-7

Rajkovic, J., Novakovic, R., Grujic-Milanovic, J., Ydyrys, A., Ablaikhanova, N., Calina, D., Sharifi-Rad, J., & Al-Omari, B. (2023). An updated pharmacological insight into calotropin as a potential therapeutic agent in cancer. *Frontiers in Pharmacology, 14,* 1160616. https://doi.org/10.3389/fphar.2023.1160616

Rasmann, S., Johnson, M. D., & Agrawal, A. A. (2009). Induced responses to herbivory and jasmonate in three milkweed species. *Journal of Chemical Ecology, 35(11),* 1326–1334. https://doi.org/10.1007/s10886-009-9719-0

Ravi, B. G., Guardian, M. G. E., Dickman, R., & Wang, Z. Q. (2020a). High-resolution tandem mass spectrometry dataset reveals fragmentation patterns of cardiac glycosides in leaves of the foxglove plants. *Data in Brief, 30,* 105464. https://doi.org/10.1016/j.dib.2020.105464

Ravi, B. G., Guardian, M. G. E., Dickman, R., & Wang, Z. Q. (2020b). Profiling and structural analysis of cardenolides in two species of Digitalis using liquid chromatography coupled with high-resolution mass spectrometry. *Journal of Chromatography. A, 1618,* 460903. https://doi.org/10.1016/j.chroma.2020.460903

Ren, Y., Ribas, H. T., Heath, K., Wu, S., Ren, J., Shriwas, P., Chen, X., Johnson, M. E., Cheng, X., Burdette, J. E., & Kinghorn, A. D. (2020). Na+/K+-ATPase-Targeted Cytotoxicity of

(+)-Digoxin and Several Semisynthetic Derivatives. *Journal of Natural Products, 83(3),* 638–648. https://doi.org/10.1021/acs.jnatprod.9b01060

Rosca, C. I., Kundnani, N. R., Tudor, A., Rosca, M. S., Nicoras, V. A., Otiman, G., Ciurariu, E., Ionescu, A., Stelian, M., Sharma, A., Borza, C., & Lighezan, D. F. (2021). Benefits of prescribing low-dose digoxin in atrial fibrillation. *International Journal of Immunopathology and Pharmacology, 35,* 20587384211051955. https://doi.org/10.1177/20587384211051955

Saxena, M., Jadhav, E. B., Sankhla, M. S., Singhal, M., Parihar, K., Awasthi, K. K., & Awasthi, G. (2023). Bintaro (Cerbera odollam and Cerbera manghas): an overview of its eco-friendly use, pharmacology, and toxicology. *Environmental Science and Pollution Research International, 30(28),* 71970–71983. https://doi.org/10.1007/s11356-022-22585-w

Schaller, F., & Kreis, W. (2006). Cardenolide genin pattern in Isoplexis plants and shoot cultures. Planta Medica, 72(12), 1149–1156. https://doi.org/10.1055/s-2006-947194

Schmelzer, G., Gurib-Fakim, A., Arroo, R., Bosch, C. H., de, R., Simmonds, M., Lemmens, R. H. M. J., & Oyen, L. P. A. (2008). *Plant Resources of Tropical Africa 11(1): Medicinal plants 1*.

Schrutka-Rechtenstamm, R., Kopp, B., & Löffelhardt, W. (1985). Studies on the Turnover of Cardenolides in Convallaria majalis. *Planta Medica, 51(5),* 387–390. https://doi.org/10.1055/s-2007-969527

Seiber, J. N., Brower, L. P., Lee, S. M., McChesney, M. M., Cheung, H. T., Nelson, C. J., & Watson, T. R. (1986). Cardenolide connection between overwintering monarch

butterflies from Mexico and their larval food plant, Asclepias syriaca. *Journal of Chemical Ecology, 12(5),* 1157–1170. https://doi.org/10.1007/BF01639002

Seiber, J. N., Nelson, C. J., & Lee, S. M. (1982). Cardenolides in the latex and leaves of seven Asclepias species and Calotropis procera. *Phytochemistry, 21(9),* 2343–2348. https://doi.org/10.1016/0031-9422(82)85202-3

Sendker, J., & Nahrstedt, A. (2009). Generation of primary amide glucosides from cyanogenic glucosides. *Phytochemistry, 70(3),* 388–393. https://doi.org/10.1016/j.phytochem.2008.11.008

Shaw, D., & Pearn, J. (1979). Oleander poisoning. *The Medical Journal of Australia, 2(5),* 267–269. https://doi.org/10.5694/j.1326-5377.1979.tb127135.x

Singh, Y., Nimoriya, R., Rawat, P., Mishra, D. K., & Kanojiya, S. (2021). Structural analysis of diastereomeric cardiac glycosides and their genins using ultraperformance liquid chromatography-tandem mass spectrometry. *Journal of the American Society for Mass Spectrometry, 32(5),* 1205–1214. https://doi.org/10.1021/jasms.1c00017

Siti-Syarifah, M., & Yunos, N. (2018). Therapeutic potential of cardiac glycosides against cancer. In *Anticancer Plants: Natural Products and Biotechnological Implements* (pp. 67–81). https://doi.org/10.1007/978-981-10-8064-7_4

Soto-Blanco, B., Fontenele-Neto, J. D., Silva, D. M., Reis, P. F., & Nóbrega, J. E. (2006). Acute cattle intoxication from Nerium oleander pods. *Tropical Animal Health and Production, 38(6),* 451–454. https://doi.org/10.1007/s11250-006-4400-x

Sun, M., Pan, D., Chen, Y., Li, Y., Gao, K., & Hu, B. (2017). Coroglaucigenin enhances the radiosensitivity of human lung cancer cells through Nrf2/ROS pathway. *Oncotarget, 8(20),* 32807–32820. https://doi.org/10.18632/oncotarget.16454

T. Higashi, N. Nakayama, K. Shimada, H. Kasai & H. Nakazawa (1999) High-performance liquid chromatography-tandem mass spectrometry of cardiac steroids. *Journal of Liquid Chromatography & Related Technologies, 22(15),* 2283-2296 https://doi.org/10.1081/JLC-100101801

Tian, D. M., Cheng, H. Y., Jiang, M. M., Shen, W. Z., Tang, J. S., & Yao, X. S. (2016). Cardiac glycosides from the seeds of Thevetia peruviana. *Journal of Natural Products, 79(1),* 38–50. https://doi.org/10.1021/acs.jnatprod.5b00611

Tian, L., Xie, X. H., & Zhu, Z. H. (2018). Calotropin regulates the apoptosis of non small cell cancer by regulating the cytotoxic T lymphocyte associated antigen 4 mediated TGF β/ERK signaling pathway. *Molecular Medicine Reports, 17(6),* 7683–7691. https://doi.org/10.3892/mmr.2018.8853

Ujvari, B., Mun, H. C., Conigrave, A. D., Bray, A., Osterkamp, J., Halling, P., & Madsen, T. (2013). Isolation breeds naivety: island living robs Australian varanid lizards of toad-toxin immunity via four-base-pair mutation. *Evolution; International Journal of Organic Evolution, 67(1),* 289–294. https://doi.org/10.1111/j.1558-5646.2012.01751.x

Wang, X., Dubois, R., Young, C., Lien, E. J., & Adams, J. D. (2016). Heteromeles Arbutifolia, a traditional treatment for alzheimer's disease, phytochemistry and safety. *Medicines (Basel, Switzerland), 3(3),* 17. https://doi.org/10.3390/medicines3030017

Wangteeraprasert, R., Lipipun, V., Gunaratnam, M., Neidle, S., Gibbons, S., & Likhitwitayawuid, K. (2012). Bioactive compounds from Carissa spinarum. *Phytotherapy research, 26(10),* 1496–1499. https://doi.org/10.1002/ptr.4607

Warashina, T., Shikata, K., Miyase, T., Fujii, S., & Noro, T. (2008). New cardenolide and acylated lignan glycosides from the aerial parts of Asclepias curassavica. *Chemical & Pharmaceutical Bulletin, 56(8),* 1159–1163. https://doi.org/10.1248/cpb.56.1159

Wilkins, M. R., Kendall, M. J., & Wade, O. L. (1985). William Withering and Digitalis, 1785 to 1985. *British Medical Journal (Clinical research ed.), 290(6461),* 7–8. https://doi.org/10.1136/bmj.290.6461.7

Woods, L. W., Filigenzi, M. S., Booth, M. C., Rodger, L. D., Arnold, J. S., & Puschner, B. (2004). Summer pheasant's eye (Adonis aestivalis) poisoning in three horses. *Veterinary Pathology, 41(3),* 215–220. https://doi.org/10.1354/vp.41-3-215

Zalucki, M. P., Brower, L. P., & Alonso-M, A. (2001). Detrimental effects of latex and cardiac glycosides on survival and growth of first-instar monarch butterfly larvae Danaus plexippus feeding on the sandhill milkweed Asclepias humistrata. *Ecological Entomology, 26(2),* 212–224. https://doi.org/10.1046/j.1365-2311.2001.00313.x

Zhang, R. R., Tian, H. Y., Tan, Y. F., Chung, T. Y., Sun, X. H., Xia, X., Ye, W. C., Middleton, D. A., Fedosova, N., Esmann, M., Tzen, J. T., & Jiang, R. W. (2014). Structures, chemotaxonomic significance, cytotoxic and Na(+),K(+)-ATPase inhibitory activities of new cardenolides from Asclepias curassavica. *Organic & Biomolecular Chemistry, 12(44),* 8919–8929. https://doi.org/10.1039/c4ob01545b

Appendix

Acronyms

ACN	Acetonitrile
AIF	All Ion Fragmentation
CAHFS	California Animal Health and Food Safety Laboratory
CC	Cardenolide-containing
CG	Cardiac Glycoside(s)
dSPE	Dispersive Solid Phase Extraction
EIC	Extracted Ion Chromatogram
GCB	Graphitized Carbon Black
LC-MS	Liquid Chromatography - Mass Spectrometry
MeOH	Methanol
N.OL-ACN	*Nerium oleander* extract in acetonitrile
N.OL-MEOH	*Nerium oleander* extract in methanol
NCC	Non-Cardenolide-Containing
PSA	Primary Secondary Amine
RT	Retention time
SAS	Statistical Analysis System
UC	University of California
UCD	University of California, Davis
UHPLC-HRMS	Ultra High Performance Liquid Chromatography - High Resolution Mass Spectrometry